THE DEVELOPMENT OF AN ENERGY EFFICIENT TEMPERATURE AND HUMIDITY BASED FAN SYSTEM FOR INDOOR ENVIRONMENTAL QUALITY IMPROVEMENT

LAYA MOHAMMED AHMED AL-HILFI

A project report submitted in partial fulfilment of the
Requirements for the award of Master of Engineering (Electrical)

Lee Kong Chian Faculty of Engineering and Science
Universiti Tunku Abdul Rahman

OCT 2020

DECLARATION

I hereby declare that this project report is based on my original work except for citations and quotations which have been duly acknowledged. I also declare that it has not been previously and concurrently submitted for any other degree or award at UTAR or other institutions.
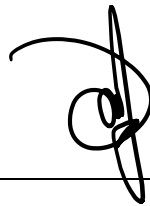
Signature   :

Name   : Laya Mohammed Ahmed Al-Hilfi

ID No.   : 2000612

Date   : 11/12/2020

APPROVAL FOR SUBMISSION

I certify that this project report entitled **"THE DEVELOPMENT OF AN ENERGY EFFICIENT TEMPERATURE AND HUMIDITY BASED SYSTEM FOR INDOOR ENVIRONMENTAL QUALITY IMPROVEMENT"** was prepared by **Laya Mohammed Ahmed Al-Hilfi** has met the required standard for submission in partial fulfilment of the requirements for the award of Master of Engineering (Electrical) at Universiti Tunku Abdul Rahman.

Approved by,

Signature   :

Supervisor   :   Wong Jianhui

Date   :   11/12/2020

Signature   :

Co-Supervisor :

Date   :

ACKNOWLEDGEMENTS

ABSTRACT

Indoor air quality (IAQ) represents a domain that encompasses diverse sub-domains that affect the human's life and comfortability inside a building such as lighting, thermal comfort, ergonomics, electromagnetic radiation, and many related factors. As global warming worsens, most of the occupant behaviour tends to increase the usage of air conditioners for better thermal comfort without any consideration of other indoor air quality factors such as CO2 and pollutant levels. A large increase in air conditioner usage was registered in Malaysia in 2009, making air conditioners the highest yearly energy consumption devices. Due to such large energy consumption, many studies urge the need for occupants to relay more on fan systems and less on-air conditioner as many are unaware with the amount of saving that can be achieved through the reduction of air conditioner usage. As such these unacceptable indoor air quality conditions that result from over-dependence on air conditioners, lack of window/door ventilation, and the minimal usage of ceiling fans have inspired the idea of building automated systems that monitor indoor air quality and provide solutions by depending on controllable environmental factors, such as humidity rate, airflow speed, percentage of CO2, CO, and temperature levels to reduce the need for air conditioners and increase the chances of energy saving. However, no previous research has shown whether an environmental-based fan system can assist in reducing energy consumption without causing any discomfort to the occupant in a humid tropical climate like Malaysia. This research aims to develop a cost-effective fan system that relies on the environmental parameter to control its speed to improve indoor air quality and reduce energy consumption while maintaining occupant's thermal satisfaction according to both ASHRAE 55 and EN 16798 standards.

TABLE OF CONTENTS

LIST OF TABLES

LIST OF FIGURES

LIST OF SYMBOLS / ABBREVIATIONS

IAQ	Indoor Air Quality
WHO	World Health Organization
CO_2	Carbon Dioxide
CO	Carbon Monoxide
APF	Annual performance factor
PMV	Predicted Mean Vote
PPD	Predicted Percentage of Dissatisfied
AC	Air Conditioner
ADC	Analog to Digital Converter
LCD	Liquid-Crystal Display
RH	Relative Humidity
PPM	parts per million
PWM	Pulse Width Modulation

LIST OF APPENDICES

- **Appendix A**

CHAPTER 1

INTRODUCTION

1.1   General Introduction

Indoor air quality (IAQ) is an emerging issue of concern that has received a great deal of attention in the past few decades from international scientific communities, governments and the World Health Organization (WHO) (Cincinelli and Martellini, 2017).

WHO has acknowledged that indoor air quality plays a massive role as a health determinant since people in urban areas spend 90% of their time indoors, which is to say 70% in work and 20% in their houses. As such, the WHO published the second edition of air quality guidelines in the year 2006, which includes a chapter that focuses mainly on indoor air quality guidelines and it is standards (Argunhan and Avci, 2018).

In addition to indoor air quality, thermal comfort has to be taken into consideration as well. Thermal comfort is a critical indoor factor that affects human performance (Mendes et al., 2013) .Both indoor air quality and thermal comfort are determined chiefly by room temperature, relative humidity, air movement rate and other related factors as shown in Figure 1.1.

Thermal comfort can be achieved and controlled via heating, cooling, and air conditioning systems. Nonetheless, the mentioned technologies have a leading role in reducing indoor air quality. Therefore, IAQ is closely related to thermal comfort, and a balance between them is needed to achieve an acceptable indoor environmental quality shown in Figure 1.1 (Cheng et al., 2014).

Human indoor comfort depends on four factors, which are indoor air quality, thermal comfort, visual comfort and acoustic comfort (named as Quite in Figure 1.1). but this research's focus is on two of these factors by trying to improve the indoor air quality with a minimum risk of overheating and reduced disruption on occupant's performance.

Figure 1.1: Indoor Environmental Quality (Cheng et al., 2014)

Despite publishing indoor air quality guidelines, the existing air quality parameters are very different from WHO's standard values; thus, researchers and engineers suggested implementing IAQ real-time monitoring systems to decode and analyse human behaviours and environmental factors to improve indoor air quality accordingly. The data gathered from IAQ real-time monitoring systems are used to provide efficient ventilation ways.

1.2   Importance of the Study

Malaysia is known for its hot, humid weather across the whole year, making the usage of air conditioners in this country much more than seasonal countries leading to a higher rate of CO2 emissions and an unfavourable indoor air quality condition most of the time. Based on studies conducted by Daiken, air conditioners have been developed to reduce energy consumption, improve human comfort and reduce global warming (Daikin Global, 2018) .

The development done by Daiken from the year 2007 to the year 2017 on air conditioners has managed to reduce the energy consumption by 10%, dropping from 863kWh to 779 kWh as shown in Figure 1.2. The improvement continues to reduce by a percentage of 10% in energy consumption from 2011 to 2017 as shown in Figure 1.2.

The tests conducted by Daiken were calculated for a Daikin 2.8-kW class air conditioners in Japan, so the consumption in Malaysia is assumed to be far more reaching around 1162 kWh in2009 (Daikin Global, 2018).
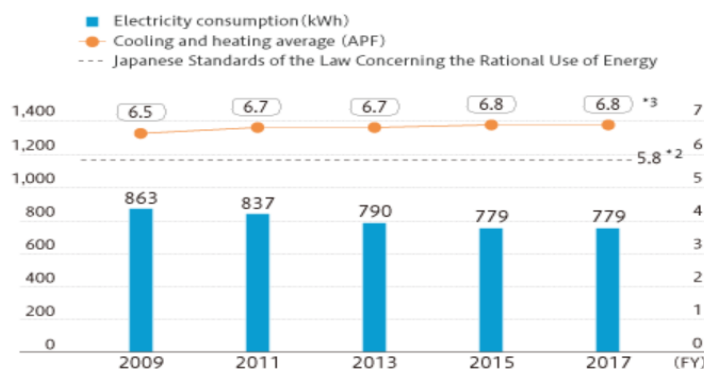
Figure 1.2: Energy consumption from Daiken Air Conditioners in years 2009-2017 (Daikin Global, 2018)

As shown in Figure 1.2, the APF (Annual performance factor), which represents the heating and cooling capacity per kWh over one year of air conditioner usage. The APF is proportional with the energy efficiency so the higher the APF, the greater the air conditioner energy efficiency.

The APF is also inversely proportional to the electricity consumption (kWh) as shown in Figure 1.2; as the electricity consumption reduces from 2009-2017, the APF shows a slight increase yearly. Based on a study conducted in China, APF rating indoors in residential areas in China ranges from 3.4 – 5.4 (Karali et al., 2020) as shown in Figure 1.3, while in Japan, the APF level exceeded six and expected to reach 6.9 by the year 2020.
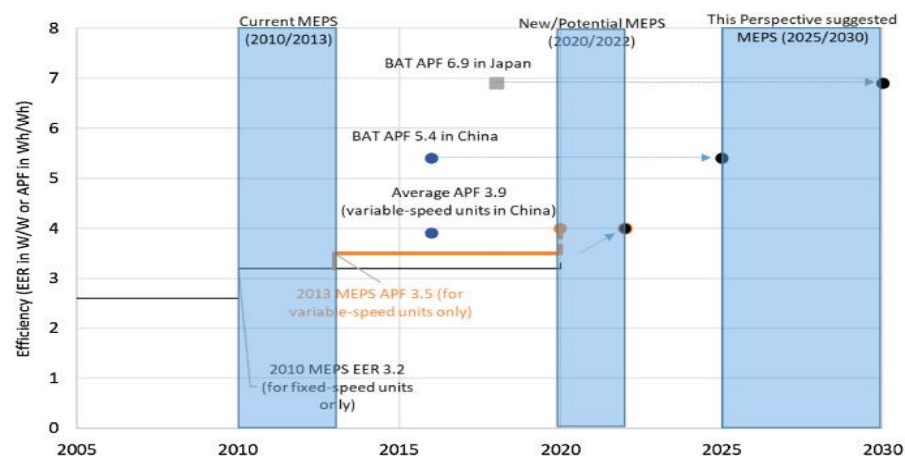
Figure 1.3: Future pathway for APF enhancement (Phadke et al., 2020)

Daiken has stated that the improvement in air conditioners and the energy consumptions reduction have resulted in a noticeable drop of 20% in CO_2 emission over the 10-year gap, which is a considerable improvement in the environment. However, depending on company improvements is not sufficient to improve indoor air quality.

Until today, sick building syndrome has been categorized as a significant occupational hazard and has contributed to a decrease in productivity, especially in countries where air conditioners are used continuously.

In 2011, the yearly energy consumption of air conditioners was recorded to illustrate the primary energy consumption sources as shown in Figure 1.4. The numbers were recorded by distributing surveys among volunteers. The number of volunteers "n" was categorized into two main groups, which are air-conditioner owners and non-air conditioner owners.

The total number of volunteers was 243, with approximately 60% (148 volunteers) of them owning air conditioners who consumed yearly energy of nearly 28GJ/year, whereas non-air conditioner owners consumed only 20GJ/year, which is 30% less (Kubota et al., 2011).
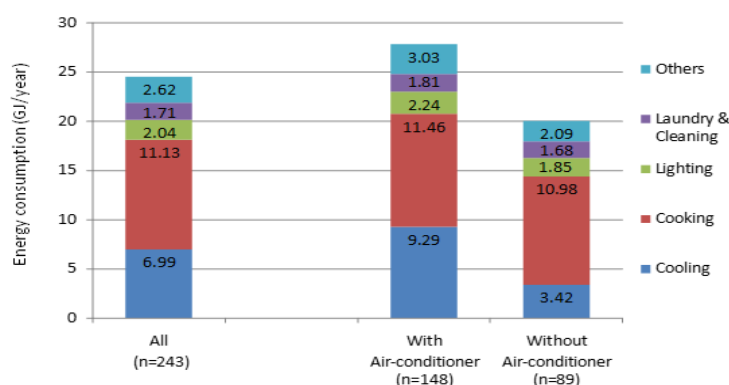
Figure 1.4: Energy consumption in residential houses in the year 2009 in Malaysia (Kubota et al., 2011)

As such, this research will study the idea of programming the fan's motor to run at different speed rates according to environmental factors to help reduce internal heat gain and control common indoor pollutants and reduce the household's yearly energy consumption.

The research will also study the amount of time reduced in terms of air conditioner usage and estimate the extent to which an environmental-based fan system helps improve temperature, humidity, air movement, to assist in expanding the idea of automatically controlled appliances that enhances the hygiene and ventilation of indoor zones.

1.3   Problem Statement

The paper written by (Leung, 2015), stated how building performance and occupant behaviour are affected by climate change. As global warming worsens, human try to cope by prolonging their time indoors and extending their use of air conditioners.

The usage of air conditioners in hot-humid climate areas such as Southeast Asian countries are the highest among all others to cope with the climate condition. As a result, the percentage of air conditioner ownership in Malaysia has reached 65 % in the year 2009, making it the highest yearly energy consumption source (Kubota et al., 2011) as shown in Figure 1.5.

Based on EnerDemand (The Global Efficiency and Demand Database), Air conditioner systems have continued to consume the highest amount of energy with an average daily usage of 6 hours and the numbers continued to increase making Malaysia the fourth highest country in terms of air conditioner energy consumption in the world as shown in Figure 1.5.
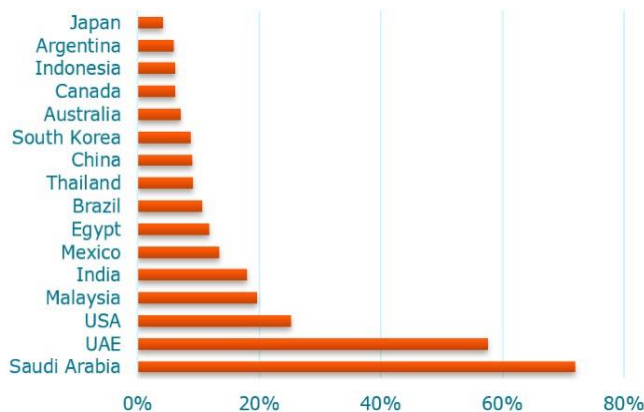
Figure 1.5: Share of air conditioning in household electricity use (based on EnerDemand: The Global Efficiency and Demand Database)

The air-conditioners are the most significant contributor, which record an average electricity consumption of 1.167 kWh yearly and daily consumption of 5.9 kWh as shown in Figure 1.6. Another previous household electricity analysis was done in the year 2017 in 10 different houses to check the average air conditioner energy consumption as shown in Figure 1.7.
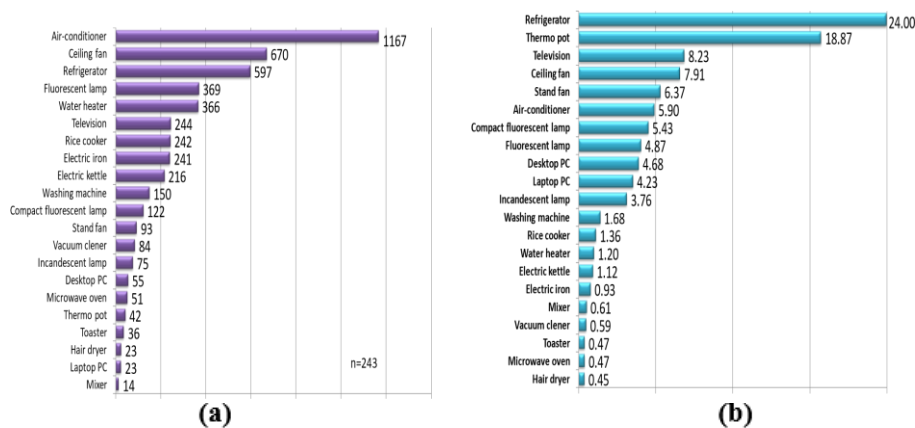
Figure 1.6: (a) Yearly electricity consumption and (b) Daily usage time in 2009 in Malaysia (Kubota et al., 2011)
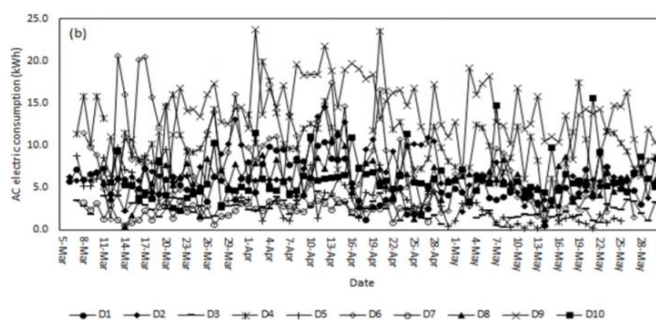
Figure 1.7: Ac electric consumption in 10 different houses over a period of 1 month (Ranjbar et al., 2017)

The studies showed, while some houses only had an electric consumption of less than 5kWh daily, some households reached 23 kWh per day, Which reflected the substantial increase from the year 2009 to 2017 (Ranjbar et al., 2017).

In addition to high energy consumption, the circulation of indoor air by AC systems is a closed loop of heat exchange that circulates indoor air and leads to the increase in gaseous pollution and results to physiological discomforts and allergic symptoms called sick building syndrome. This syndrome is accompanied by symptoms such as headache, skin irritation and breath shortage.

To avoid sick building syndrome, adequate ventilation is necessary through exhaust fans, ceiling fans and open window/doors. Ventilation importance was mentioned in the Energy and Building Journal, stating that the elevation of airspeed can offset the impact of increased room temperature, provide occupant comfort and contribute to a potential saving of cooling energy as recommended in modern standards (ASHRAE 55 2004, ISO 7730 2005 and EN 15251 2007).

The percentage of saving when increasing the air velocity and providing adequate ventilation by using ceiling fans, desk fans, tower fans or standing fans are 17-48 % without the usage of air conditioners and maintaining indoor relative humidity (RH) at a range (20%<RH<60%) (Schiavon and Melikov, 2008).

Thus, based on previous researches, a fan system is the best alternative to improve indoor air quality and provide thermal comfort (Zhai et al., 2015) and therefore, an investigation will be conducted in this research to study whether an environmental fan system that changes its speed according to weather condition can provide an energy-saving alternative to air conditioners while maintaining human comfort and proper air circulation in warm and humid environments.

1.4 Aim and Objectives

This research aims to develop an energy-efficient temperature and humidity-based fan system through a two-week analysis of a residential room's indoor air conditions to achieve a more sanitized, low polluted, and cost-effective alternative to air conditioners.

The objectives of the project are as:

I. Design and simulate an indoor air quality monitoring system.

II. Develop an indoor air quality monitoring system to investigate the acceptable limits of temperature, humidity and air movement that maintain thermal comfort for room occupants.

III. Design an Energy Efficient Temperature and Humidity Based Fan System, where the fan's motor changes according to the acceptable limits set.

1.5   Scope and Limitation of the Study

Most indoor areas in Malaysia are known for their cold and humid climate, where thermal adaptation occurs due to low-temperature exposure for a very long time. In return, a human's ability to tolerate heat will reduce. Extended air conditioner usage will eventually reflect negatively on human health, which can be avoided by minimizing the air conditioner's operating time

In this study, the main focus is to improve indoor air quality and maintain thermal comfort by varying the fan speed according to environmental factors such as humidity, temperature, CO2, and CO levels and analyse how human body temperature will react in different environmental circumstances and will program the fan system according to the most comfortable situation.

The study will also emphasize on the systems benefits in terms of energy efficiency that will later on result lowering the household's costs and indoor air pollution.

As for limitations, thermal comfort levels and indoor air quality will be set by studying human body temperature reaction instead of distributing questionnaires among volunteers to rate their thermal comfort by following a comfort index as previous studies have done and that is due to a restricted movement order that is currently being practised.

1.6   Contribution of the Study

The findings of this study illustrate the effectiveness of environmental fans in terms of improving one's health and providing a more comfortable and sanitized environment. This research also analyzed the resulted reduction in terms of energy consumption and air conditioner activation hours when implementing the environmental fan in a hot and humid country.

CHAPTER 2

LITERATURE REVIEW

2.1 Background

2.1.1 Indoor Air Quality (IAQ)

Indoor air quality is defined by the American Occupational Safety and Health Administration as a description of indoor air condition in terms of many environmental factors, such as temperature, humidity, airflow rate (air ventilation), and pollutant levels.

The indoor air quality has been discussed lately in a more frequent manner as many researchers have linked bad IAQ to multiple chronic diseases due to the inhalation and exposure to many pollutants and particulate matter (PM 2.5) (Chan et al., 2016), while other researches have linked bad IAQ with a range of irritations and cancer-causing effects (Spengler and Sexton, 1983).

In 2015, the United States Environmental Protection Agency announced that indoor air quality had been neglected for a very long time leading to indoor air pollutant levels to reach 2-5 times worse than outdoors (US EPA, 2015).

IAQ is influenced by many factors as shown in Figure 2.1, such as humidity, CO_2, CO, bacteria, viruses, dust, odour and PM2.5, to name a few. Despite all these factors contributing to IAQ condition.

Nonetheless, this research paper will be focusing mainly on the improvement of indoor air factors that can improve with proper air circulation (temperature, humidity, airflow, CO_2 and CO levels) (Schulze et al., 2017).
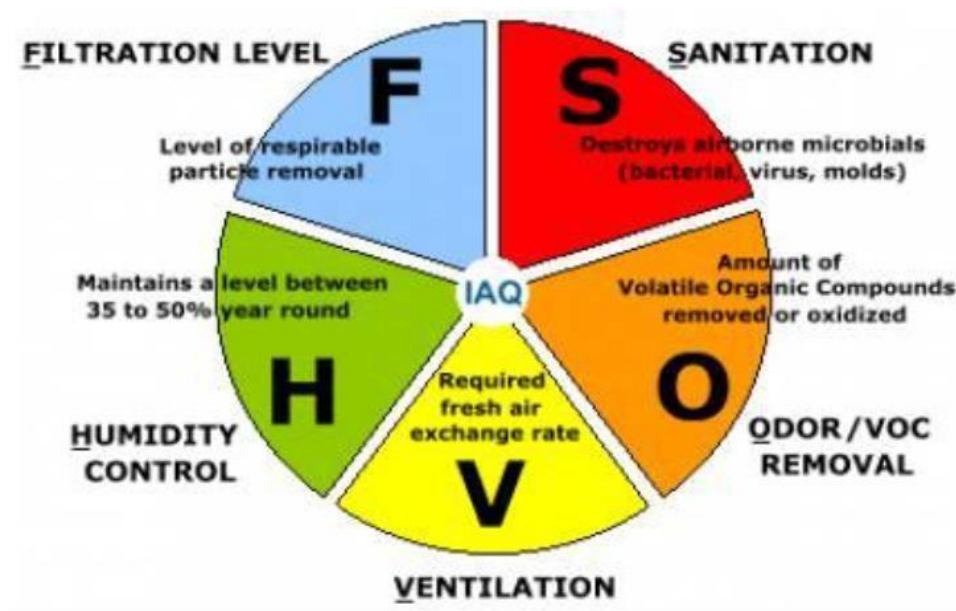
Figure 2.1: Factors influencing the IAQ (Khare and Katiyar, 2001)

Each one of these factors has a negative impact on one's health, while some pollutants show instant symptoms, other may cause damage on the long run as shown in Table 2-1.

Table 2-1: IAQ Pollutants With Their Health Effects (Leung, 2015)

Type of indoor air pollutant	Sources	Health impacts
PM	Cooking stoves; fireplaces; smoking; outdoor air	Respiratory and cardiovascular illnesses
SO_2	Cooking stoves; fireplaces; outdoor air	Impairment of respiratory function
NO_2	Cooking stoves; fireplaces; outdoor air	Irritate the lungs and lower resistance to respiratory infection
CO	Cooking stoves; fireplaces; water heater; outdoor air	Highly toxic and fatal at a conc. 700 ppm
Ozone	Air cleaning device with high voltage; outdoor air	Asthma and allergic triggers
VOCs (such as formaldehyde, turpenes)	Building materials including carpet, plywood (emit formaldehyde); Paint and solvents; Clothing (after dry cleaning) (emits tetrachloroethylene, or other dry cleaning fluids); air fresheners, incense, other scented items; certain plants (emit turpenes)	Some are carcinogenic; can also trigger the formation of photochemical oxidants, such as peroxyacyl nitrates (PAN) and aldehydes, which cause eye irritation
Radon	Exuded from earth and rocks such as granite and gneiss in certain locations with low ventilated air and trapped inside houses	Radioactive; leading cause of lung cancer in non-smokers
Biological air pollutants (gasses and airborne particulates)	Pets (dander), human (dust from minute skin flakes and decomposed hair), dust mites (enzymes and μm-sized fecal droppings), inhabitants (methane), wall and air-duct (mold)	Increase risk for people with breathing problems, such as asthma sufferers, and with compromised or underdeveloped immune systems

Based on the pollutant sources mentioned in Table 2.1, the possibility of improving IAQ by removing pollutant sources is extremely low as some of these sources are important to human's everyday (Leung, 2015), therefore researchers seek to find substitute methods to enhance IAQ without causing thermal discomfort or disturbance in occupants daily activities.

2.1.2 Brief History on Indoor Air Quality Awareness and Improvement

Air pollution is a phenomenon that existed way longer than some may assume, going back to the Greeks and Romans' time. The Greeks and Romans were aware that crowded cities and mines caused stuffiness and understood the adverse effects that were associated with polluted air despite lacking complete knowledge of how the lungs work and how breathing is achieved scientifically through the respiratory system (Boschi, 1999).

Leaping forward through history in December 1952 where the worst air pollution disaster in history occurred in London due to combustion products being trapped at ground level as a result of adverse weather conditions (Kelly and Fussell, 2015).

That crisis resulted in a death toll that ranged from 4000-12,000 and led to the direct incentive to pass the Clean Air Act in 1956, which was considered as a milestone in environmental protection by historians (Kelly and Fussell, 2015).

After several other epidemic outbreaks occurred at the beginning and mid of the 19th century, the importance of air quality improvement and providing a hygienic environment was recognized by governments, researchers and engineers. That started the idea to regulate indoor temperature by using different air pressures and circulating the airflow in a manner that provides a healthy and sanitarian environment (Van Der Tempel et al., 2011).

More improvements were made after C. P. Yaglou completed his research in early 20th century, which included indoor airflow limits that achieve thermal comfort to occupants. That research served as a basis for ventilation standards until the year 1990 (Van Der Tempel et al., 2011).

Natural ventilation was also studied after realizing that by opening and closing windows, a flow rate is induced and thus improving the air quality.

Nevertheless, that depended on several factors such as the temperature between indoor and outdoor, weather condition and wind speed rate, which is why natural ventilation alone cannot provide the necessary air quality improvement

In 1939, history witnessed the first prototype of an air conditioner. Packard Motor Company was the first company to sell air-conditioner that provided cooling the summer and heating in the winter (Shah, 2009).

Air-conditioner function involves taking the air from the room to heat and cool it and then recycling the air back to the room (Shah, 2009).
The air conditioner invention led to the reduction of air quality as it is accompanied by many drawbacks such as the increase in CO_2 level along with other gaseous pollutants such as CO, SO_2, NOX, O_3, radon, and VOCs.

These chemical materials cause harm to the human's health, especially VOC's as it causes many instant symptoms such as headache, eye, nose, throat irritations, coughs, dizziness, and nausea (Yu et al., 2009). Based on the drawbacks mentioned above, the air conditioner cannot replace a ventilation system, despite many may assume so. However, most rooms are currently only equipped with air conditioners and ceiling fans with no exhaustion fans or ventilation systems.

Another issue is that most residential apartments and offices are built in a sealed indoor environmental manner, where isolation is achieved between indoor areas and natural outdoor environments (Boddy and Krigger, 2001).

To avoid Sick Building Syndrome, WHO has listed down the procedures that must be achieved to maintain a good IQA, for instance, undergoing air conditioner maintenance every six months and conducting an audit every two years to ensure indoor air quality is acceptable and conforms to the specifications.

Even so, the WHO guidelines and requirements can only be implemented in office, companies, and entertainment centres but residential areas may not conduct the policies due to a busy schedule or for the sake of cutting costs. Subsequently, the air conditioner invention has reduced indoor air quality instead of improving it. The reliance on air conditioners due to Global warming has increased substantially in recent years, making removing air conditioners from human lives impossible.

Therefore, a balance between fans, air conditioners, and natural ventilation has to be achieved to provide thermal comfort and a good IQA for humans in all environments.

2.1.3   Factors of Thermal Comfort

Based on a research conducted in the technical university in Denmark, temperature and humidity showed a strong influence on the perception of indoor air quality. By controlling those two factors in coordination with each other a good IQA and thermal comfort were achieved (Fang, 1998).

The results were obtained by conducting tests at three levels of temperature (18 °C, 23 °C, 28 °C) and three levels of humidity (30 %, 50 % , and 70 %) according and by using ventilation and air conditioners in a manner that avoids a high pollution level (Fang, 1998).

In 2018, a similar research was conducted to achieve thermal comfort and a good IQA taking into consideration six factors instead of only two, which are relative humidity, air flow rate, air temperature, activity level, clothing insulation and radiant temperature (ÖZDAMAR and UMAROĞULLAR, 2018).

These factors are used to calculate the Predicted Mean Vote (PMV), which is a model stands among the most recognized thermal comfort models as shown in Figure 2.2. The method of calculating the PMV (Predicted Mean Vote) is called Fanger's method (Chaudhuri et al., 2016).
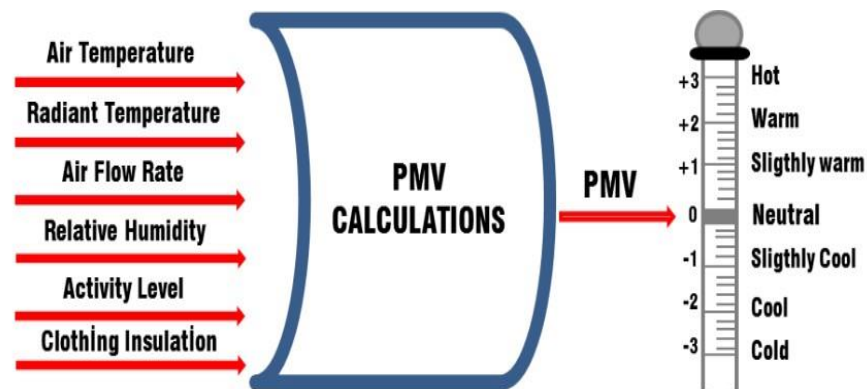
Figure 2.2: Fanger's method illustration (ÖZDAMAR and UMAROĞULLAR, 2018)

The PMV index is:

$$\text{PMV} = (0.303e^{-0.036}M + 0.028) \times L \tag{2.1}$$

Where: M = metabolic rate   L = thermal load

And this can be calculated manually or by using a PMV online calculator, that will later categorize thermal comfort sensation from +3 (Hot) to -3 (cold) or just categorized as acceptable or not depending on the objective of the research or the setting of the online calculator chosen.

The PMV model is widely used and is validated by the American professional association of heating, ventilation, air conditioning and refrigeration systems (ASHRAE) and the European standard for indoor environmental parameters (EN-16798), incorporating it as a method to indicate and calculate the thermal comfort in buildings (Ihtsham et al., 2015).

Another research conducted in 2001 by De Dear named as "The adaptive model of thermal comfort and energy conservation in the built environment" have also concluded that the PMV model is acceptable for thermal comfort prediction.

PMV model was also used in a Malaysian research to evaluate the thermal comfort named as "A case study of the Climate Factor on Thermal Comfort for Hostel Occupants in Universiti Sains Malaysia" published in 2011. The study relied its thermal comfort level based on the PMV model (Wafi et al., 2011). In addition to PMV, another index was also mentioned in all the previous research, which is the PPD (Predicted Percentage of Dissatisfied) that quantifies the number of dissatisfied people with the given thermal environment (in percentage).

The PPD is reliant on the PMV calculated (Carlos and Da Silva, n.d.) through the following equation:

$$PPD = 100 - (95. e^{-(0.03353.PMV^4+0.2179.PMV^2)})$$ (2.2)

A curve was shown in Fanger's studies that illustrated the PMV and PPD variations and its relation to each other similar to an inverted Gaussian distribution (Carlos and Da Silva, n.d.) as Shown in Figure 2.3.
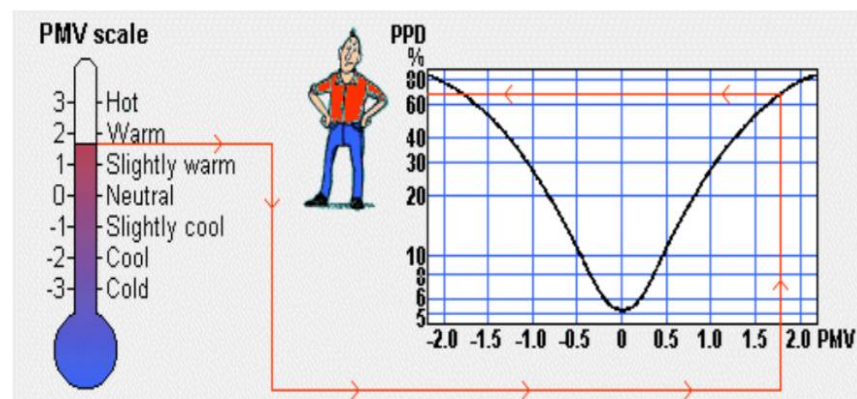
Figure 2.3: PMV And PPD Index (Carlos and Da Silva, n.d.)

Thermal comfort zones are defined in three classes named A, B and C classes, where there PMV values range from -0.2 to 0.2; -0.5 to 0.5 and -0.7 to 0.7 respectively and there PPD values are below 6%, 10% and 15% and the class selection depends on the standard followed in the chosen country of research (Carlos and Da Silva, n.d.).

In order to comply with ASHRAE 55, the thermal limit is the point scale of PMV between -0.5 and 0.5, whereas the EN-16798 follows a scale between -0.7 and +0.7 as a representation of a comfortable thermal condition for building occupants (Carlos and Da Silva, n.d.) .

During this research, the main concern is checking the room thermal condition compatibility to ASHRAE Standard 55-2017 and EN-16798 by calculating the PMV, however the PPD will also be looked over to ensure the satisfaction of the occupants.

2.2   Research Conducted to Build Thermal Control and Improve IAQ Systems

2.2.1   Introduction

This section will focus on studying and analyzing previous research conducted to improve thermal control and indoor air quality in controllable factors such as temperature, humidity, and airflow. Studies that examine uncontrollable factors such as the number of people in the room, clothing insulation, and ambient temperature will not be taken into consideration

2.2.2   Air Quality Monitoring Systems

Previous research papers that emphasize on indoor air quality, started by monitoring the present air quality in order to assess the situation, for example a study conducted in 2016, where an IAQ monitoring system was designed to detect one variable (temperature) across different periods and the outcome was displayed on an LCD (Liquid Crystal Display) reflecting the air quality status (shown in Figure 2.4) (Ehiagwina and Onawola, 2016).

 The system received an input from a temperature sensor in the form of an analog signal. The signal was later converted to a digital signal through an ADC (analog to digital converter) and is sent to the microcontroller to perform calculations/operations and finally display the outcome on the LCD.
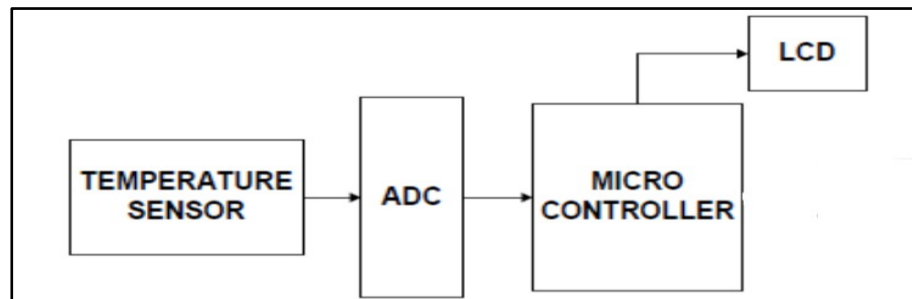
Figure 2.4: Temperature monitoring system hardware architecture (Ehiagwina and Onawola, 2016)

Figure 2.5 shows a more improved indoor air quality monitoring framework where the connection between the system units is wireless. This system consists of an additional section called the data server and access point, which is used to provide internet connection (Li et al., 2014).

To sum up, air quality improvement and thermal comfort can only be achieved when the present environmental status is known, therefore, the first objective in this research was set to design an air quality monitoring system to monitor the present environmental status and investigate the acceptable limits of temperature, humidity and air movement that maintain thermal comfort for room occupants.
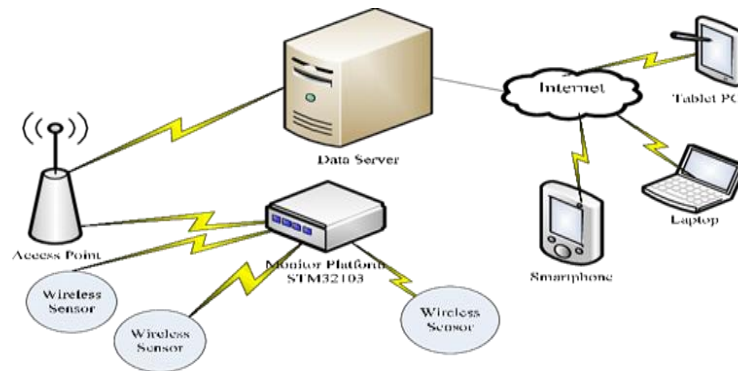
Figure 2.5: The framework for the overall design of the air quality monitoring system (Li et al., 2014)

2.2.3   Previous Thermal Comfort Research in Residential Areas

Thermal comfort has been studied for several years to help reduce the air-conditioner's electricity usage while maintaining thermal satisfaction.

A previous research studied thermal comfort residential buildings in four different adaptive strategies (AC- cooling on, Heating on, Fan on and Door/window open) in a four-season country (Sydney, Australia), where the temperature fluctuates between 5°C to 40°C (Kim et al.. 2017).

Figure 2.6 illustrates the likelihood of activation with the increase of temperature at different behaviours individually, while figure 2.7 shows all the different behaviour outcome in one plot for comparison.

The first behaviour was AC-Cooling on (A), representing the probability of Air-conditioner activation in response to an increase in temperature (shown in Figure 2.6). The likelihood of Air conditioner activation started to increase gradually starting from 30°C and reaching its peak (80%) at 40°C.

The second behaviour (B) was open/close windows, where the curve showed more than 50 % of the participants are expected to open doors and windows at a temperature ranging from 20°C to 32 °C. The curve's peak is around 25 °C at a percentage of 68 % of participants.

The third behaviour was the Fan on (C). The study conducted showed that fan usage was consistently below 40 % across the entire temperature range, which is considered low when compared to the AC on percentage.

The final behaviour involved heater usage which will not be discussed as heater refers to the heating system that increases room temperature in winter. So based on this research, a high rate of air conditioner usage was recorded, followed a low rate of fan system usage at the same temperature, which resulted in a higher electricity usage and a higher electricity bill.
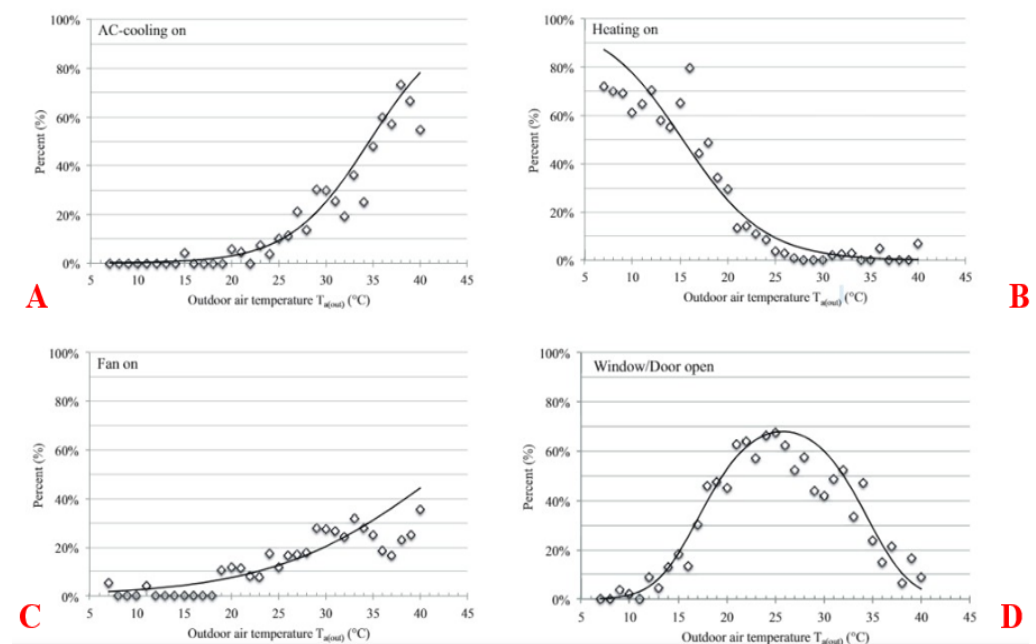
Figure 2.6: The percentage of different adaptive strategies as a function of outdoor air temperature (Separated) (Kim et al., 2017)

Figure 2.7 illustrates the percentage of different adaptive strategies a function of outdoor air temperature, which in short are the same results shown in Figure 2.6, however combined together, making it easier for comparison.
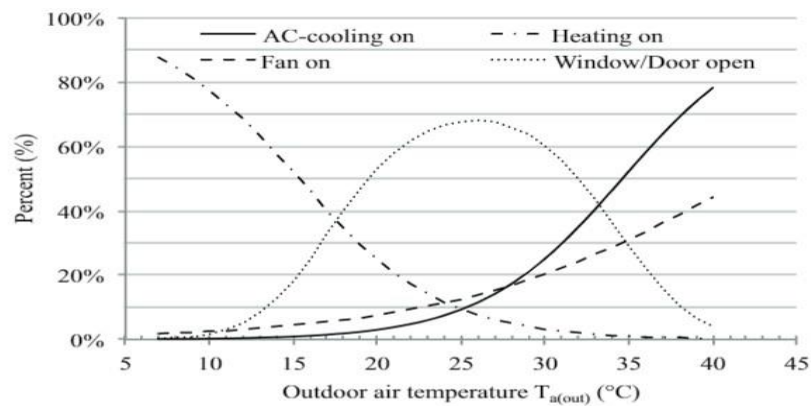
Figure 2.7: The percentage of different adaptive strategies a function of outdoor air temperature (Combined) (Kim et al., 2017)

To provide thermal comfort an assumption will be made based on this research that 80 % of humans tend to activate air conditioners when temperatures are above 35°C as well as low fan system usage at temperatures above 35 °C. Ventilation was achieved by opening windows and doors, yet the rate of opening doors windows decreased substantially with the increase of temperature. Those assumptions will help find a balance to improve air quality with thermal comfort at a minimal amount of energy.

2.2.4 Previous IAQ Improvement Systems Designed

Figure 2.8 shows the architecture of the wireless sensing and control system design. The system was connected to ARIMA forecast software to collect the air quality for comparison (Yu and Lin, 2015).

The gathered data from ARIMA forecast software was compared with the input data coming from the temperature, humidity and air quality sensors and analysed the environmental conditions.
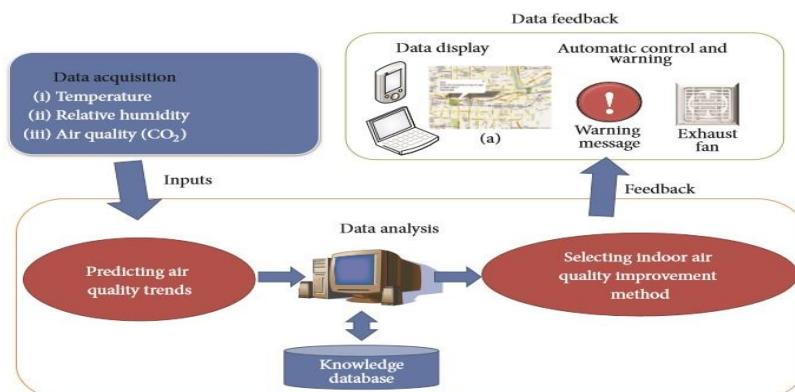
Figure 2.8: Control system flow chart (Yu and Lin, 2015)

The computation, calculation and prediction is done by the micro-controller (Yu and Lin, 2015). The research assumed a hardware schematic and circuit structure and was simulated online. Thus, the connection is between the simulation model and Arima forecast with no real data.

A similar research was conducted in India in the year 2017 (Sipani et al., 2017) and another conducted Nigeria (Purnomo et al., 2016). Both depended on temperature and humidity factors to control the motor in a fan system to provide better IAQ. Both studies involved circuit schematic and designs by using the same humidity sensor called DHT11 and temperature sensor called LM35.

Despite completing the design and successfully running the system, nevertheless, no sign of indoor air quality and humidity improvement analysis and the results only shows a successful coordination of motor speed with the change of temperature.

In 2016, a research was conducted in Siberia by 4 engineers to build a system that can provide thermal comfort along with air quality improvement in classrooms by controlling the class windows automatically based on the indoor and outdoor temperature, mean radiant temperature, airspeed and CO_2 level (Stazi et al., 2017).

The procedure was done by collecting data using temperature, air speed and CO_2 detection sensors and the data collected were used as limits to control the window (Stazi et al., 2017).

The signals obtained from the sensors are sent to the data logger (Datataker DT500), which stores the data and later on transmits the data to the controlling software (LabVIEW 2014).

The control method applied to the controller depends on comparing the actual environmental data with the data limits and would act according to the difference between the two data as shown in Figure 2.9.
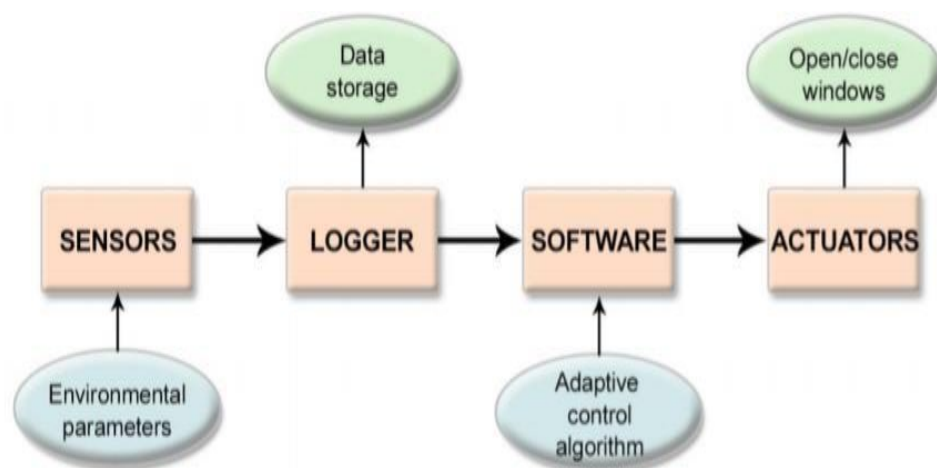
Figure 2.9: Hardware architecture of IAQ and thermal comfort automatic system for open/close window condition (Stazi et al., 2017)

The research showed that classrooms are mostly stuffy when the outdoor temperature is above 22°C and the operative temperature is above 24 °C and are less stuffy when the temperature in winter when the outdoor temperature is below 6 °C and below 16 °C for operating temperature.

Those limits set the windows to open/ close at different proportions to provide thermal comfort for students. Based on the above research, the outdoor/operating temperatures are considered to be the most driving factors for indoor air quality improvement when compared to CO_2 concentration and Airflow rate.

However, CO_2 concentration and airflow rate have to be measured constantly when designing the system to ensure proper good air quality and proper ventilation as shown in Figure 2.10.
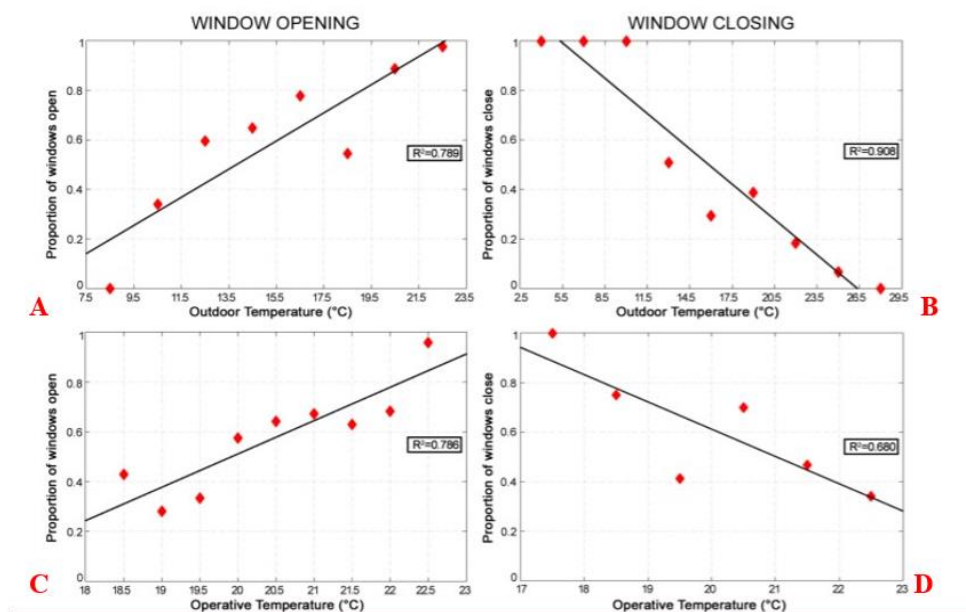
Figure 2.10: Linear regression analysis (Stazi et al., 2017)

The Y-axis in Figure 2.10 represents the amount of open/close window, in other words when the proportion is 0.2 in open window condition (A and C) means that 20 % of the window is open. The same goes for close window condition, where a proportion of 0.2 means the window is 20% closed (B and D).

The research clearly shows the likelihood of the windows being fully open is under conditions where the outdoor temperature is higher than 23C as the rooms tend to get stuffier, while the possibility of the windows closing gets higher the more the outdoor temperature goes below 20C.

Although the research has provided good room ventilation but based on studies done in the 19th century (Van Der Tempel et al., 2011) (mentioned in section 2.1.2), natural ventilation will not be able to provide adequate indoor air quality alone and thus an additional tool is needed.

A research conducted in 2015 argues that celling fans can provide human comfort in a warm and humid environment by conducting tests in a climate chamber set at three different temperature values (26°C, 28°C and 30°C) and two relative humidity rates (RH 60% and 80%) with sixteen subjects (both males and females) and were exposed to 7 levels of air speed ranging from 0.05 m/s to 1.8 m/s (Zhai et al., 2015).

The subjects were asked to describe their thermal sensation, comfort, eye dryness and air movement acceptability for 2 hours and 15 minutes while changing the ceiling fans speed.

Fan speed levels	off	1	2	3	4	5	6
Fan 1 mean (m/s)	0.05	0.30	0.68	0.86	1.20	1.65	1.82
Fan 2 mean (m/s)	0.05	0.33	0.75	0.83	1.24	1.57	1.78
Nominal air speeds (m/s)	0.05	0.30	0.70	0.85	1.20	1.60	1.80

Figure 2.11: Fan speed test conditions (Zhai et al., 2015)

Test conditions	T (°C) and RH (%)	ET (°C)	Air speeds (m/s)						
			<0.1	0.30	0.70	0.85	1.20	1.60	1.80
1	26, 60	26.3	•	•	•	•			
2	26, 80	27.0	•	•	•	•			
3	28, 60	28.5	•		•	•	•		
4	28, 80	29.7	•			•	•	•	
5	30, 60	30.7	•			•	•	•	
6	30, 80	32.6	•				•	•	•

Figure 2.12: Temperature and humidity test condition (Zhai et al., 2015)

The first condition was when the fan was turned off, where the percentage of participants requesting for a cooler environment was only 25% at 26°C. That percentage increased to 100 % when the temperature was set at 30 °C. The rest of the tests were done by adjusting the fan at different speed rates. Most subjects were fine as the temperature elevated with the air movement until condition 6 (30 °C and a relative humidity of 80 %), where subjects felt uncomfortable even when the air movement even at air speed of 1.8 m/s (Zhai et al., 2015).

As a result, ceiling fans are considered to be effective at most times except when the humidity exceeds 80 % with a temperature above 30°C so celling fans can be used for IAQ improvement and thermal comfort under certain temperature and humidity levels.

Based on the research conducted over the years, a temperature and humidity-based system for indoor air quality improvement and thermal comfort is in need to provide a comfortable, hygienic and sanitary environment and reduce the reliance on air conditioner.

The system must achieve a balance between the usage of celling fan and air conditioner with constant monitoring of CO_2 and CO percentage and air flow rate to ensure good room ventilation and pollutant control.

2.3 Indoor Air Quality and Thermal Comfort Analysis in Malaysia

2.3.1 Indoor Air Quality in Malaysia

The indoor air quality assessment is needed to gauge the level of pollutants that are generated by indoor and outdoor resources, such as air conditioners, pest control, housekeeping, renovations and other building occupant activities. The Industry Code of Practice (ICOP) on Indoor Air Quality has mentioned the recommended indoor air conditions as shown in Table 2.2.

Table 2-2: ICOP Indoor Air Contaminants and Their Acceptable Limits

Indoor Air Contaminants	Acceptable limits		
	ppm	mg/m³	cfu/m³
Chemical contaminants			
(a) Carbon monoxide	10	-	-
(b) Formaldehyde	0.1	-	-
(c) Ozone	0.05	-	-
(d) Respirable particulates	-	0.15	-
(e) Total volatile organic compounds (TVOC)	3	-	-
Biological contaminants			
(a) Total bacterial counts	-	-	500*
(b) Total fungal counts	-	-	1000*
Ventilation performance indicator			
(a) Carbon dioxide	C1000	-	-

Previous research has emphasized on CO2 concentration as well, recommending a concentration of not more than 800 ppm rate for an occupied room with good air exchange and highlighting that a CO2 of 1000 ppm may lead to drowsiness and poor air quality (Raza et al., 2017).

Table 2-3: Indoor Air Quality Classification (Raza et al., 2017)

Order order	Parameter	Unit	Excellent class	Good class	Limit for IAQ
1	Air temperature	°C	20 to <25.5	<25.5	22.5-25.5
2	Airborne bacteria	cfu/m³	<500	<1000	500
3	Relative humidity	%	40 to <70	<70	<−70
4	Respirable suspended particles (PM$_{10}$)	μg/m³	<20	<180	150
5	Carbon dioxide	ppmv	<800	<1000	1000
6	Carbon monoxide	ppmv	<1.7	<8.7	9
7	Formaldehyde	ppbv	<24	<81	100
8	Toluene	ppbv		290	
9	Xylene	ppbv		333	
10	Benzene	ppbv		5	

Table 2-4: Indoor Air Parameter's Acceptable Limits Used in This Research

Parameter	Acceptable Limit
CO2 concentration (ppm)	**<800**
CO concentration (ppm)	**< 8.7**

2.3.2 Thermal Comfort in Malaysia

Thermal comfort in residential buildings in Malaysia was analysed in the year 2015, by taking an example of a house demo in both Kuala Lumpur and Kuching as shown in Figure 2.13 (Jamaludin et al., 2015), however only the data obtained in Kuala Lumpur will be used. since this research is done in Kuala Lumpur district.
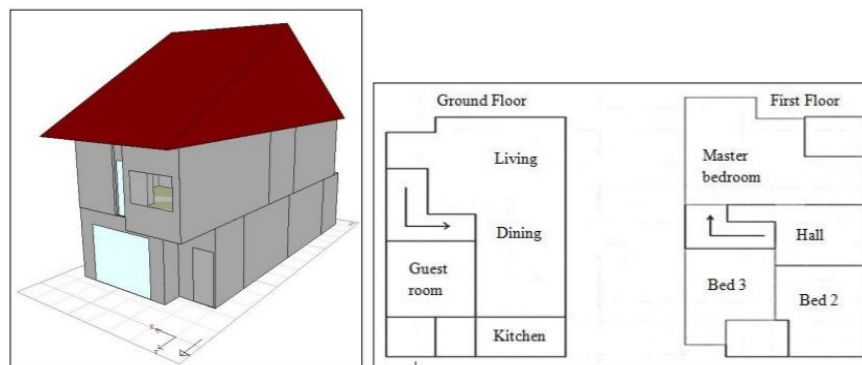
Figure 2.13: House indoor and outdoor plan (Jamaludin et al., 2015)

Table 2-5: Zone properties of the simulated residential building model (Jamaludin et al., 2015)

Zone properties	Description
The type of active or passive system used	Natural ventilation
Comfort band (environmental temperature range for comfort system):	(recommended by MS1525:2007)
Lower band	23°C
Upper band	26°C
The occupants' metabolic rate	Sedentary activity: 70W (5 persons)
The occupants' clo value (thermal insulation of clothing)	1.0

The research analysed the temperatures indoors at different hours of the day in all house rooms, showing that the highest room temperature was recorded in the Master Bedroom, followed by the dining/living room and the kitchen. The highest room temperature in Kuala Lumper was recorded at a value of 32.5°C at 2pm in the Master bedroom, while the Dining/living room recorded a value of 32.4°C.

The graph shown as shown in Figure 2.14 also illustrates that the temperature between 1pm – 7pm fluctuates between 31°C and 32.5 °C in all the rooms, resulting in the most uncomfortable time in terms of thermal comfort (Jamaludin et al., 2015).
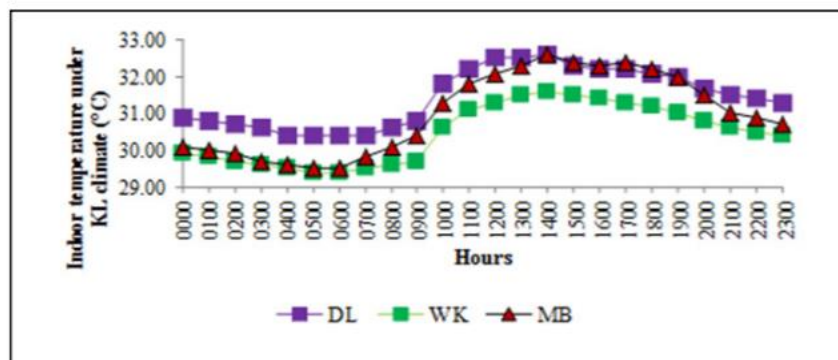
Figure 2.14: Indoor temperature across the day in DL (Dinning/Living). WK (Kitchen) And MB (Master Bedroom) (Jamaludin et al., 2015)

This research was linked to another research conducted in 2009 in Malaysia that showed the energy consumption in the Master bedroom recorded the highest monthly in terms of air conditioner usage frequency (98%) (shown in Figure 2.15), while other bedrooms recorded only 50%, making the Master bedroom the main location for this research (Kubota et al., 2011).
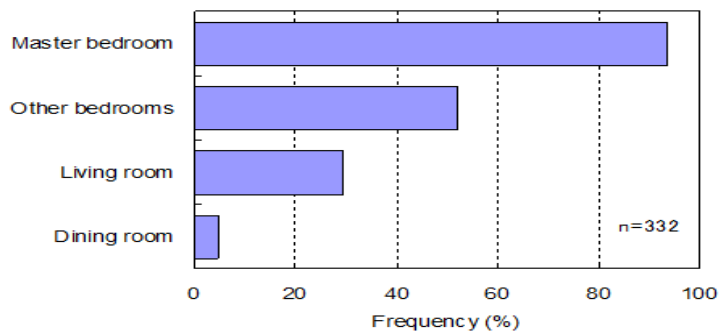
Figure 2.15: Air conditioner usage frequency based on the rooms in which air-conditioners are installed (Kubota et al., 2011)

2.4 Fan System as An Energy Efficient Alternative to Air Conditioners

Air conditioners are known to pose a threat to the environment and a huge contributor in the decrement of indoor air quality, yet in addition to environmental threats and occupant's health, its energy consumption is ranked one of the highest in every household.

Alternative concepts of cooling were suggested by previous research to improve the indoor environment in addition to the reduction of energy consumption such as increasing fan usage instead of total reliance on air conditioners.

2.4.1   Fans Energy Saving Possibility

In 1996, The ACEEE (The American Council for an Energy-Efficient Economy) summer study on energy efficiency in buildings discussed thoroughly whether or not the usage of fans contributes to energy savings. The study was later published under the name "Are Energy Savings Due to Ceiling Fans Just Hot Air?"(James et al., 1996)

The simulation and measurements were done in three cities in the United States of America – Jacksonville, Orlando, and Miami by measuring the energy-saving percentage when using ceiling fan alone with no air conditioner.

The base run was setting the thermostat at 78°F (25°C) without opening ceiling fans, followed by another test that involved the activation of a ceiling fan without the change of the thermostat setting.

The difference between the first experiment and the second led to an increase of 10.5% average cooling energy in all three cities (shown in Table 2.7). The following experiments involved a gradual increase in the thermostat setting by a set rate of 0.5 °F point in each consecutive experiment.

The tests led with positive results as the cooling energy saving recorded 2.6 % when the thermostat is set at 79°F and saving of 14.9% at 80°F. The maximum savings difference between the three cities at any thermostat set point simulated was approximately 18% (James et al., 1996).

Table 2-6: Simulation Seasonal Energy Savings By Thermostat Temperature (James et al., 1996)

T-state °F (Fan Status)	Jacksonville		Orlando		Miami	
	Energy Use (KWh)	% Savings	Energy Use (KWh)	% Savings	Energy Use (KWh)	% Savings
78 (w/o fans)	2772	Base	4030	Base	5670	Base
78 (w/ fans)	3091	− 11.5	4443	− 10.2	6230	− 9.9
78.5 (w/ fans)	2891	− .3	4180	− 3.7	5871	− 3.6
79 (w/ fans)	2700	2.6	3927	2.6	5520	2.6
80 (w/ fans)	2338	15.7	3448	14.4	4840	14.6

The study concluded that many occupants are unaware of the amount of saving's that can be achieved by using fans instead of air conditioner, while other claim that despite using ceiling fans, no energy saving was noticeable. The reason behind that is most occupants leave fans open when rooms are unoccupied and 33 % of respondents admit of leaving the fan open 24 hours (James et al., 1996).

Another reason returns to the fact that thermal comfort studies done with varying wind speeds, humidity levels, and temperatures are limited and extrapolations may not be accurate, claiming that fans have great savings potential and further studies are needed to achieve maximum energy saving (James et al., 1996).

The study focused on ceiling fans, but other fans can provide the same energy saving potential when referring to their wattage ratings.

2.5 **Fan Design Used in The Research**

Since all the fans can provide energy saving when being compared to air conditioners, the type of fans will be decided based on its thermal comfortability to occupants. The comparison will be based on previous research.

2.5.1 **Ceiling Fan's Thermal Comfort Analysis**

A research was conducted in California in a classroom by placing two fans and removing the air conditioner. The test was conducted by varying the speed and room temperature and checking the thermal comfortability by distributing a survey for occupants to rate their thermal comfortability. The speed of the fan ranged from 0.3m/s to 1.8m/s at room temperature that varied between 26 °C to 33°C (Arens et al., 2013).
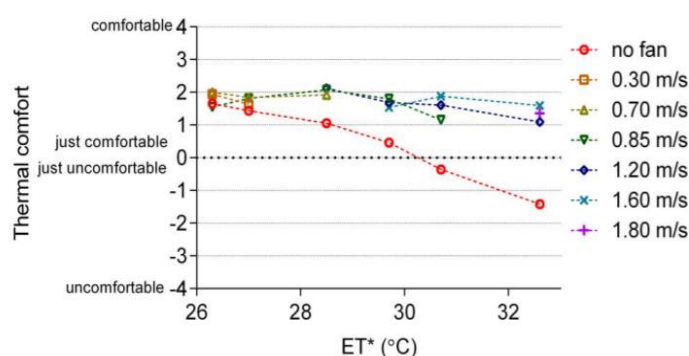
Figure 2.16: Thermal Comfort Rate Vs Room Temperature By Varying Fan Speed (Arens et al., 2013)

Table 2-7: Thermal Comfort Index Description (Polese et al., 2014)

Index	Thermal comfort	Hypothetical activity
4	very comfortable	People enjoy their circumstances
2	comfortable	Normal situation in massive houses
+0	just comfortable	Normal situation in light houses
-0	just uncomfortable	People feel a little bit uncomfortable
-2	uncomfortable	People start to look for help
-4	very uncomfortable	Lethal circumstances

From Figure 2.16, the most uncomfortable condition was rated when no fan was activated at temperatures above 29°C. The research also mentioned that only speed values of 0.85 m/s, 1.2m/s, 1.6 m/s and 1.8m/s showed cool thermal sensation at temperatures above 28°C, while the rest of the speed values showed no significant difference and all occupants felt uncomfortable at high temperatures (Arens et al., 2013).

At the highest temperature (33°C), occupants feel a comfortability of 1-2 when the speed fan is higher than 1.2 m/s, which is a motor speed when adjusted at approximately 70% of the duty cycle. As for temperatures below 29°C a speed higher than 0.7 m/s gives a comfortability of 2, which is approximately 50% duty cycle of the motor's speed.

As for freshness and air quality rating, a survey was also distributed to rate the freshness from 4 to -4, where 4 represents "extremely fresh" and -4 represents "stuffy" (shown in Figure 2.17) (Arens et al., 2013).

Since air quality was not the main focus in this research, so only surveys were conducted to rate the perceived air quality without using a sensor to measure the pollutant rate. The perceived air quality survey also gave a rating choice that ranges from -4 to 4, where 4 represents "very acceptable" and -4 represents "very unacceptable" (shown in Figure 2.18) (Arens et al., 2013).
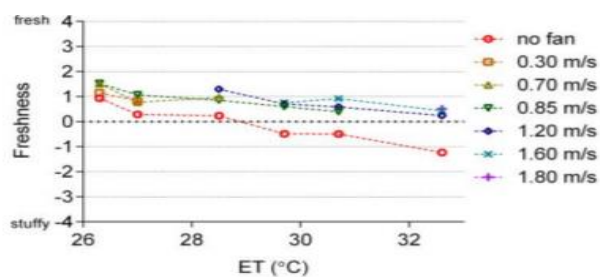
Figure 2.17:Freshness Vs Room Temperature at different fan speed (Arens et al., 2013)
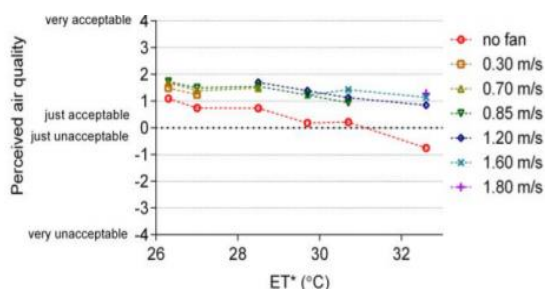
Figure 2.18: Perceived Air Quality Vs Room Temperature by varying fan speed (Arens et al., 2013)

The freshness and perceived air quality were ranked similar to the thermal comfortability, where occupants felt most uncomfortable when no fan was open and felt most comfortable at fan speeds higher than 1.2 m/s as the temperature approaches 29°C.

2.5.2 Standing Fan's Thermal Comfort Analysis

A pervious conducted a research by using an energy efficient standing fan to analyse the thermal comfort of occupants in the classroom. The fan has 3 levels of speed named as "High", "Medium" and "Low" each placed 3 meters from one another and are placed 1.5 meters away from the occupant as shown in Figure 2.19. (Mun et al., 2019).
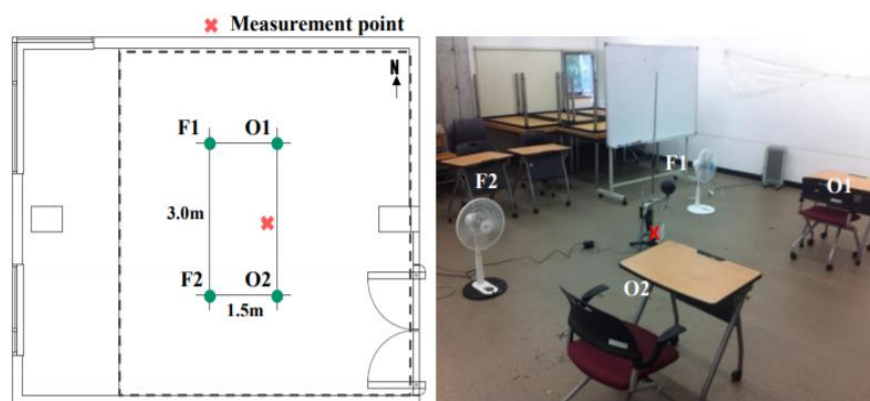
Figure 2.19: Placement of fans (Mun et al., 2019)
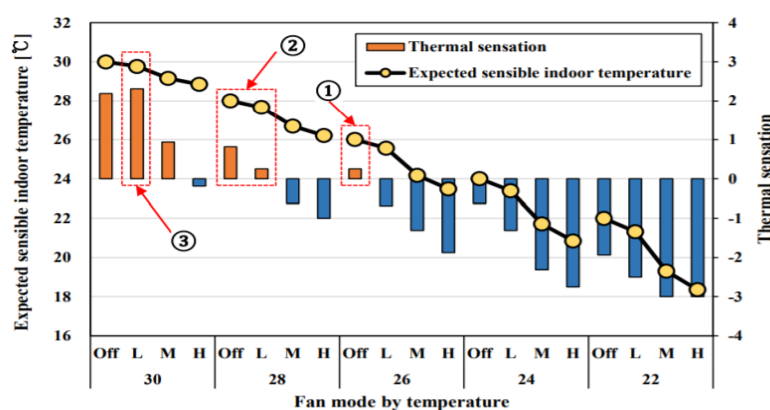
Figure 2.20: Thermal Sensation Rate Vs Room Temperature by varying fan speed (Mun et al., 2019)

In Figure 2.20, the dotted line is the indoor temperature, and the orange bar represents when the thermal sensation is above 0, while the blue bar represents when thermal sensation is below 0. As for the thermal sensation index is ranked opposite of thermal comfort, where values below 0 represents a cooler sensation and the values above 0 represents a hotter sensation as shown in Table 2.10.

Table 2-8: Thermal Sensation Index (Mun et al., 2019)

Thermal sensation	vote
+3	Hot
+2	Warm
+1	Slightly warm
0	Neutral
-1	Slightly cool
-2	Cool
-3	Cold

The research ranked the most uncomfortable situation was under conditions indoor temperature = 30°C and the fan is set as "High" (circled as condition 3), while the second most uncomfortable condition is an indoor temperature of 28°C with the fan set as "High" or "OFF" (circled as condition 2) and the least uncomfortable situation was when the temperature is adjusted at 26°C and a fan is "OFF" (circled as condition 1) (Mun et al., 2019).

The rest of the conditions shows a thermal sensation ranging from -1 (slightly cool) to 3 (cold). Still, the relative humidity was not measured, which may explain why comfortability decreased substantially when the temperature reached 30°C (Mun et al., 2019). To conclude, the standing fan can provide an acceptable thermal comfort but at a rate less than ceiling fans.

2.5.3　　　　Table Fan's Thermal Comfort Analysis

The research was conducted in China in a university by placing desk fans at reading tables, while increasing its speed under different temperature conditions. The test evaluated both the thermal sensation (following Table 11) and thermal comfort (following table 2.10) (He et al., 2017).
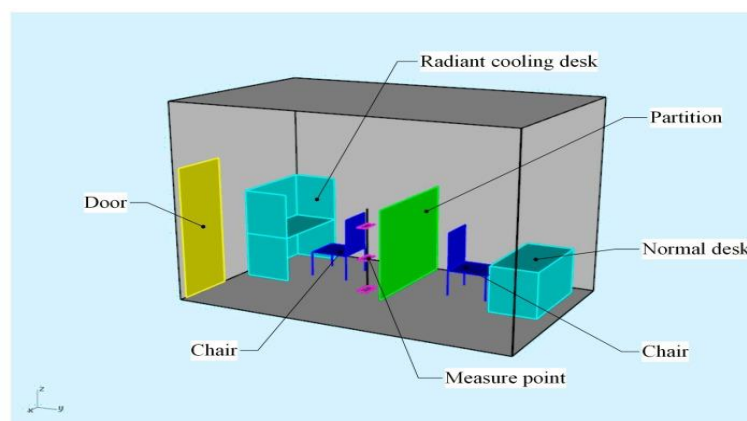
Figure 2.21: Location of measuring point (He et al., 2017)
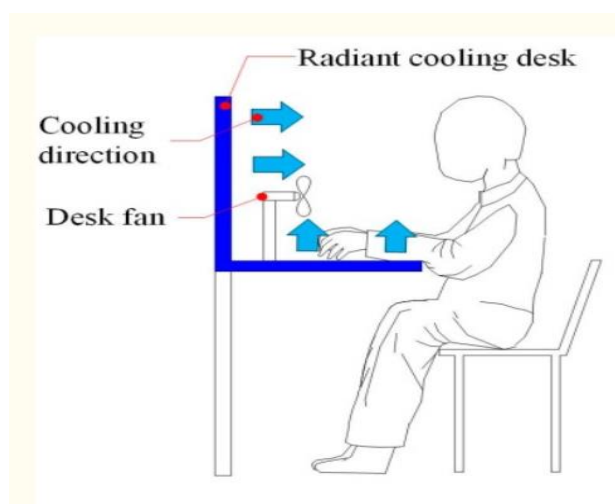
Figure 2.22: Placement of desk fan (He et al., 2017)
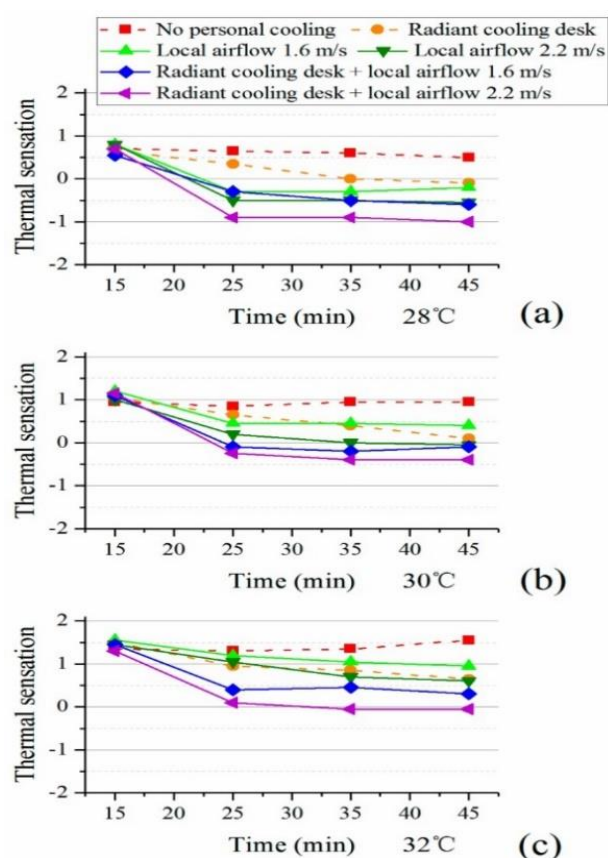
**Figure 2.23: Thermal Sensation Vs Time By Varying Fan Speed at
different indoor temperatures (He et al., 2017)**

As a result of the thermal sensation analysis, the sensation varied between

slightly warm (1) and slightly cool (1) across the whole procedure, making no

significant change despite the fan sits maximum speed of 2.2 m/s (He et al.,

2017).

The research also highlighted that during the whole experiment, the rating never reached -2 (cool), making desk fan's effect on occupant's thermal comfortability low. The same was done by using the thermal comfort index (He et al., 2017).
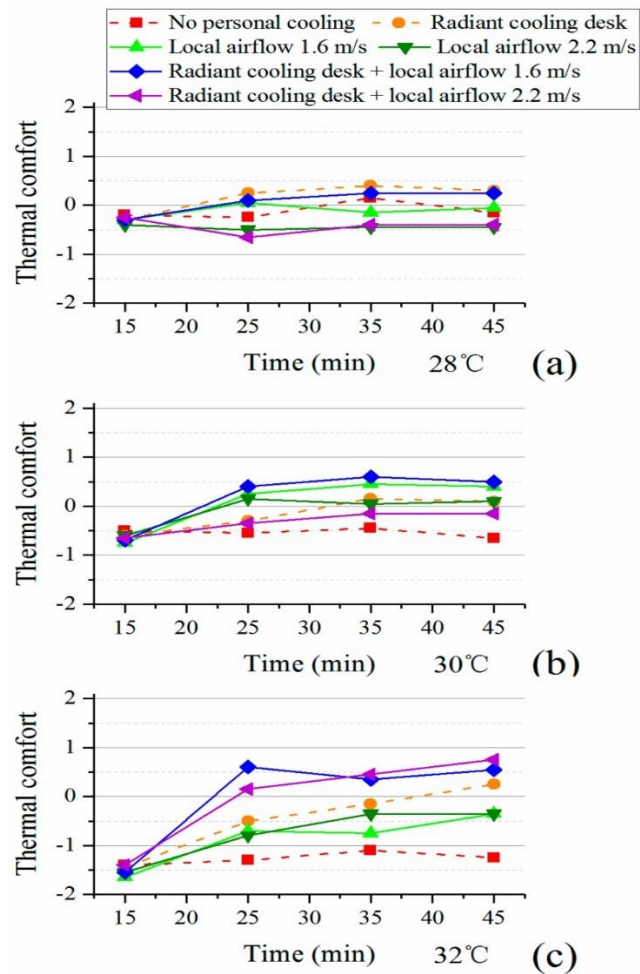
Figure 2.24: Thermal Comfort Vs Time By Varying Fan Speed at different indoor temperatures (He et al., 2017)

Thermal comfort results showed a similar outcome to the thermal sensation as the results vary from -1 (uncomfortable) to 1 (just comfortable). The results showed a slight improvement in the thermal comfort status for occupants despite adjusting the speed of the fan at its highest level (2.2 m/s) (He et al., 2017).

Based on these results, it can be shown that thermal comfort is improved much more with the usage of ceiling fans and standing fans, which is why this research will be focused on using only ceiling fans and standing fans.

2.6   Literature Review Conclusion

To summarize, historically, the idea of pollution and thermal discomfort started a very long time ago but lacked attention and awareness. That continued until the crisis in 1952 in Britain that led to the implementation of the Clean Air Act (mentioned in section 2.1.2).

Since then, researchers, scientists, and engineers have focused on providing a better indoor and outdoor environment. But despite the considerable contribution and effort, discomfort, stuffiness, and lack of freshness are symptoms that humans still encounter daily.

Based on the previous researcher's outcome as mentioned in the literature review, bad indoor air quality results from over-dependence on air conditioners, lack of window/door ventilation, and the minimal usage of ceiling fans.

That inspired the idea of building automated systems that monitor indoor air quality and provide solutions by depending on controllable environmental factors, such as humidity rate, airflow speed, percentage of CO_2, CO, and temperature levels.

Solutions involved sending alert messages, opening/closing windows, and using a ceiling fan. Among those purposed ideas, the usage of a ceiling fan was proven to be the most effective in terms of providing a suitable airflow with thermal comfort, energy-saving, and less air conditioner reliance.

However, up until now, all research has focused on fan control software development with little focus on real-collected data. Thus, the results are all assumptions by relying on the weather forecast and depending on simulation results.

Therefore, no confirmation is given on how effective an environmentally based fan system is in providing necessary indoor air quality improvement with thermal comfort.

For that reason, the indoor air quality and thermal comfort will be analyzed across two weeks by relying only on ceiling/standing fan to achieve a PMV level that complies with the ASHRAE Standard 55-2017 and EN-16798.

During the two weeks, the data gathered will be used to create the environmental fan's benchmark, which is the point of reference for its working to ensure a healthy air quality without causing thermal discomfort.

The system will be designed on energy-efficient concepts to achieve the fan's maximum savings potential.

CHAPTER 3

METHODOLOGY

3.1   Indoor Air Quality Monitoring System Development

To build a temperature and humidity-based fan system, the indoor air quality, and thermal comfort were evaluated in terms of different fan speed levels in a residential apartment's Master bedroom by using an air quality monitoring system for two weeks.

The indoor air quality system was developed according to the requirements needed in the research, which are the temperature level (in Celsius), relative humidity rate, CO_2 level (in ppm), CO level (in ppm), and the room's airflow. The microcontroller used to analyze and display the results is an Arduino.

3.1.1   Temperature and Humidity Measurement

The humidity and temperature were measured through DHT22, which is a module that includes two sensors, the first is an NTC temperature sensor and the other is a humidity sensing component placed in a case as shown in Figure 3.1.
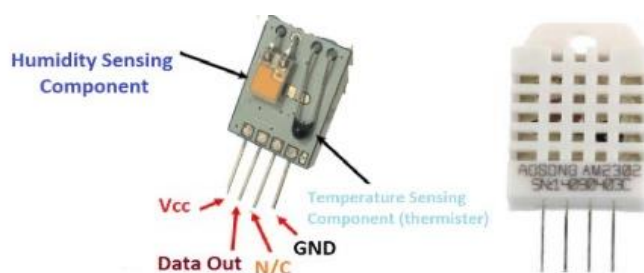
Figure 3.1: DHT22 Structure in datasheet

The output of the sensor is a calibrated digital signal, which is why the output of the sensor is connected to the digital pin in the microcontroller (Arduino). The sensing element is connected to an 8-bit single chip computer.

The sensor is suitable for harsh applications and is categorized as small size, low consumption of energy and long-distance transmission capability (around 20m), making it suitable for usage in an air quality monitoring system.

Table 3-1: DHT22 specifications listed in the data sheet

Model	DHT22
Power supply	3.3-6V DC
Output signal	digital signal via single-bus
Sensing element	Polymer capacitor
Operating range	humidity 0-100%RH; temperature -40~80Celsius
Accuracy	humidity +-2%RH(Max +-5%RH); temperature <+-0.5Celsius
Resolution or sensitivity	humidity 0.1%RH; temperature 0.1Celsius
Repeatability	humidity +-1%RH; temperature +-0.2Celsius
Humidity hysteresis	+-0.3%RH
Long-term Stability	+-0.5%RH/year
Sensing period	Average: 2s
Interchangeability	fully interchangeable
Dimensions	small size 14*18*5.5mm; big size 22*28*5mm

The working of the DHT22 is different from analog sensors as the analog sensors will give a reading that can be converted to a voltage value and easily displayed, however, the DHT22 is a digital signal that will give an output of 0 and 1.

The DHT22 starts by sending the humidity values first than followed by the temperature values. Both the data gathered will be a 16-bit data and are sent only 8-bits at a time. A logic of 1 is represented when a 50 µs long low pulse is followed by a 70 µs long high pulse, as for the logic 0, its represented when a 50 µs long low pulse is followed by a 26µs long high pulse as shown in Figure 3.2:
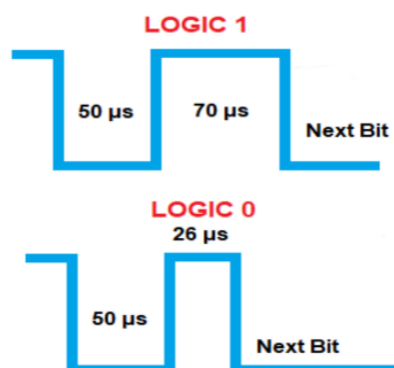
Figure 3.2: Logic 0 and Logic 1 in DHT22 shown in datasheet

The Logic 1 and logic 0 might not be represented with the exact values. Therefore, when the actual low pulse ranges between 48µs to 55µs, a value of 50 µs will be read and if the low pulse is followed with a high pulse that ranged between 68 µS to 75 µs, a logic of 1 will be considered, while if the low 50 µs pulse is followed with a high pulse that ranges between 22 µs to 30 µs, the logic 0 is read.

Hence, the device ends with a parity byte (which is a byte that can be appended to a binary), the parity byte will only be shown after two bytes of humidity and two bytes of temperature are sent out, and thus, resulting in a parity byte.

Parity byte = humidity high byte + humidity low byte + temp. high byte + temp. low byte
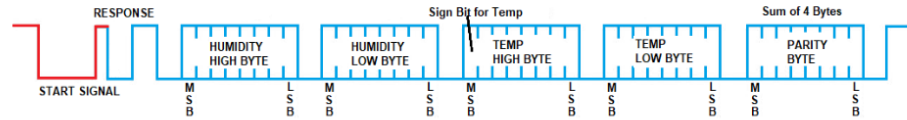
Figure 3.3: The timing diagram when a DHT22 sends out a single humidity and temperature reading (DHT11 Datasheet)

After coding the DHT22 accordingly to read the humidity and temperature, the following results was given when placing the sensor at a desk height (76cm – 89cm) and the air conditioner is open at a temperature of 27°C.
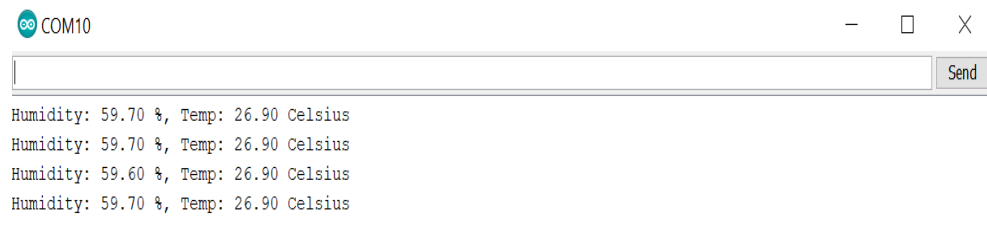
Figure 3.4: The humidity and temperature value where the air conditioner is set at 27°c

Another test was conducted on another day with no air conditioner, which showed a much higher temperature as shown in Figure 3.5 and Figure 3.6.
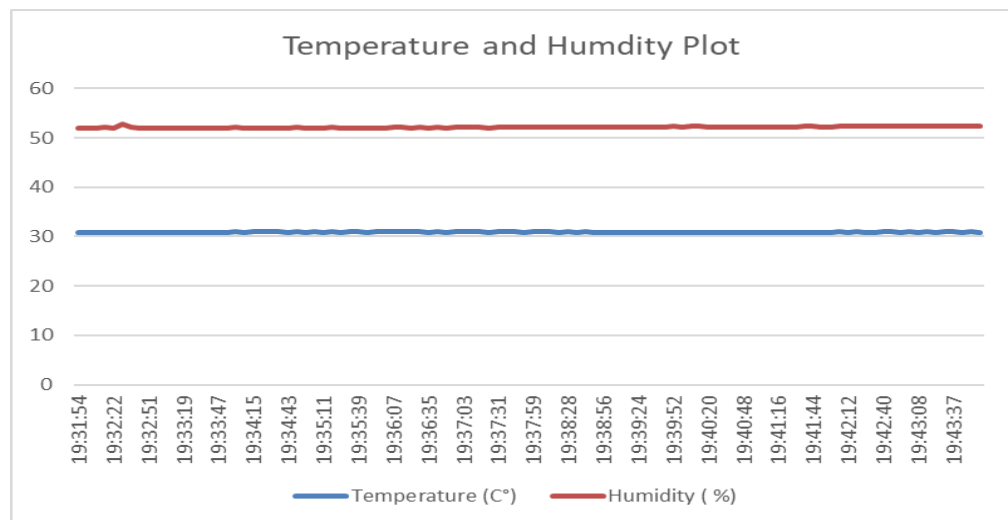
Figure 3.5: Humidity (Blue) and Temperature (Red)
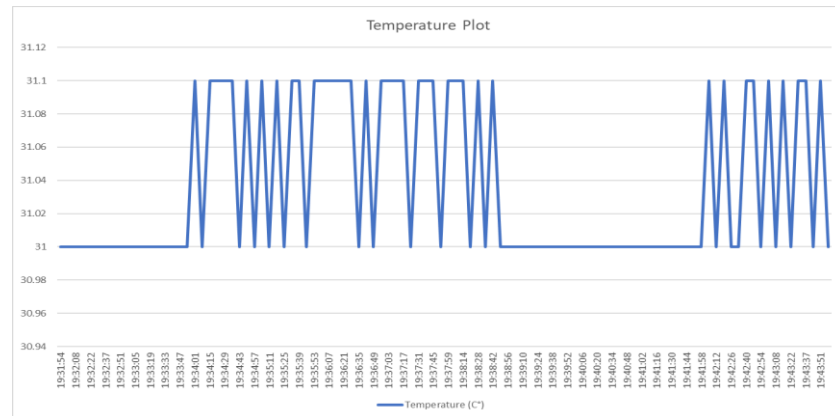
Figure 3.6: Temperature (Celsius)
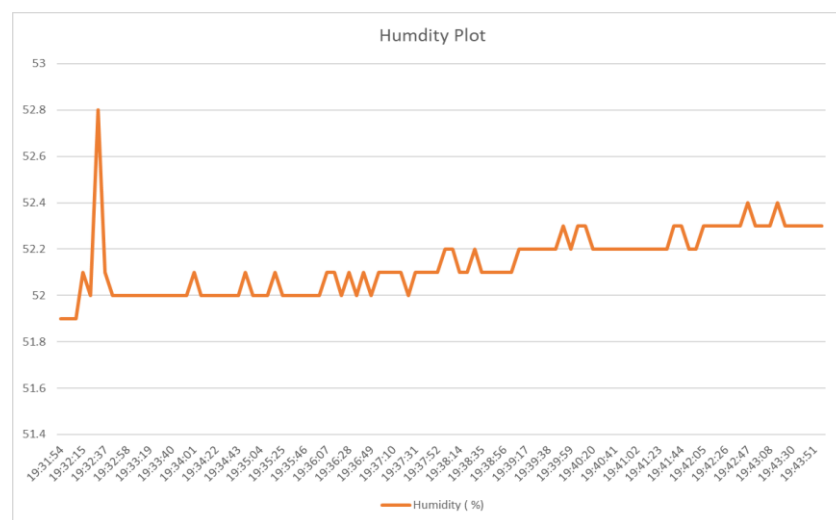
Figure 3.7: Relative Humidity (in Percentage %)

In Figure 3.7, the humidity of the room ranged from 51.9% to 52.8%, while the temperature as shown in Figure 3.6 ranged from 31°C to 31.1°C, so the Temperature and Humidity sensor is operating correctly.

3.1.2 Measuring the CO2 By Using Air Quality Sensor MQ-135

The MQ-135 is a sensor that detects and measures the concentration of different gases in the environment. It can be used to give an overall air quality by measuring the concentration of NH3, NOx, alcohol, Benzene, smoke and CO2 and comparing its values to the standard values assumed in the MQ-135 Library.

The MQ-135 consist of a Library that can be used when using different Micro-controllers such as and Atmega328, making it easier for coding. The structure of the MQ-135 (shown in Figure 3.8):
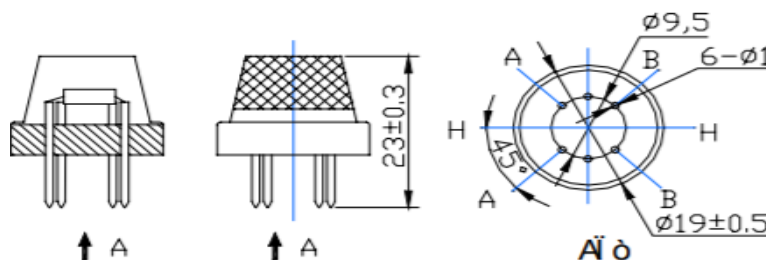
Figure 3.8: MQ-135 Sensor

The circuit diagram for the MQ-135(shown in Figure 3.9):
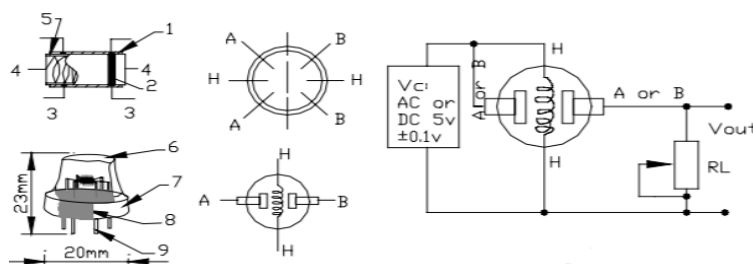
Figure 3.9: MQ-135 Circuit

The MQ-135 is made of a sensor composed of Micro AL203 ceramic tube and a Tin Dioxide sensitive layer. The sensing electrode is fixed with a heater under a crust made from plastic and stainless-steel net as shown in Figure 3.9. The heater is needed since the sensor used is an electrochemical sensor.

By heating the sensor to a certain temperature, the sensors sensitive surface will react and will allow certain gases and particles to penetrate it and thus the detection and measurement will be possible.
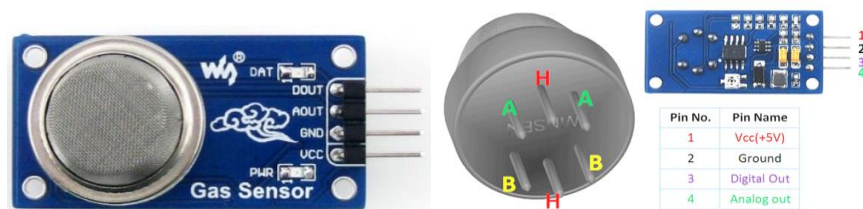
Figure 3.10: MQ-135 IC

The MQ-135 sensor consists of 6 pins, two of them are named H, which are the ones used to power up the heater, while the other 4 pins are connected to the sensor, so the output can be connected to either A or B, the pins A and B are repeated in order to ease its usage as a bridge when building the PCB (printed circuit boards).
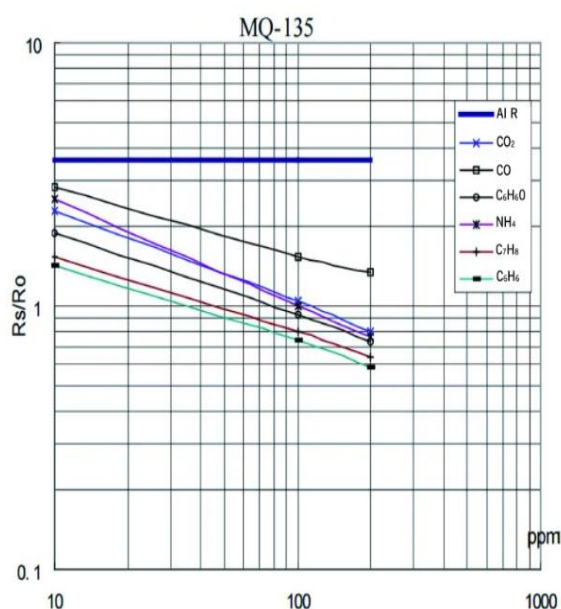
Figure 3.11: The Sensitivity Characteristics of the MQ-135

Figure 3.11 expresses the behaviour of the gas with respect to the resistance ratio in exponential not linear. The resistance ratio is Rs/R0, which is a constant in clean air, as Rs is the sensor resistance that will change when any gas is detected, while the R0 (also called Rzero) will remain constant.

 The value of R0 (Rzero) was fixed at 76.63, however that value changes when adding a resistor across the output, as the higher the load resistance, the higher the sensitivity of the sensor and it is advisable to add a load resistance from 10KΩ-22KΩ.

The figure also illustrates the typical sensitivity characteristics of the MQ-135 for different types of gases such as CO_2 and NH4 when the temperature is set at 20C ± 2 and the humidity is 65% ± 5%, while supplying the heater with a voltage of Vh = 5V ± 0.1 and supplying the sensor with Vc = 5V ± 0.1 and connecting the sensor with a load voltage of 20 KΩ.

To detect the concentration of the CO_2 in the room. The first step is to obtain the value of the R0, which was detected by coding the microcontroller (Arduino) to find the R0. The value of R0 changes slightly with time, which is why an average value was calculated and used to find the PPM of the CO_2. During the experiment, the sensor was placed at a desk height (76cm – 89cm) with a load resistance of 22kΩ, 78 samples were taken giving an average of 333.5Ω (shown in Figure 3.12).
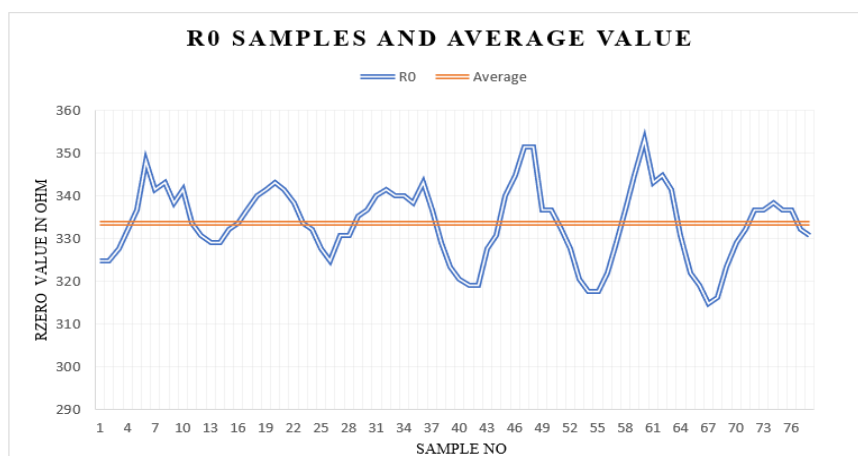
Figure 3.12: R0 Samples and Average Value

After obtaining the R0 value, the Arduino was coded to detect the CO2 concentration. The test was done indoors while opening windows and allowing a good air flow.

Based on the ICOP 2010, the value of CO2 concentration should be less than 1000 ppm, otherwise the air is considered as poor quality, however it is recommended that the concentration doesn't exceed 800 ppm to provide a healthier room environment.

Before the results are monitored, the sensor needs to be pre-heated to wait for the heating coil heater) to reach the necessary temperature for the sensing layers to function correctly and achieve thermal equilibrium.

The duration of thermal equilibrium differs each time the sensor is used as it depends on multiple environmental factors such as the room temperature that may speed up or slow down the process of heating as shown in Figure 3.13.
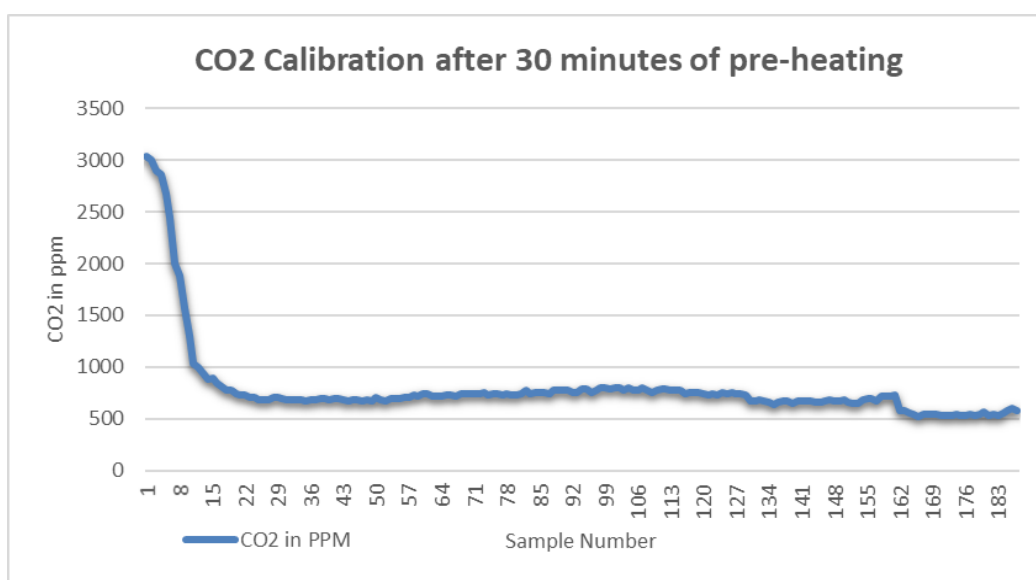
Figure 3.13: MQ-135 thermal equilibrium after 30 minutes of preheating

After the thermal equilibrium was completed the CO2 concentration ranged around 400ppm -500 ppm in a residential apartment when the windows and door was open providing good air circulation as shown in Figure 3.14 and Figure 3.15.
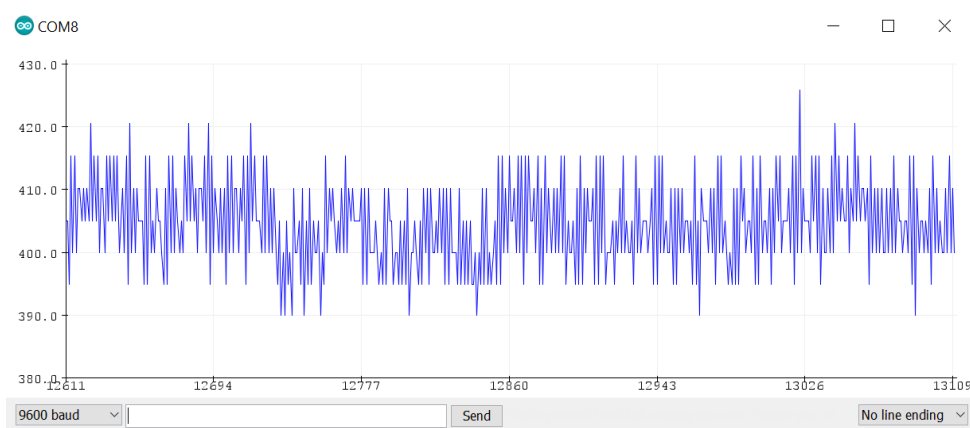
Figure 3.14: The illustration of CO2 Concentration (ppm) Vs The Number Of Samples (Using Arduino Serial Monitor)

250 samples were gathered and plotted using Excel to show a clearer graph as shown in Figure 3.15.
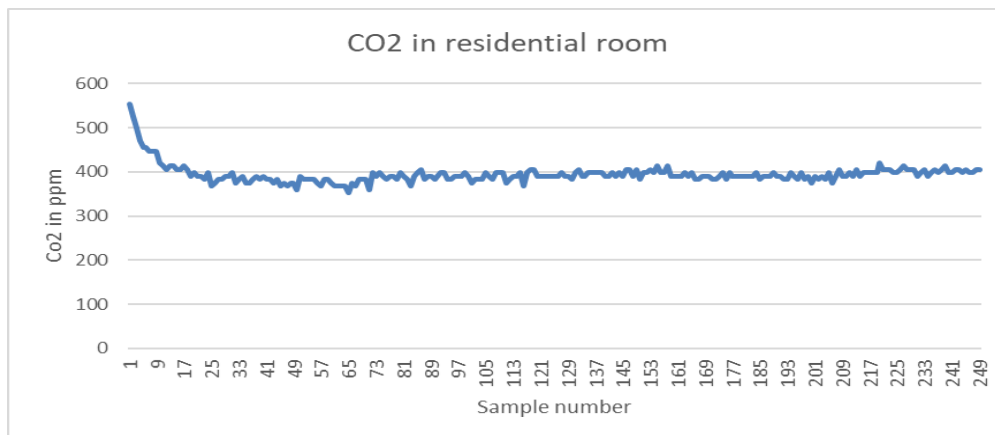
Figure 3.15: CO2 Concentration In ppm Vs the Number of Samples

3.1.3   Measuring the Carbon Monoxide (CO) by using air quality sensor MQ-7

The MQ-7 is a sensor built to detect and measure Carbon Monoxide (CO) in the air. It can detect CO at values ranging from 20 ppm to 2000 ppm.

The sensor's output can be in both digital and analog form and needs a 5V supply to function. The sensor is recommended to be connected to a load resistance of 10KΩ before connecting it to a microcontroller.

The structure of MQ-7 is composed out of a micro ceramic tube and a Tin Dioxide sensitive layer (gas sensing layer), an electrode (Au) and a Heater coil are fixed into a crust made from plastic and stainless-steel net.
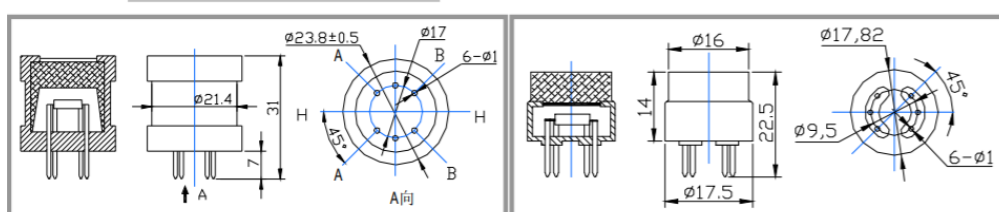
Figure 3.16: MQ-7 structure and configuration

Before the usage of the sensor, a preheating step is needed. The preheating is suggested to be more than 1 hour and less than 48 hours. The preheating ends when the values start to stabilize.
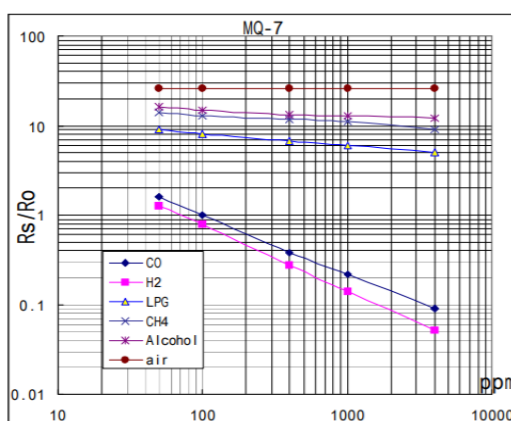
Figure 3.17: MQ-7 sensitivity characteristics

The value shows that the CO PPM can reach up to 2000 ppm under certain circumstances. The sensitivity chart shown in figure 3.17 was recorded with the usage of a load resistance of 10KΩ, a humidity of 65 % and a temperature of 20 °C.

The CO sensor value was coded to convert the analog reading to milli-volt and later converting the milli-volt value to CO reading in ppm (Anguera et al., 2018). The Arduino default reading setting for analog reading are 8-bit PWM, but that can be changed to 12 bits so that the input reading can give an outcome from 0 to $2^{12} = 4096$ rather than limiting the outcome to a range between 0 to 2^8=256.

The increase in the outcome range is for precaution purposes, since the reading coming from the sensor will be analog reading so we are unaware of how high it can reach in terms of very high temperatures.

$$V = analogreading \times (\frac{power\ supply\ voltage}{4096}) \quad\quad\quad (3.1)$$

Where V is the analog value in Milli-volt. In this project a supply of 5V is used.

$$V = analogreading \times (\frac{5V}{4096})$$

As for the value of ppm, the analog value in Milli-volt (V) can be converted following the below equation (Anguera et al., 2018)

$$Value\ of\ ppm\ for\ CO = 3.027 \times e^{1.0698 \times V} \quad (Anguera\ et\ al.,\ 2018) \quad\quad (3.2)$$

After setting up the sensor, the microcontroller (Arduino is used in the testing) was programmed to read the value of the CO, however, preheat was needed at each activation to heat the coil and reach thermal equilibrium
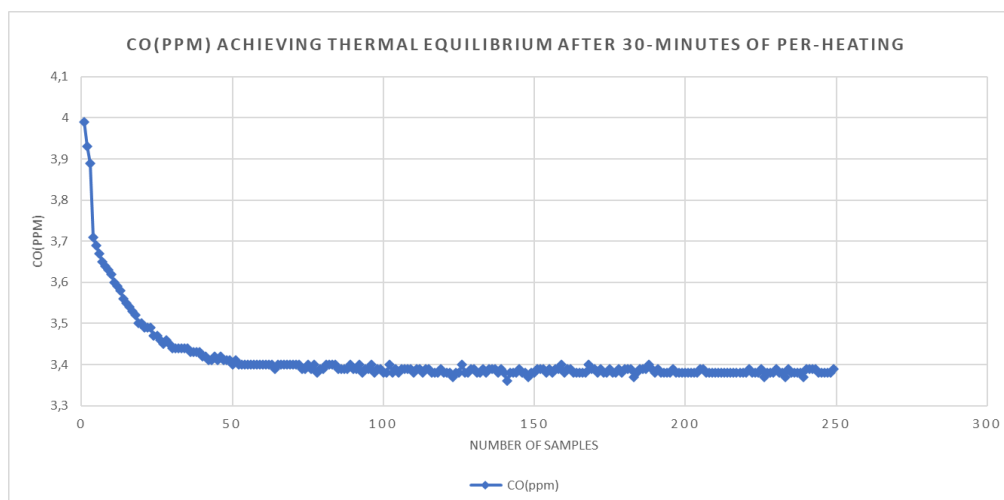
Figure 3.18: Thermal equilibrium after 30 minutes of preheating

The duration of pre-heating changes from time to time depending on multiple environmental factors such as the room temperature that may affect the speed of the sensor's thermal equilibrium.

From figure 3.18, a clear thermal equilibrium was illustrated as the sensor starts by detecting a high value as mentioned in the data sheet as shown in Figure 3.17 and starts to decrease until stabilizing at a certain value. Once a stabilization occurs meaning the sensor is ready to be used.

3.1.4 Air Flow Speed

Since most airflow devices and wind speed meters are expensive, the airflow was determined using the hall effect sensors. The hall effect sensors are made out of a thin layer of P-type semiconductor and are activated with the help of an external magnetic field, so the need to use magnets is necessary.

The hall effect sensors were connected to a power supply and that allows current to pass through the plate when a magnet is placed at the rated distance. The magnetic flux will exert a force on the semiconductor and thus deflecting the electrons on one side while deflecting the positive charges on the other side as shown in Figure 3.19 a (Ramsden, 2006).

So, if a voltmeter is placed across the plates, a voltage is detected, that voltage will be discovered using the microcontroller. The air flow speed can be determined by the strength of the voltage signal or the frequency of voltage detection.

One main element that has to be taken into consideration is the air gap between the magnets placed and the hall effect sensor as long air gaps will weaken the magnetic flux density as shown in Figure 3.19 b (Ramsden, 2006).
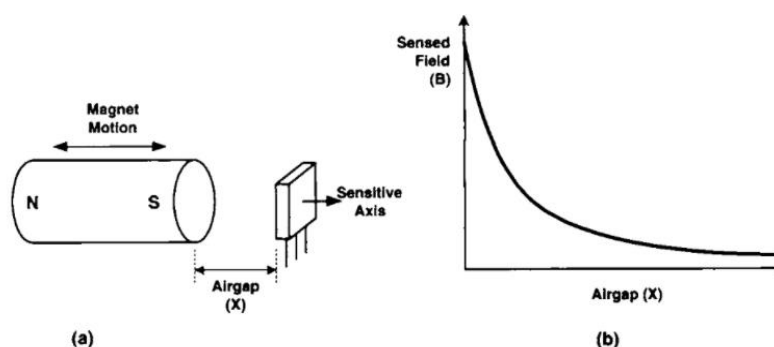
Figure 3.19: (a) Hall Effect (B) And Magnetic Flux Density Vs Airgap (Ramsden, 2006)

There are two ways to use the hall effect sensors, one is the Head-On sensing, and another is the Slide-By sensing (Ramsden, 2006) depending on the location of the magnets with respect to the hall effect sensor.

The Slide-By sensing was used in this experiment as magnets were placed onto wind turbines to achieve voltage detection by sliding the pole-face of the magnet pass the sensor.

To measure the air flow in the experiment, the air flow was rated from 1 to 5, where one represents the lowest speed and 5 represents the highest speed when using a ceiling fan.

The hall effect device was used to measure the speed. The device consists of two magnets that are connected on a two-blade small wind turbine, which will pass by the hall effect sensor.

The distance between the magnets and the hall effect sensor are kept within a distance of less than 40mm as the hall effect sensor used can detect magnetic flux at a maximum air gap of 40mm. The placement of the hall effect sensor with respect to the wind turbine was adjusted so that Slide-By sensing is achieved as shown in Figure 3.20.

Air gap between the magnet and hall effect sensor is maintained at value less than 40 mm
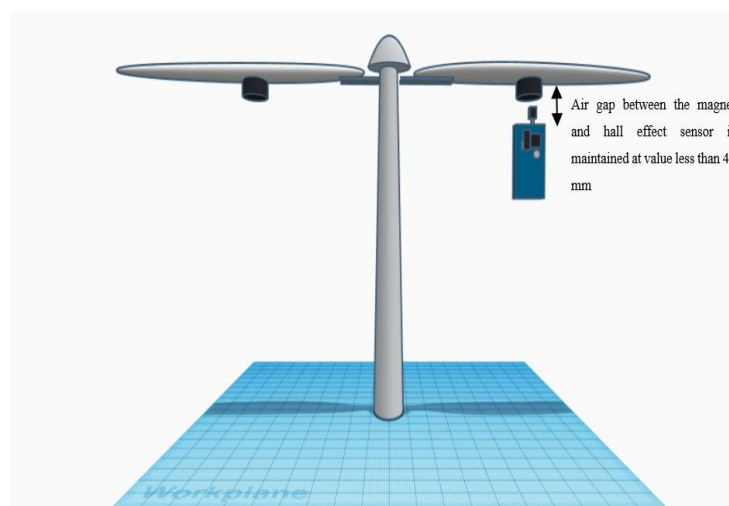
Figure 3.20: Placement of hall effect sensor with respect to the magnets and wind turbine drawn in Tinker CAD software

This placement showed the following results, when connecting the sensor to the microcontroller (Arduino) and coding the microcontroller to read the analog signals from the senor.

The coding was done in a way that will give a zero outcome when the hall effect sensor is aligned with the magnets and will increase when the magnet moves away from the sensor, So, a whole revolution is the distance that starts from zero points and heads back to it again.

The maximum rating before reaching the zero point is the point furthest from the magnet, which means it's the distance to complete one revolution. The faster the air flow is, the faster the turbine goes and comes back to the zero point and the distance to complete one revolution will decrease.

3.1.4.1 Air Flow Speed Testing Using Ceiling Fan

The ceiling fan's module used has a voltage that vary from 220V-240V and wattage of 80 with a maximum rated speed of 300RPM and an air delivery of 270m³/min (CFM Cubic feet per minute of 8828 CFM). The ceiling fan had a blade span of 60 inches, 14-degree blade pitch and 3 blades.

To get the wind speed MPH (mile per hour), an online calculator was used to approximate expected MPH based on the CFM and blade span. The online's calculation is not based on formula but based on previous collected data since there is no formula to convert CFM to MPH.

The calculator was chosen based on the similarities between the fan used in the experiment and the fan manufactured by the company. Based on the similarities, the Hansen company's fan of a 60-inch blade with a 14-degree blade pitch and 3 blades is similar to the fan used in the research as shown in Figure 3.21.
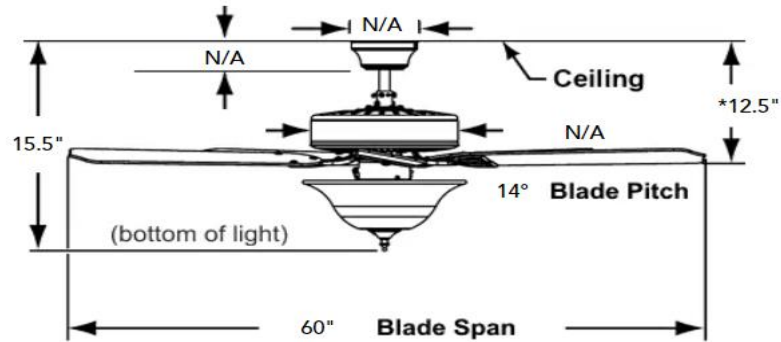
Figure 3.21: Hansen's company's ceiling fan structure
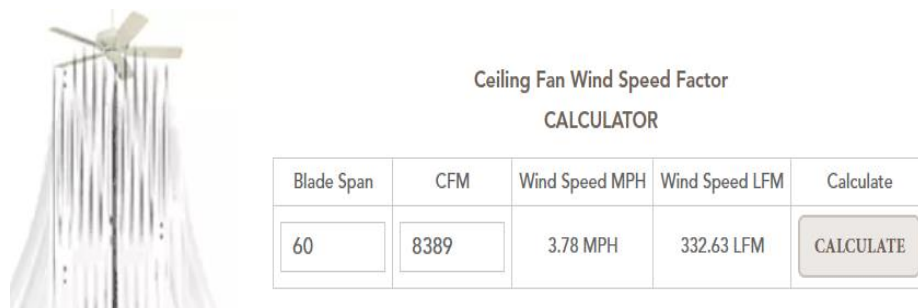
Figure 3.22: Wind speed air flow calculation using Hansen company's calculator

So, an online calculator was used to measure the MPH (Miles per Hours). The MPH (Miles Per Hour) calculated was 3.78 for level 5 (highest speed), and the MPH was converted to m/s (Meter/second) using the following formula:

$$\frac{Miles}{hours} \times \frac{1600 \; meters}{1 \; mile} \times \frac{1 \; hour}{3600 \; second} = \frac{meter}{second} \qquad (3.3)$$

That gave an approximated maximum air flow of 1.6898 m/s ($\approx$ 1.7 m/s), the same approach was used to calculate the air flow at different fan speed levels.

Table 3-2: Ceiling Fan Specifications

Speed rate of fan	Speed	Air Delivery (CFM)	Air Flow M^3/s	Air Flow MPH	Air flow m/s
5	300 RPM	8828	270	3.78	1.7
4	257 RPM	7562.65	231.3	3.41	1.524
3	215 RPM	6326.73	193.5	2.85	1.27
2	173 RPM	5090.813	155.7	2.29	1.02
1	130 RPM	3825.467	117	1.72	0.768

The first test was performed using a ceiling fan located in the master bedroom. The placement of the senor was at position 1 as shown in Figure 3.23, which is directly below the ceiling fan, where the air speed can be detected easily as shown in Figure 3.24 (Babich et al., 2017).
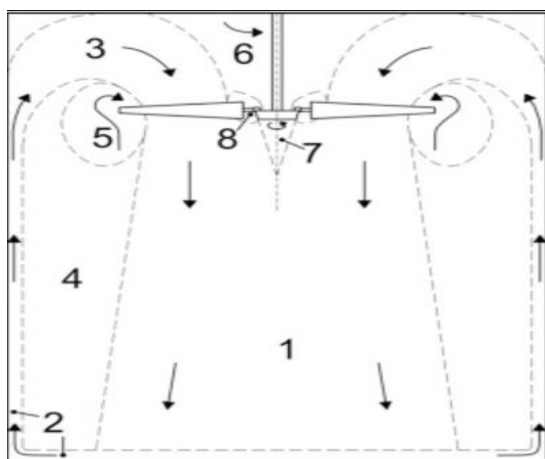
Figure 3.23: Ceiling fan's air flow regions (Babich et al., 2017)

These air flow regions were described in Table 3.3.

Table 3-3:Air flow region descriptions (Babich et al., 2017)

Region	Agreement	Key characteristics
1	Good	Highest higher speed, significant swirling component, divergent flow
2	Good	Very low air speed near walls (moving upward) and ceiling
3	Good	Increasing air speed and development of swirling component
4	Good	Very low air speed and negligible effectiveness of the fan
5	Weak	Local air recirculation underestimated by the CFD model
6	Good	Low air speed, recirculation area
7	Good	Air not driven downwards due to the blockage caused by the motor of the fan
8	Weak	Local air recirculation underestimated by the CFD model

The previous research also used a simulation software (ANSYS) as shown in Figure 3.24, that shows the air flow rate of a ceiling fan and the room is measured in precise when the detector is placed directly below the fan, while the air speed near the walls and ceiling are very low it is difficult to be detected.
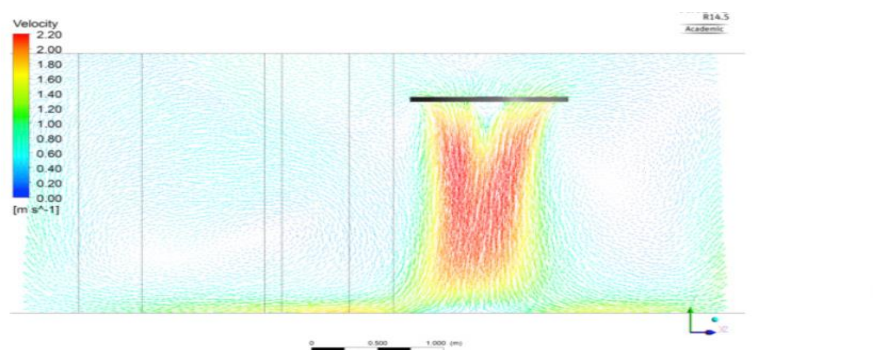
Figure 3.24: Air flow generated by the ceiling fan simulation using ANSYS Software (Babich et al., 2017)

So as the placement were followed accordingly, the data gathered at speed levels 1-5 were recorded using Excel by connecting the microcontroller (Arduino) to excel and was plotted (shown in Figure 3.25 – Figure 3.29)

Figure 3.25: Ceiling fan speed detected by Arduino at speed level 1
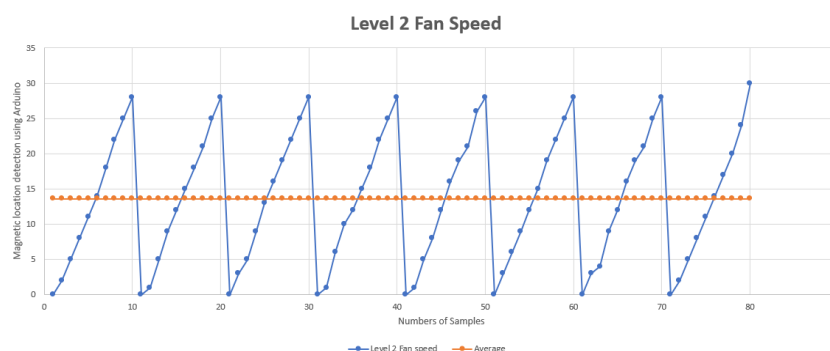
Figure 3.26: Ceiling fan speed detected by Arduino at speed level 2

Figure 3.27: Ceiling fan speed detected by Arduino at speed level 3

Figure 3.28: Ceiling fan speed detected by Arduino at speed level 4
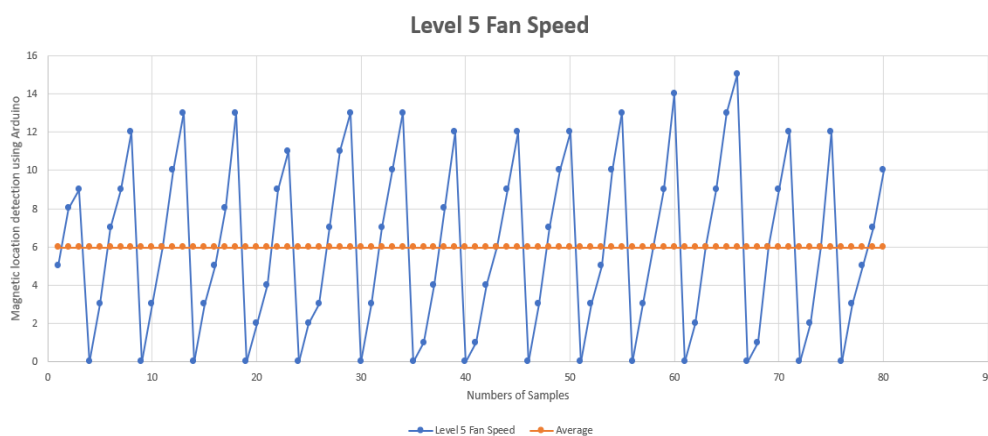
Figure 3.29: Ceiling fan speed detected by Arduino at speed level 5

All the testing was done by gathering 80 samples with a difference of 5miliseconds (5ms) between each sample: thus, total testing time for all speed levels was around 400ms. The figures show 80 samples in the X-axis, while a magnetic location reading in the Y-axis.

The magnetic location reading records zero when the magnet is aligned with the hall effect sensor and increases as the magnet move further away. The number recorded before the end of the revolution is considered the distance taken for one magnet to go from the zero point and back to it again.

The recording in the Y-axis is an Arduino analog reading, which can be converted to voltage; however, in this experiment, the Arduino reading was used for a more straightforward approach. So, it can be shown in Figure 3.25 to Figure 3.29, the rotation of the wind turbine increases as the speed increases within the same period.

In contrast, in Figure 3.25, only five wind rotations were achieved within 400ms, while in Figure 3.28 around 14 rotations were completed. The distance for one rotation was also noticed to be decreasing as the level of speed increases. The average length for one rotation was calculated and recorded as shown in Table 3.4.

Therefore, to determine the airflow in the room while investigating the acceptable limits of air movement that maintain thermal comfort for room occupants, the outcome of the Arduino was compared to Table 3.4 and an approximate air flow rate was assumed accordingly.

Table 3-4: Ceiling fan ratings based on hall effect sensor

Level Speed	Y-axis Revolution distance reading (Average)	Number of samples per revolution	Number of revolutions	Total number of samples
1	21.6125	14	5	80
2	13.5875	9	7	80
3	9.1	6	11	80
4	6.675	5	≈ 14	80
5	5.98	3-4	≈ 15	80

Table 3-5: Ceiling fan specifications

Level Speed	Y-axis Revolution reading (Average)	Number of samples per revolution	Air Delivery (CFM)	Air flow m/s
1	21.6125	14	3825.467	0.768
2	13.5875	9	5090.813	1.02
3	9.1	6	6326.73	1.27
4	6.675	5	7562.65	1.524
5	5.98	3-4	8828	1.7

For example, if during this research the Y-axis Revolution distance reading (Average) was recorded to be 13, Table 3.5 was used flow so that an evaluation of the indoor air quality and thermal comfort can be achieved. Based on Table 3.5 if an average of 13 of Y-axis Revolution distance was given by the Arduino the air flow is assumed to be 1.02 m/s.

Thus, the determination of the air delivery and air flow of the room when using a ceiling fan was determined by comparing the results with the standards established in Table 3.5.

3.1.4.2 Air Flow Speed Testing Using Standing Fan

The Standing fan module used was a Pensonic Stand Fan | PSF-45 with 3 speed levels and has a voltage that vary from 220V-240V, with a maximum rotational speed of 1220 RPM and a minimum rotational speed of 950 RPM. The maximum power consumption of 50W and the air delivery is 54 m³/min (CFM Cubic feet per minute of 1906.99 CFM).

Table 3-6: Standing fan specifications based on performance label

Speed rate of fan	Speed	Air Delivery (CFM)
3	1220 RPM	1906.99
2	1020 RPM	1594.36
1	950 RPM	1328.64

The fan was compared by a previous research published by the IES (The institution of engineers) in Sri Lanka (Attalage and Sugathapala, 2001), where the performance of different pedestal fans was analysed at a 80 cm distance between the fan and the measuring point (named as X) as shown in Figure 3.30.
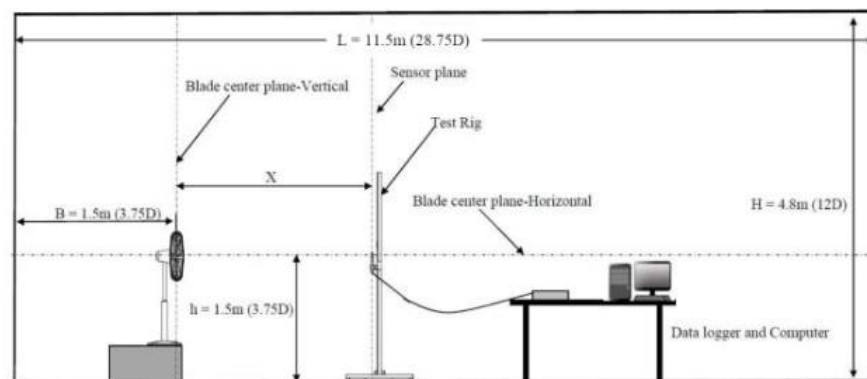
Figure 3.30: Test setup (Attalage and Sugathapala, 2001)

The experiment used 4 different fan types as shown in Table 3.7, where Fan B and the Pensonic Stand Fan | PSF-45 used are almost the same, having approximately the same rotational speed (RPM), frequency, voltage level, power consumption and regulator position, therefore a similar air flow is expected.

Table 3-7: The specifications of the 4 fans used in the previous research (Attalage and Sugathapala, 2001)

Fan Type	Regula-tor Position	Current (A)	Voltage(V)	Frequency(Hz)	Power consumption(W)	Power factor	Rotational speed (RPM)	Annual Power consumption (kWh)
A	1	196.1	242.4	50.1	47.86	1	1231	138.87
	2	211.6	243.5	50.1	52.1	1	1310	153.17
	3	249.1	240.7	50.12	56.54	0.946	1370	165.23
B	1	173.2	221.6	50.2	35.44	0.945	970	103.6
	2	185.1	219.8	50.15	40.14	0.968	1100	116.7
	3	210.2	224.6	50.15	47.57	1	1230	139.5
C	1	150.5	218.8	50.25	32.45	0.97	940	94.57
	2	162	226.4	50.15	36.26	0.988	1080	106
	3	174.5	225.8	50.1	38.84	1	1240	114.2
D	1	149.9	210	50.1	30.67	0.968	1235	90.18
	2	160.2	215.2	50.05	34.09	0.991	1310	97.71
	3	184.7	215.1	50.2	38.88	0.992	1375	114

The air flow for each fan type was recorded by the research and the average air flow was calculated at all three regulator positions (shown in Table 3.8).

Table 3-8 : Measurement of average velocity of all 4 fan types (Attalage and Sugathapala, 2001)

Fan Type	Regulator	Oscillation per minute	Average Velocity (m/s)	Oscillation Angle
A	1	4.14	0.54	90°
	2	4.73	0.55	
	3	5.21	0.66	
B	1	3.02	0.47	95°
	2	3.52	0.52	
	3	4.28	0.6	
C	1	3.41	0.36	90°
	2	4.09	0.38	
	3	4.8	0.45	
D	1	5.54	0.54	75°
	2	5.9	0.55	
	3	6.13	0.66	

Based on Table 3.8, the previous research has assisted in approximating the average velocity expected at each speed level. The research's setup was also used by placing the standing fan at a distance of less than 1m (approximately 75cm making it similar to the previous research where the distance was measured to be almost 80 cm) away from the desk, while placing the Wind detection device on the desk (Desk height used is 77cm) as shown in Figure 3.31.
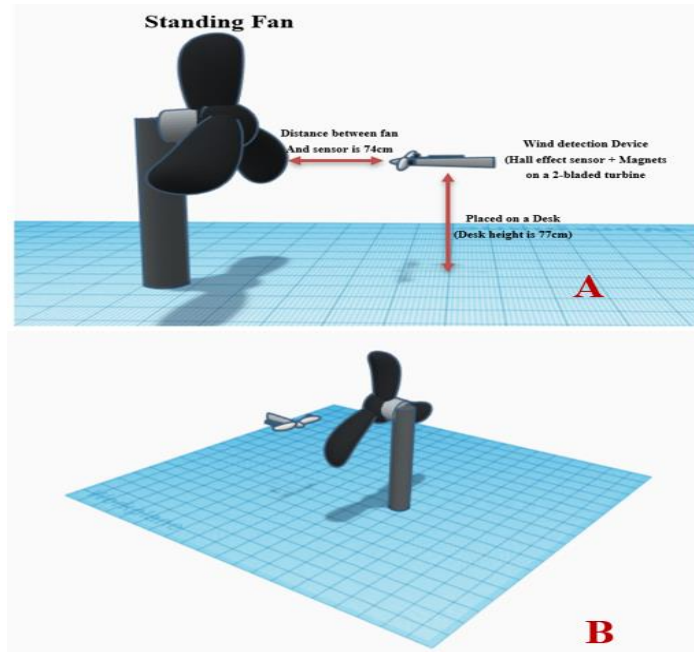
Figure 3.31: Placement of Air Flow Detection Device (A) An 3D View (B)

The procedure to test the air flow detection device was the same as the one done in the ceiling fan testing. All 3 speed levels were tested.
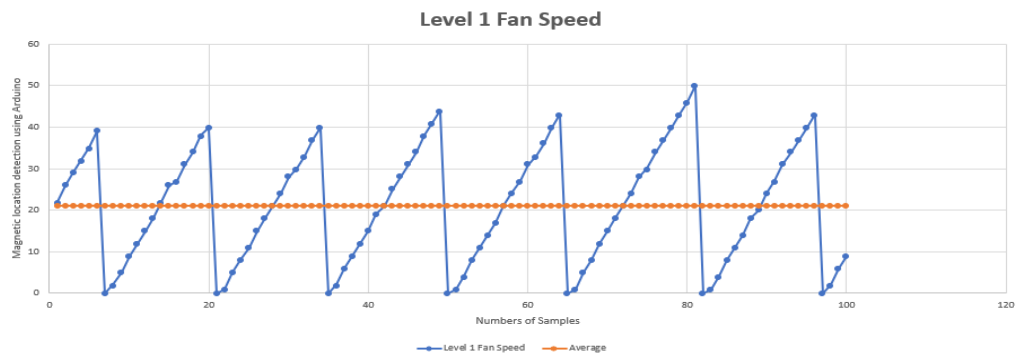
Figure 3.32: Standing Fan Speed Detected by Arduino At Speed Level 1
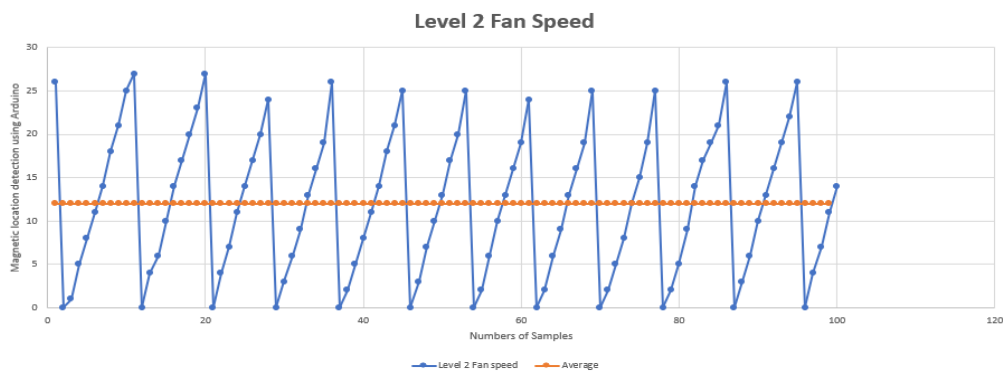
Figure 3.33: Standing Fan Speed Detected by Arduino At Speed Level 2
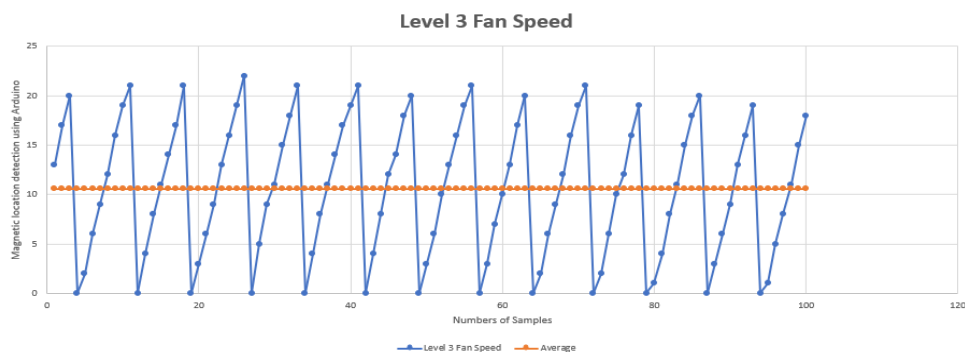
Figure 3.34: Standing Fan Speed Detected by Arduino At Speed Level 3

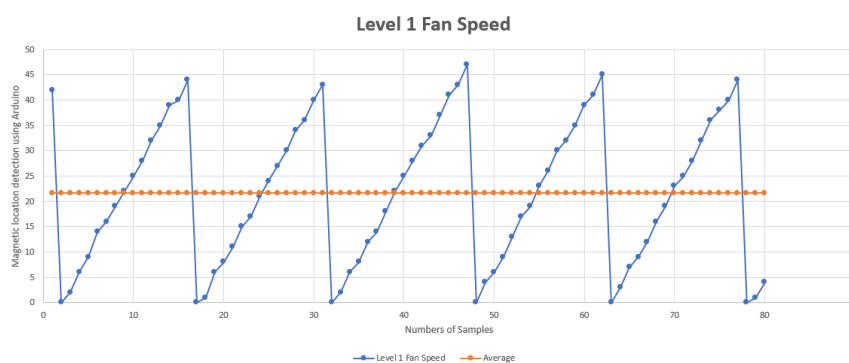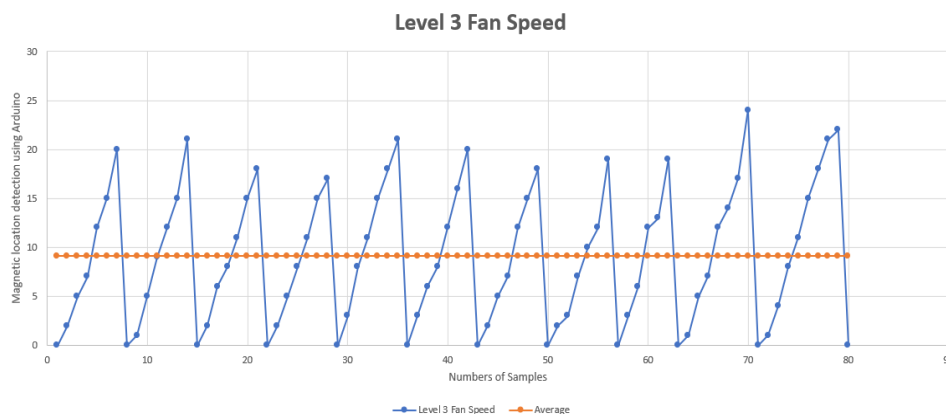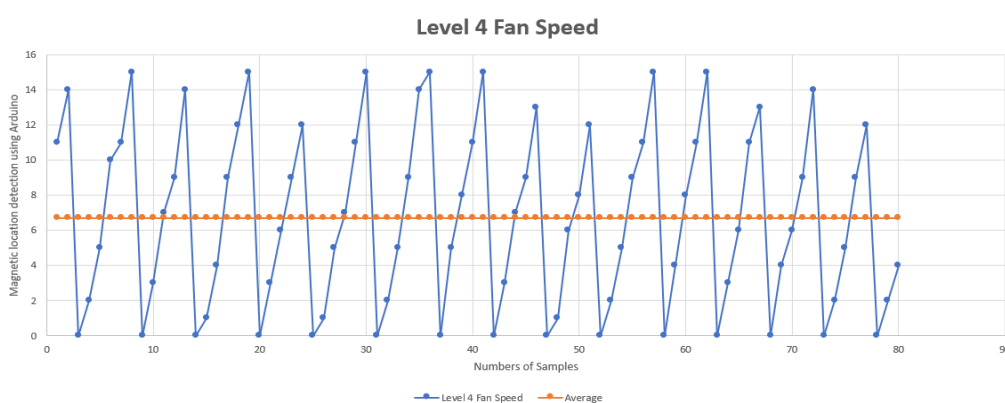All the testing was done by gathering 80 samples with a distance of 5mS between each sample, so the total testing time for all speed levels was around 500mS. The Figures 3.32- 3.34 show 80 samples in the X-axis, while a magnetic location reading in the Y-axis. The recording in the Y-axis is an Arduino analog reading.

The outcome for the standing fan shows that the number turbine rotations decreases as the fan speed increase, recording 7 revolutions within 500ms when the speed level was at 1 and 12 revolutions when the speed was fixed at 3. The average length for one rotation was calculated and recorded in Table 3.9.

Table 3-9: Standing fan ratings based on hall effect sensor

Level Speed	Y-axis Revolution distance reading (Average)	Number of samples per revolution	Number of revolutions	Total number of samples
1	21.09	12-13	≈ 7	80
2	11.95	8-9	11	80
3	10.56	7-6	≈ 13	80

Table 3-10:Standing fan specification

Level Speed	Y-axis Revolution reading (Average)	Number of samples per revolution	Speed	Air flow m/s
1	21.09	12-13	1220 RPM	0.6m/s
2	11.95	8-9	1020 RPM	0.52 m/s
3	10.56	7-6	950 RPM	0.47m/s

3.1.4.3   Air Flow Speed Detection Summary

After conducting tests and setting the standards for both the ceiling fan and the standing fan, the indoor air quality can be investigated by referring to Table 3.5 when using a ceiling fan and Table 3.10 when using a standing fan.

3.1.5   Connection of Indoor Air Monitoring System and Digital Devices

The connection between the air monitoring system and the digital device was designed to be wired, expect for the air flow data collection was made to be wireless due to the movement of the room airflow differ from one day to another and from time to another.

Therefore, the connection of the hall sensor was done in a wireless form so that the wind detection device is portable, while the rest of the sensors are connected via USB wire. Due to the two different communication methods, two microcontrollers where used, one to gather the airflow data, while the other gathers the rest of the environmental elements as shown in Figure 3.35.
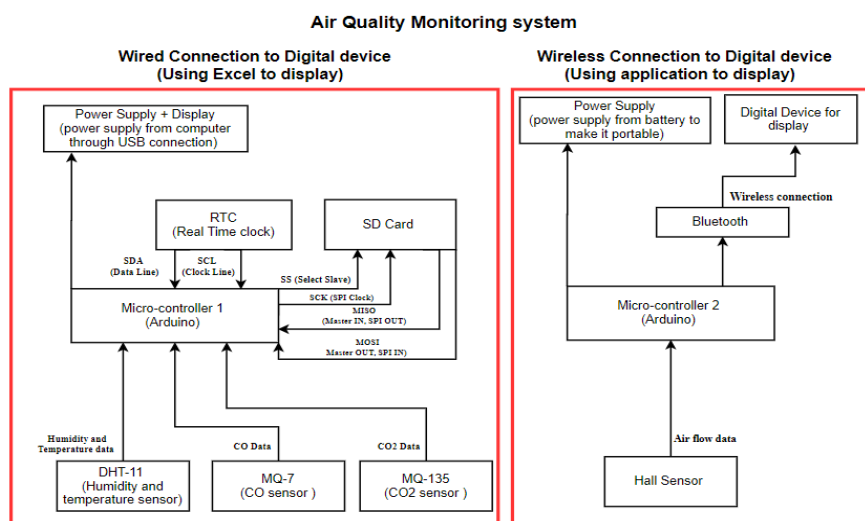
Figure 3.35: The hardware architecture for the air quality monitoring

3.1.5.1 The Wired Connection Between the Air Monitoring System and Digital Device Setup

The wired connection was made by connecting the microcontroller (Arduino) to the digital device using a USB (Universal Serial Bus). The microcontroller was connected to an SD card module (Secure Digital) and an RTC module DS3231 (Real-Time Clock Module).

The SD Card module allows the user to communicate with the memory card and perform read/write the information on them. The size of the memory depends on the SD card applied to the module.

The module used was a MicroSD card module with an SPI (Serial Peripheral Interface) interface driver as shown in Figure 3.36. The SPI is commonly shown in embedded systems and is an efficient and straightforward interface, however, it can be slow if the transferred data is significant such as cameras or any other digital devices. Still, in this research, small data was transferred, making SPI a suitable approach (Ujjan et al., 2019).
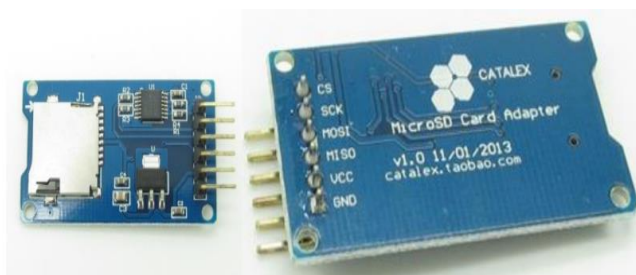
Figure 3.36: MicroSD card module (SD Card Module Datasheet)

In this project, the Arduino (microcontroller) was the master, and the SD card module was the Slave (shown in Figure 3.37).

In SPI, when a bit is shifted out of the MOSI, another will be shifted in on the MISO line using a level shifter, making the MISO the output from the SD card module, while the MOSI is the input to the SD card module (Saha et al., 2014).

Those bits will later be transferred into words in different sizes that can then be printed out in the SD card. The SD card module is often used with a real clock module so that the time and date of the data storing is printed along with the data.

As for the Slave pin in the SD module, it was used by Arduino to enable and disable the communication, for example, if the slave select pin is low, it will communicate with the Master and if it is high, it will ignore the Master (Saha et al., 2014).
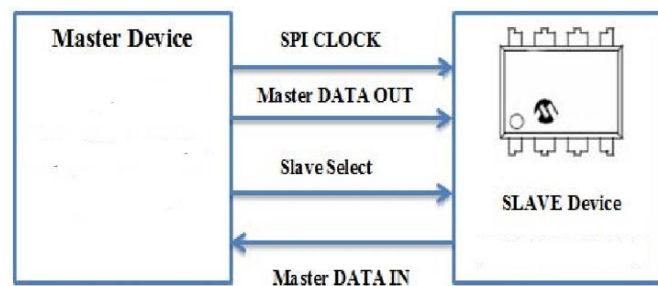
Figure 3.37: Connection between the Master (Arduino) and the Slave (SD Card Module) (Saha et al., 2014)

After the connection and coding were complete, the data was stored in the SD card as well as the creation of an Excel file where the same data stored in the SD card was written in the excel file (shown in Figure 3.37). The usage of an excel file was done using coding and the reason why excel data was used as it helps easier recording and plotting the outcome if needed.

As for the RTC module DS3231, which is the real-time clock integrated with a TCXO (temperature compensated crystal oscillator), it was used to display the second, minute, hour, day, month and year in either the 24-hour or 12-hour format with an AM/PM indicator.
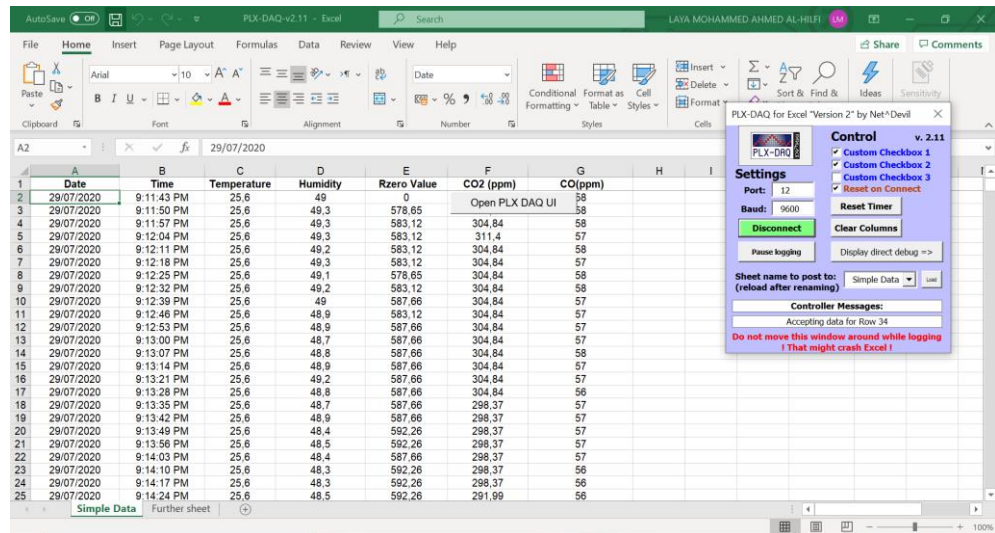
Figure 3.38: Excel file created to record the data

Figure 3.38 illustrates the data gathered from the microcontroller after all the sensors are connected. In the excel file the date and time is recorded for each data gathered. It can be shown that the excel file is connected to COM 12 (communication port), which is where the microcontroller is connected.

From Figure 3.35, it can be shown that the DHT 11, MQ-135, and the MQ-7 are all sensors connected to the microcontroller, whereas the RTC and SD card are modules that are used to record the data.

The power supply block represents the digital device (computer or laptop). The data sent from the system to the digital device was recorded automatically using Excel as well as saved in the SD card placed.

3.1.5.2   The Wireless Connection Setup to Gather the Airflow Data

The only data missing data from the excel table shown in Figure 3.38 is the airflow, which was constructed as a separate circuit as the location of the airflow detector vary with the type of fan used so a different microcontroller was used to detect the airflow.

The coding of the airflow detector is programmed to notify the user whether the hall effect sensor can detect the magnets or not. The connection detection is beneficial to prevent any errors in the data recorded as some cases during airflow detector's rotation, the magnets may shift slightly and thus a loss of connection occurs.

The microcontroller was programmed to show a message " detecting" when a connection is achieved and does not connect when there is no connection (shown in Figure 3.39).

The wireless connection was done via Bluetooth and that is by using a Bluetooth module named "Hc-05", which was connected to the second microcontroller (Arduino) so that the data gathered by the microcontroller was sent to the digital device via Bluetooth.

Figure 3.39: Air flow detection data recorded automatically in excel

The data was shown onto the digital devices by designing an application using MIT App Inventor (shown in Figure 3.40 and Figure 3.41). The MIT App inventor uses graphical user interface and uses Open Blocks Java library to code the function of the application.

The graphical user interface can be shown in Figure 3.40, where the application's design is done, while the block programming is shown in Figure 3.41.
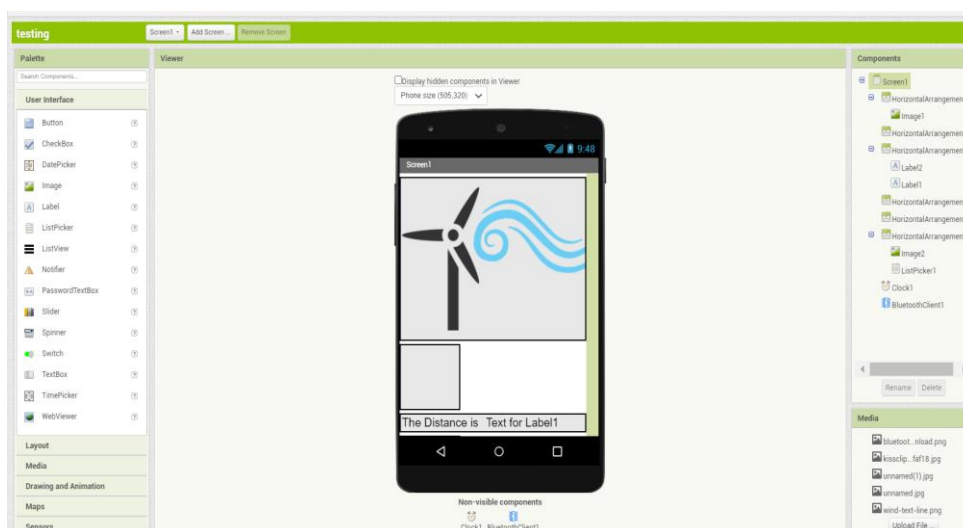
Figure 3.40: MIT App Inventor Designer to design the applications background and illustration
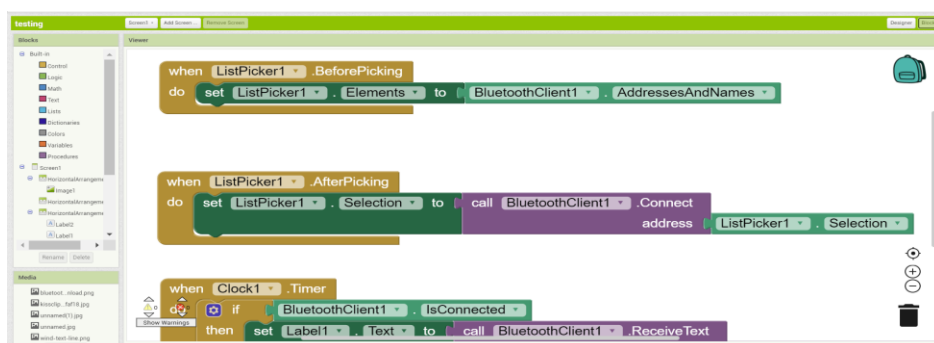
Figure 3.41: MIT App Inventor open blocks Java library to program the application

After the coding was complete, the application successfully displayed the data gathered by the microcontroller onto a digital device (Android and IOS mobile phone) via Bluetooth connection as shown in Figure 3.42.
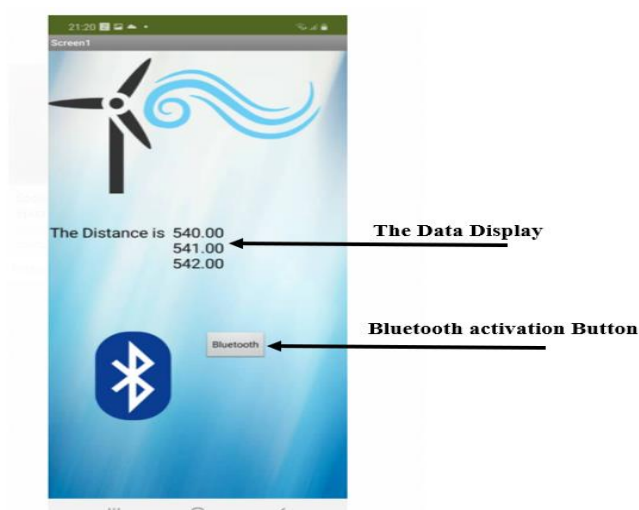
Figure 3.42: The application successfully displaying the data using an Android mobile phone

3.2 Air Quality Monitoring System's Physical Circuit

The air quality monitoring system was constructed to gather the data related to the depiction of concentrations of pollutants and thermal conditions. The physical circuit for the monitoring system as shown in Figure 3.43.

Figure 3.43: The indoor air quality monitoring system physical circuit

Figure 3.43 shows the overall system, where it can be shown that two Blue USB is connected to power the two microcontrollers. The first microcontroller (Arduino 1) was powered by connecting it to a digital device and the data collected was shown in an excel file as shown in Figure 3.38, displaying the CO concentration in ppm, CO2 concentration in ppm, Rzero value, Humidity and temperature.

The second microcontroller (Arduino 2) was connected to a battery making it portable and that data gathered was displayed using the application designed via Bluetooth connection, making it portable. Arduino 2 is only connected to the hall sensor and displays the distance between the magnet and the hall sensor to indicate the room air flow.
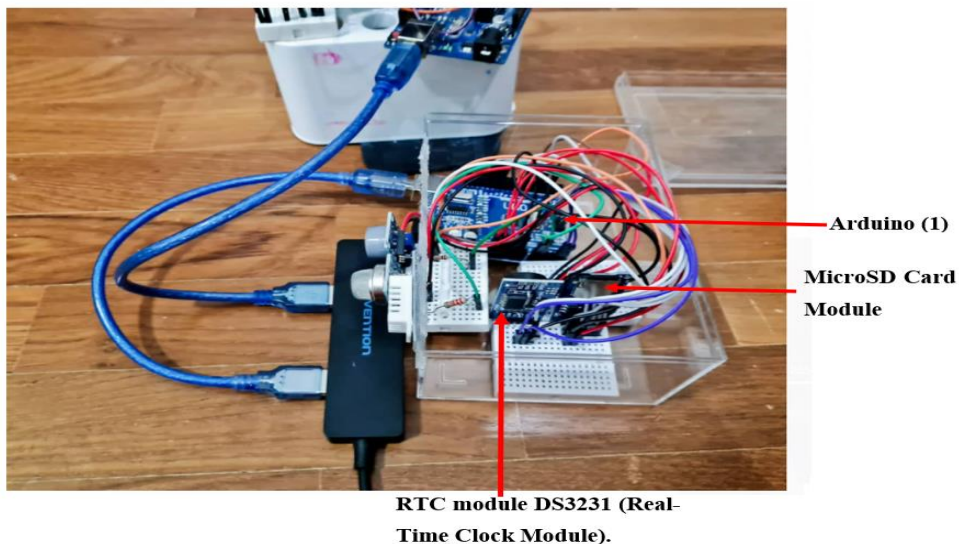
Figure 3.44: Illustration of the SD card and Clock module connection

Figure 3.44 shows the connection of the SD module and the Clock module to the Arduino 1. The SD module works in coordination with the clock module to ensure all the data stored with the date and time of collection.

Figure 3.45 shows the connection of the sensors to the microcontroller, illustrating their location outside the container in order to detect the weather condition correctly, as for Figure 3.46, it shows the hall sensor and distance away from the magnet and wind turbine.
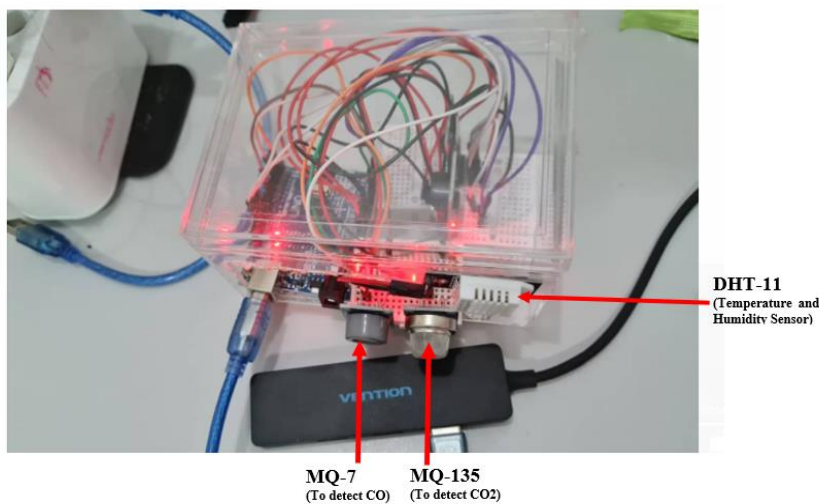
Figure 3.45: Illustration Of MQ-7, MQ-135 And DHT-11 connection (Wired Connection to Digital Device)
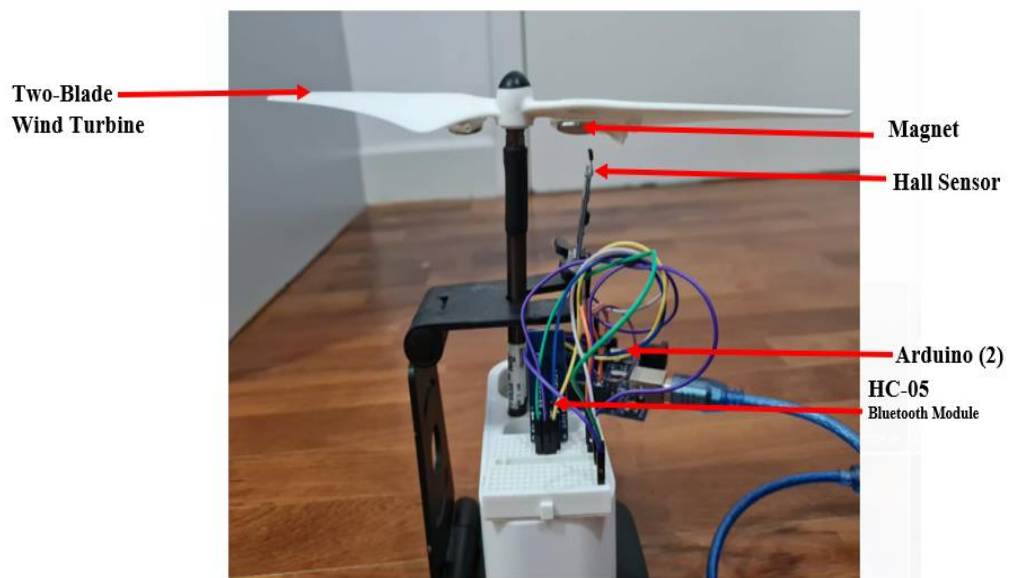
Figure 3.46: The hall sensor connection to the microcontroller (Arduino) and Bluetooth module

3.3 Testing Environment

After successfully activating the air quality monitoring system, the testing focused on gathering data from the master bedroom since it recorded a percentage of 98% in terms of air conditioner activation frequency from a sample number of 332 residents in Malaysia based on a previous research in 2011 (Kubota et al., 2011) (Refer to Figure 2.15).

The replica of the room and the apartment used in the testing was designed as shown in Figure 3.47 to Figure 3.49 for a better optimal experience. The apartment is 1410 sq. Ft with 2 rooms and 2 bathrooms.
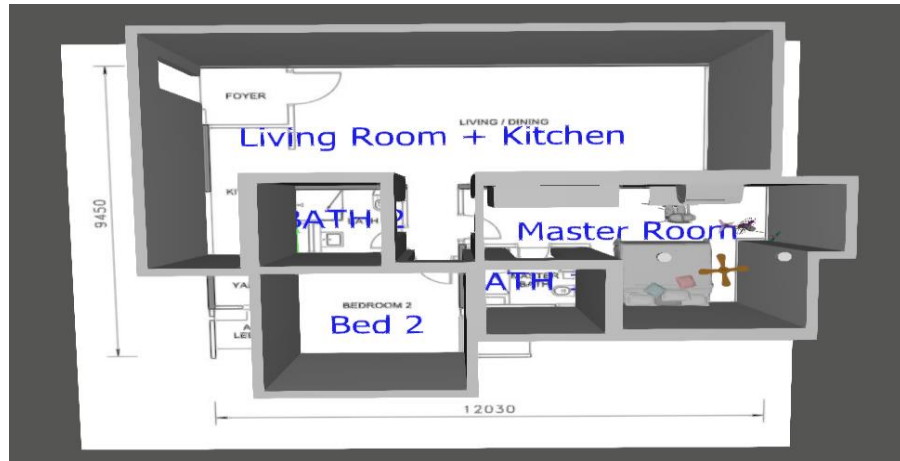
Figure 3.47: Apartment floor plan

Figure 3.48: Master bedroom replica (3D)
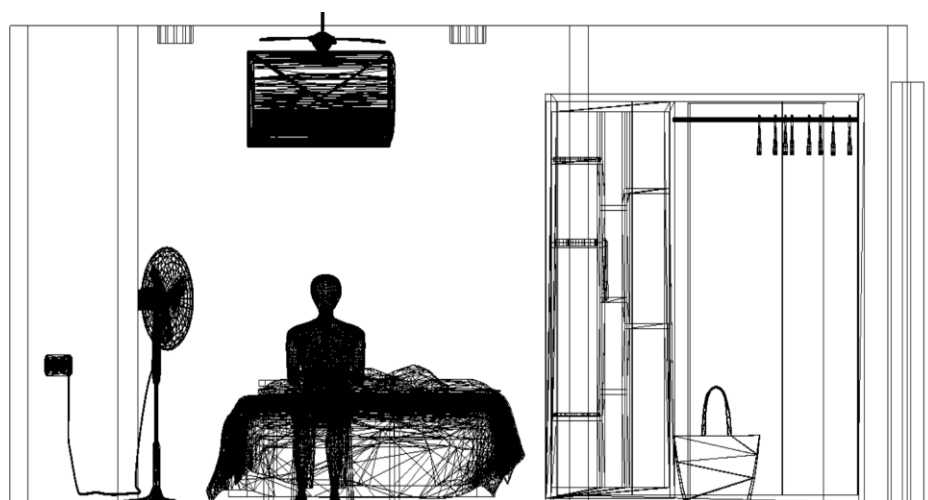
Figure 3.49: Master bedroom replica (2D)

The testing is conducted with the following placements:

- The testing was conducted to illustrate the thermal comfort and indoor air quality for a sitting person in quite position.

- The metabolic rate was fixed at 1met assuming that the volunteer sitting in a quite position practicing exercise with limited movement such as reading, writing or typing onto a digital device.

- The placement of the standing fan is (27-30) inches away from the volunteer, which is approximately 68cm- 76cm.

- The table used have a height of 29.5 inches (74.9cm).

- The clothing level was fixed to be typical summer indoor clothing. which is 0.5 clo according to CBE Thermal Comfort Tool.

- The placement of the hall sensor was placed directly below the fan at position 1 (refer to figure 3.23), so the sensor was adjusted on the bed to measure the rooms air flow (shown in Figure 3.48)

- The detection for the other environmental elements was done by placing the rest of the sensors and Arduino 1 onto the desk to indicate the air quality situation at the same position as the sitting resident (shown in Figure 3.48)

Figure 3.50: Testing dimension and circuit position

3.4   Thermal Comfort Analysis

After collecting the data using the indoor air quality, the thermal comfort condition is analysed by using the PMV method, which was done using the CBE Thermal Comfort Tool.

The CBE Thermal Comfort Tool allows the user to input all five thermal comfort parameters, which are humidity, operative temperature, airflow, metabolic rate and the clothing level and illustrates the output in the form of a psychrometric chart that indicates the range of temperature and humidity levels that are comfortable to the occupant as shown in Figure 3.51.

The Thermal comfort tool indicates the PMV/PPD value as well as highlighting the comfort zone range in blue (shown in Figure 3.51). The tool also shows whether the weather conditions comply with the chosen standard or not.
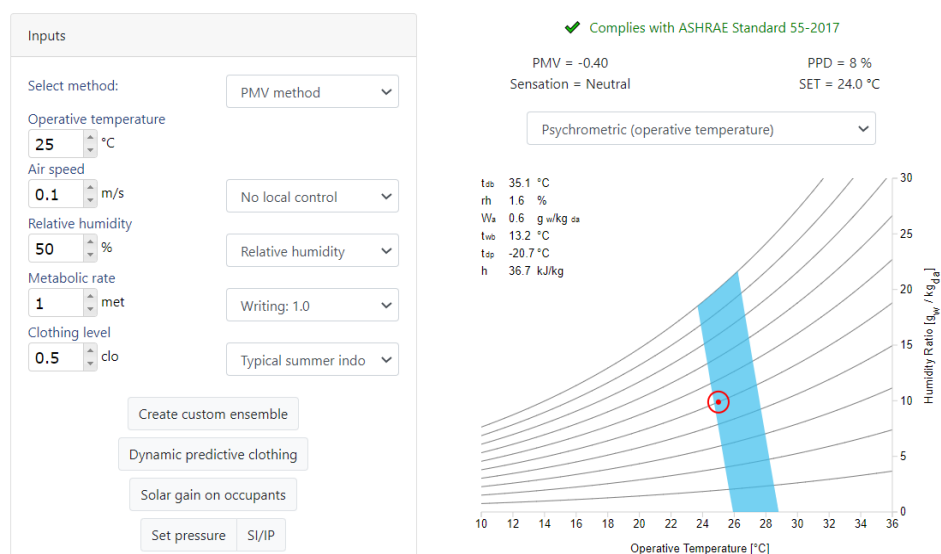
Figure 3.51: Temperature-Humidity Psychrometric Chart (ASHRAE-55)

Figure 3.51 shows an example, where the PMV was calculated to be -0.4 and the PPD was 10% and according to the ASHRAE-55, a range from -0.5 to 0.5 of PMV with a PPD equalling or less than 6% has to be followed so. Therefore, the conditions placed are complying within the ASHRAE standards.

As for the EN-16798, a Temperature-Humidity psychrometric chart, however, six parameters are used instead since the EN-16798 takes into consideration the air temperature and the ambient temperature, which in other words is the outdoor temperature and indoor temperature as shown in Figure 3.52.

The EN-16798 follows range from -0.7 to 0.7 of PMV with a PPD equalling or less than 15% has to be followed, and that explains why the thermal condition was described as Neutral (complied EN-16798) when the PMV was recorded as 0.53 and PPD of 11% in the example shown in figure 3.52.
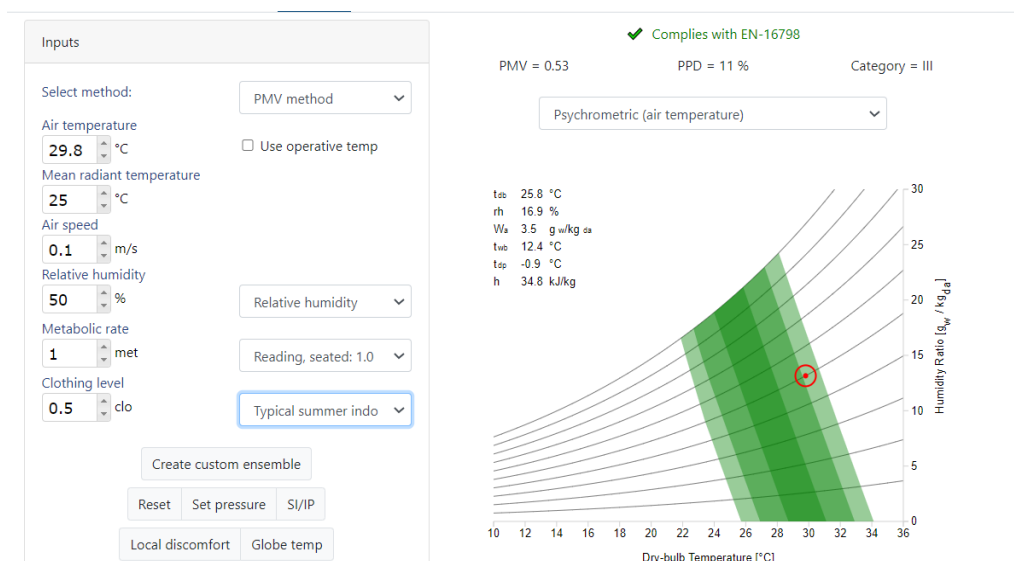
Figure 3.52: Temperature-Humidity Psychrometric chart (EN-16798)

During this research, the PMV and PPD values was collected by using this thermal tool, keeping in mind that the PMV and PPD values remain unchanged whether it's using the ASHRAE-55 standard or EN-16798 under the same weather conditions.

The only change is whether the PMV and PPD values comply with both of them, one of them or with neither of them as shown in Figure 3.53.

Figure 3.53: Thermal Comfort Tool following ASHRAE-55 (A) And EN-16798(B) at the same weather conditions

3.5 **Fan Motor Control Strategy Based on Collected Data**

The speed control of the fan motor according to environmental conditions, was done through PWM (Pulse Width Modulation) signal. The PWM refers to the method of applying a signal with a changeable width to the motor to control its speed by controlling its activation and deactivation time (Arredondo et al., 2004).

The PWM signals complete duty cycle is 100%, where the fan is operated 100% of the time and is never closed. When the duty cycle is decreased, the activation time will decrease and deactivation time with an increase, for example, an 50% duty cycle meaning that the fan is activated 50% of the time and turned off 50% of the time that can be shown in figure 3.54.

The PWM signal's duty cycle is proportional to the fan speed, so any increase to the duty cycle will increase fan speed, and vice versa and that feature was utilized to control the motor (Arredondo et al., 2004).
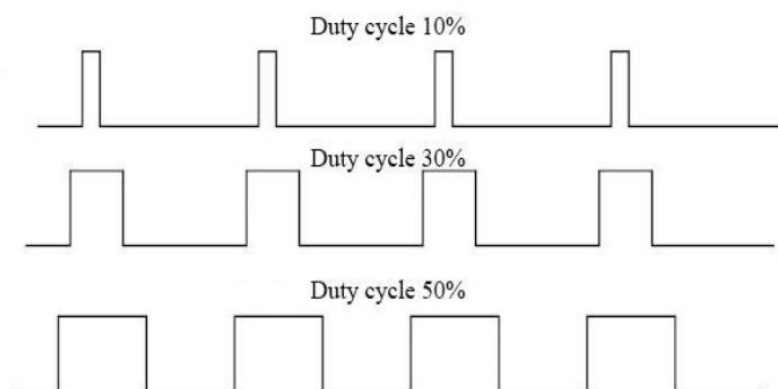
Figure 3.54: PWM duty cycle examples (Zur et al., 2019)

The same method was used in a research conducted in 2017, where a single-phase induction motor's speed was controlled by varying the duty cycle of the PWM. The research also plotted the relationship between the duty cycle and both speed and voltage as shown in Figure 3.55.

Figure 3.55 A, shows the voltage increase proportionally with the increase of duty cycle, where its y-axis represents the voltage in Volt and the x-axis represents the duty cycle in percentage, while Figure 3.55 B, shows the proportional relationship between speed and the duty cycle (Manickam, 2017). The same concept was used to control the fan in this experiment.
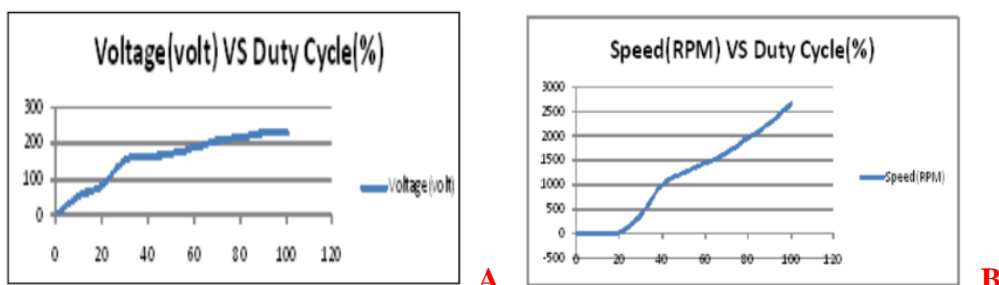
Figure 3.55: (A) Voltage Vs Duty Cycle Plot And (B) Is Speed Vs Duty Cycle Plot (Manickam, 2017)

As for the direction of the fan system, the usage of an H-bridge electronic circuit was used, which allows to control the direction of the motor to run in either forward or backward direction.

The H-bridge consist of 4 switches with work in synchronize with each other to control the motor, for example when switch 1(S1) and switch 4 (S4) are closed, the motor will rotate in clockwise direction as shown in Figure 3.56.

Results	S1	S2	S3	S4
Forward	1	0	0	1
Reverse	0	1	1	0
Motor free	0	0	0	0
Motor brake	0	1	0	1
Motor brake	1	0	1	0
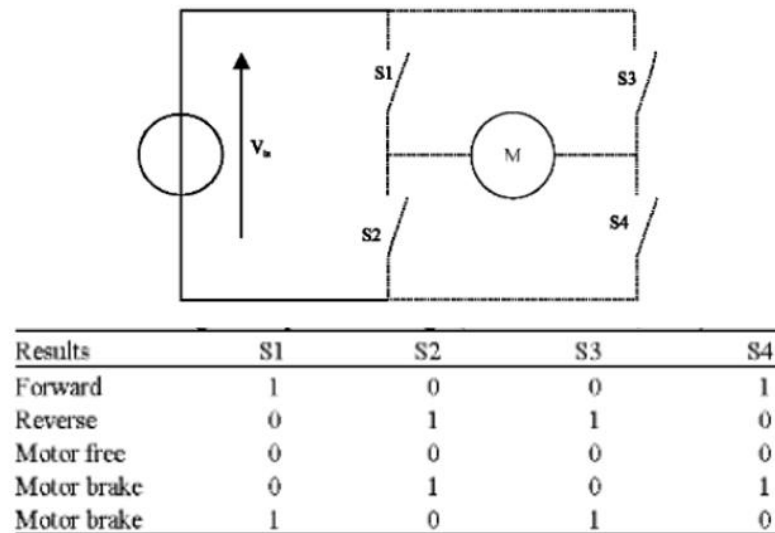
Figure 3.56: H Bridge circuit (Raheem Hatem, 2019)

Nevertheless, the motor controlled is a fan motor and the need for direction change is not necessary therefore only the clockwise direction was used in this experiment.

3.6 Energy Efficient Temperature and Humidity Based Fan System Framework Architecture

The Temperature and humidity fan system controls the speed of the fan by relying on the weather changes occurring in the surrounding environment to achieve both thermal comfort and indoor air quality.

The two main variables controlling the speed of the fan are the humidity and temperature. At the same time, the rest of the variables such as airflow, CO_2 level and CO level was monitored throughout the fan system's operation to ensure its control within the ASHRAE 55 and EN 16798 Standards.

The signals coming from the four sensors was transferred to a microcontroller to conduct the computation and produce the outcome accordingly. The outcome was transferred later on to a decoder to change the result to a set of signals capable of controlling the speed and direction of the fan system as shown in Figure 3.57.

The system also included a second microcontroller that is in charge of receiving the signals from the decoder and controlling the speed of the motor by generating the suitable PWM duty cycle as discussed in section 3.5 and managing the direction by sending a signal to the H-bridge drive as discussed in section 3.5.

In addition to controlling the fan motor, the system also involved a set of alert LEDs to signal if the room environment is no longer suitable for human occupancy and can result in health complications if the situation continued as shown in Figure 3.57.
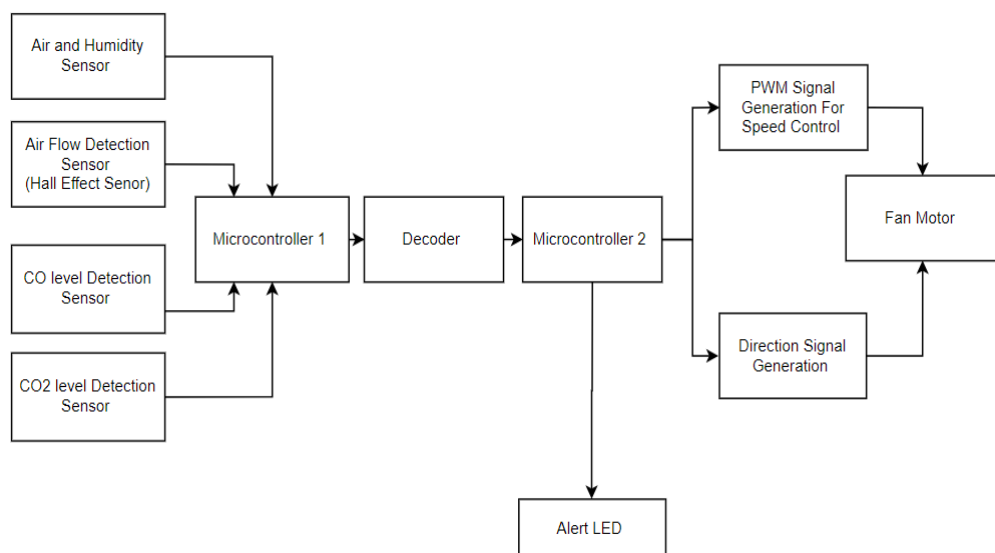
Figure 3.57: Energy Efficient Temperature and Humidity Based Fan System framework architecture

CHAPTER 4

RESULTS

4.1   Overview of Results Chapter

In this Chapter, three different case studies were discussed and analyzed. The first case studied the changes in weather condition when the door is open and closed. While the second and third cases studied the environmental changes on two different weeks during different ceiling fan and standing fan speed levels.

The three case studies helped obtain the final benchmark-setting that achieved both IAQ and thermal comfort, which later assisted in designing the humidity and temperature fan system.

After completing the three case studies, the energy-saving was estimated and discussed to illustrate the environmental fan's benefits. Finally, the fan system circuit structure was designed according to the results obtained, demonstrating the changes in the environmental fan speed according to different weather changes.

4.2   Testing Results

4.2.1   Case Study 1: Open Door Vs Closed Door Testing

The first testing was done to compare between the indoor air quality conditions when the door is closed and when the doors is opened to provide the best indoor air quality conditions for the occupant. The comparison was done in terms of temperature, Humidity, CO_2 level and CO level.
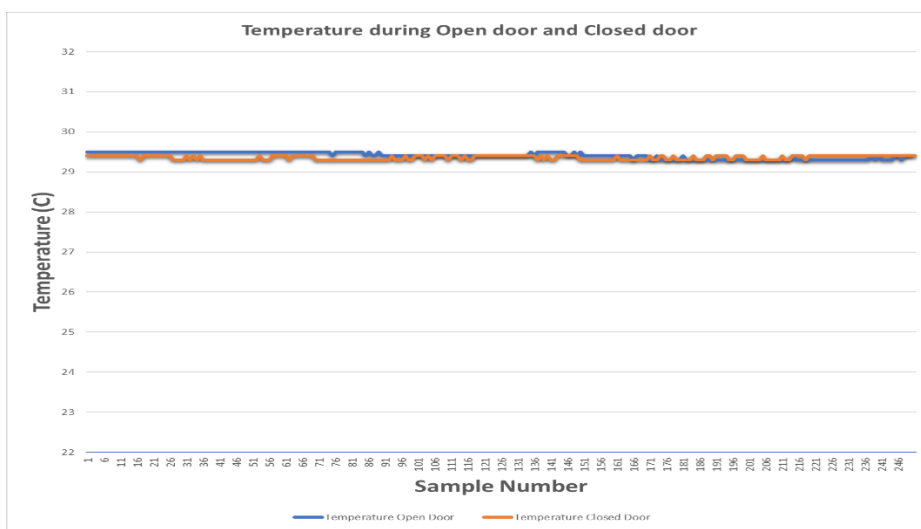
Figure 4.1: Temperature Levels During Open-Door and Closed-Door Conditions
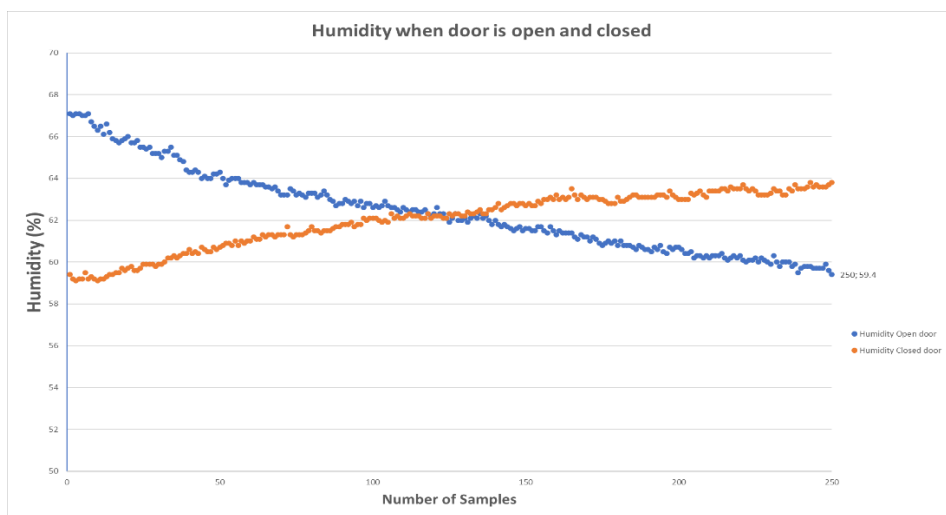
Figure 4.2: Humidity levels during Open-Door and Closed-Door conditions
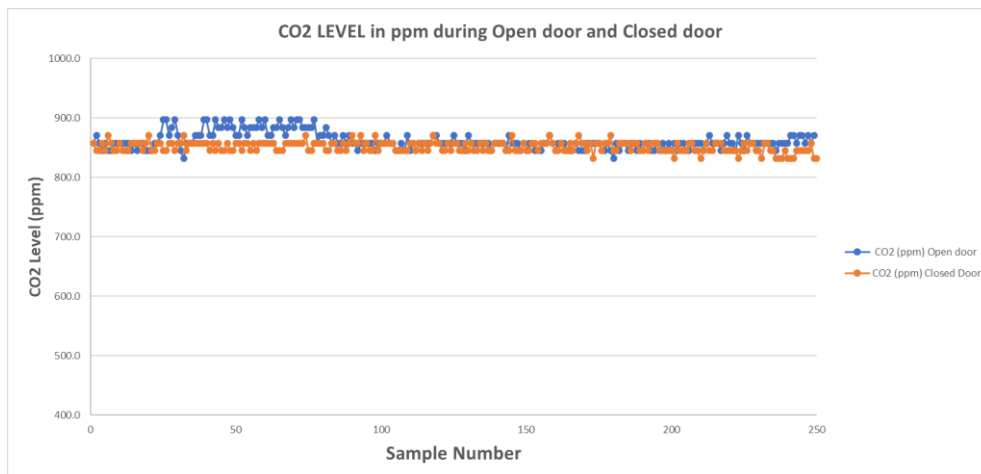
Figure 4.3: CO2 levels during Open-Door and Closed-Door conditions
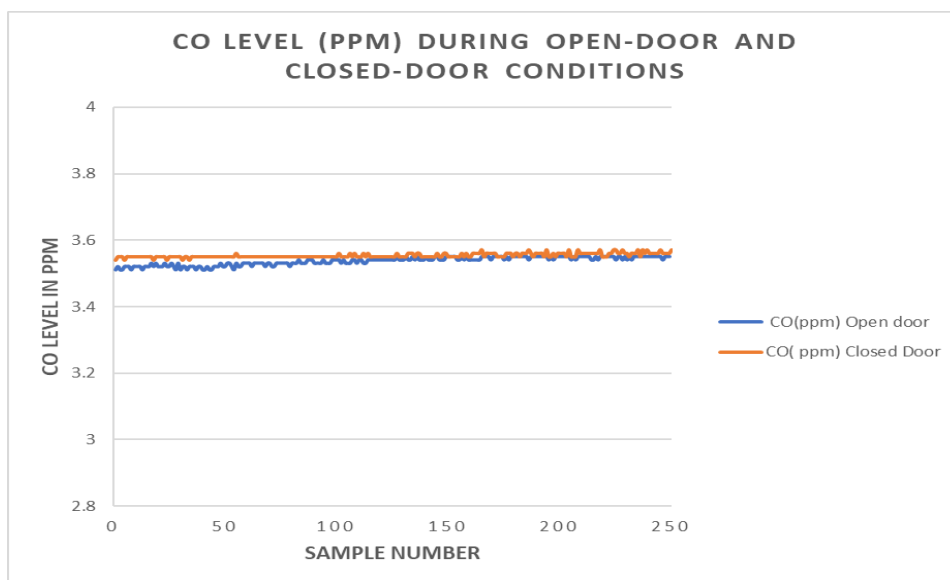
Figure 4.4: CO levels during Open-Door and Closed-Door conditions

From the comparison between the open-door and closed-door conditions, it can be shown that the temperature did not change over the 250 samples as shown in Figure 4.1; however, a clear change can be shown in terms of humidity levels, indicating that the humidity during open-door condition gradually decreases from 67% to 59.4%. whereas the closed-door state records a slow increase in humidity levels from 59% to 63.9% as shown in Figure 4.2.

As for the CO2 and CO levels illustrated in Figures 4.3 and Figure 4.4, no change can be noticed during the 250 samples taken. Therefore, the door remained open during the rest of the testing to achieve the best humidity level for the occupant and achieve a better thermal comfort condition.

4.2.2 Indoor Air Quality and Thermal Comfort Testing Procedure

In this research, two weeks of testing was conducted. The testing involved two reference points; the first reference point represented the weather condition before the ceiling fan activation while the second reference point represented the weather condition before the standing fan activation to assist in the before/after comparison.

All the tests included the temperature, humidity, CO2 level, CO level measurements at different fan levels followed by the PMV calculation through the CBE Thermal Comfort Tool that reflected its compliance with ASHRAE Standard 55-2017 and EN-16798.

The beginning of all the trials started at speed level 1, whether with the usage of ceiling fan or standing fan. In contrast, the end is when the environmental conditions comply with both standards, therefore no need to increase the fan speed any further.

All data were represented through daily, and weekly plots for comparison purposes except for day 1, where the data table was included in detail to thoroughly explain how the plots were drawn

4.2.2.1 Case Study 2: Week 1 Indoor Air Quality and Thermal Comfort Analysis at Different Ceiling Fan and Standing Fan Speed Levels

4.2.2.1.1 Testing on 18-Oct-2020 (Day 1)

Table 4-1: Day 1 Testing Data (18-Oct-2020)

	CEILING FAN								
	Ref 1 Point Pre-testing: Temp= 35.2 C° Humidity =50% Co2 = 616 ppm CO = 3.27ppm								
	Fan Speed		**Temperature(C°)**	**Humidity (%)**	**CO2 (ppm)**	**CO (ppm)**	**Wind speed**	**PMV**	**Sensation**
18-Oct (Outside) **28°C** **77%**	Level 1	Average	33.82	46.15	273.8	3.285	0.768 m/s	1.38	Slightly warm (Doesn't Comply)
	Level 2	Average	31.0336	58.6156	248.6	3.289	1.02 m/s	0.7	Slightly warm (Doesn't Comply)
	Level 3	Average	30.6944	52.9672	282.6	3.305	1.27 m/s	0.48	Neutral (Does comply)
	STANDING FAN								
	Ref 2 Pre-testing: Temp =30.4 C° Humidity=53% CO2=285,7ppm CO=3,248ppm								
	Fan Speed		**Temperature(C°)**	**Humidity (%)**	**CO2 (ppm)**	**CO (ppm)**	**Wind speed**	**PMV**	**Comment**
	Level 1	Average	30.172400	51.2096	290.74	3.2847	0.47 m/s	0.63	Slightly warm (Doesn't Comply)
	Level 2	Average	30.0648	49.1656	295.65	3.2987	0.52 m/s	0.36	Neutral (Does comply)

From Table 4.1, it can be shown that there are two reference point, the first is the weather conditions pre-ceiling fan activation and the second is the pre-standing fan activation. Other data involve the fan speed, temperature, humidity, CO2, CO and wind speed as well as the PMV and the sensation, which were plotted along with the reference point for comparison in two different charts, one representing the ceiling fan and the other representing the standing fan as shown in Figure 4.5.

(A)   (B)
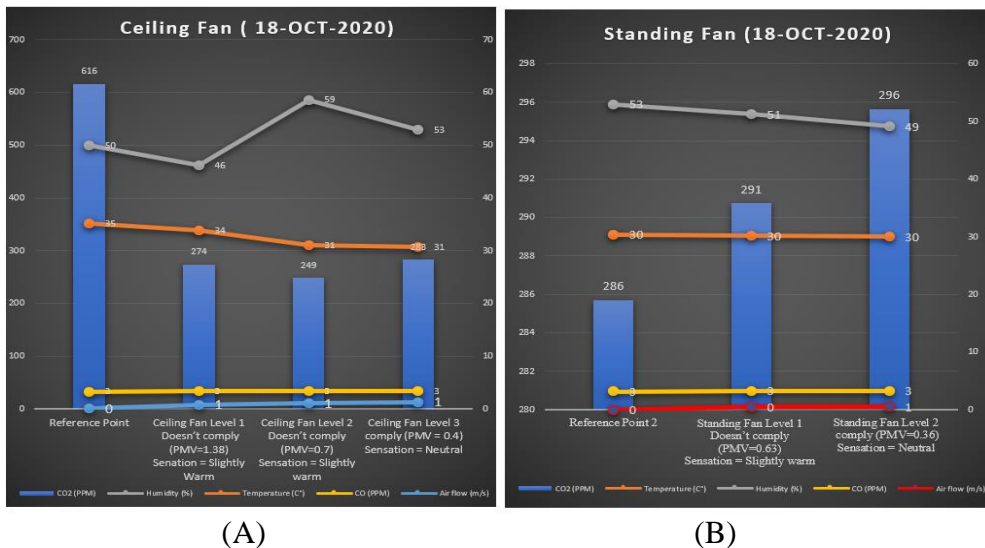
Figure 4.5: Ceiling Fan Data (A) and Standing Fan Data (B) (18-OCT-2020)

The figure above represents the changes in terms CO2, temperature, humidity, CO and airflow at different fan speed level when using a ceiling or a standing fan. Both graphs plot the reference point as well to see whether an improvement or deterioration occur in terms of air quality situation before and after activation to help choose the most suitable fan type and set acceptability limits in terms of thermal comfort and air quality according to the data collected.

4.2.2.1.2 Testing on 19-Oct-2020 (Day 2)
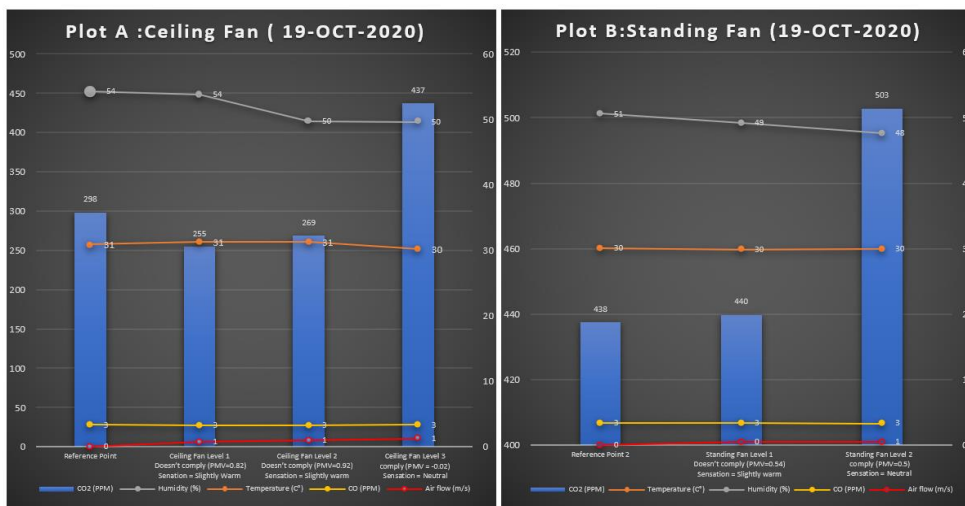
Figure 4.6: Ceiling Fan Data (A) and Standing Fan Data (B) (19-OCT-2020)

4.2.2.1.3 Testing on 20-Oct-2020 (Day 3)
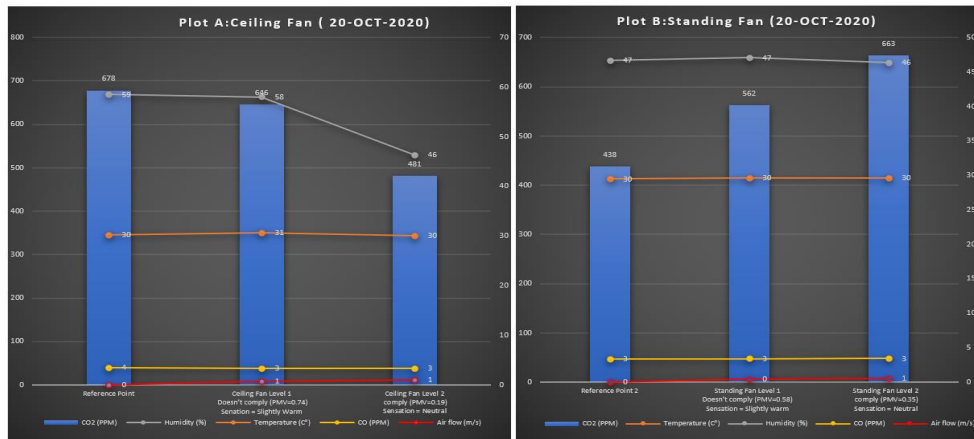
Figure 4.7: Ceiling Fan Data (A) and Standing Fan Data (B) (20-OCT-2020)

4.2.2.1.4 Testing on 21-Oct-2020 (Day 4)
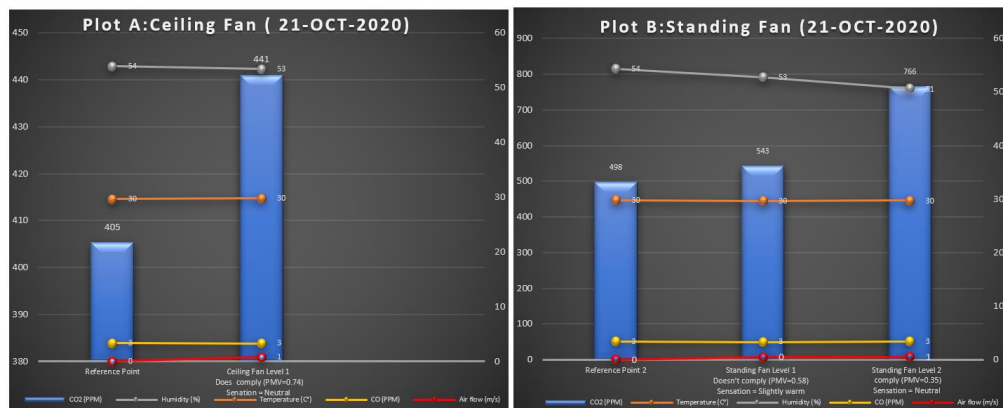
Figure 4.8: Ceiling Fan Data (A) and Standing Fan Data (B) (21-OCT-2020)

4.2.2.1.5 Testing on 22-Oct-2020 (Day 5)
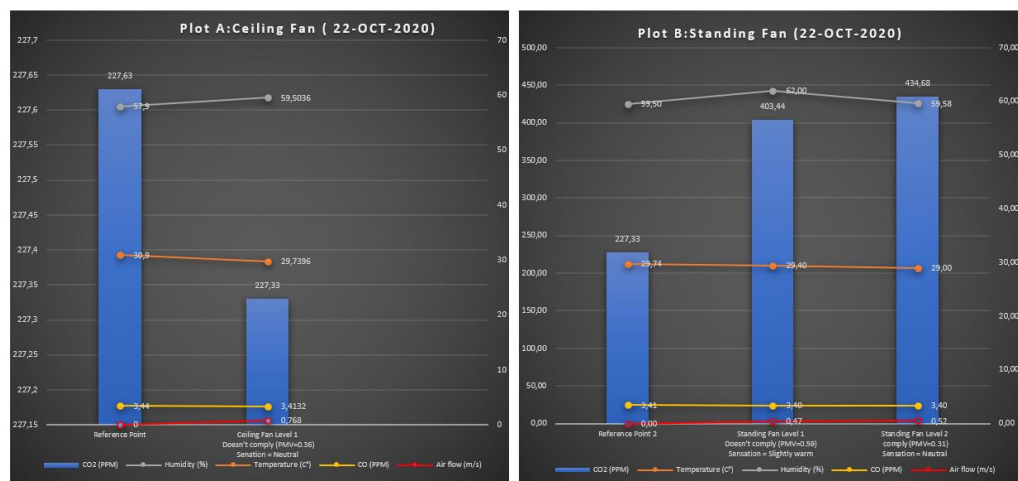
Figure 4.9: Ceiling Fan Data (A) and Standing Fan Data (B) (22-OCT-2020)

4.2.2.1.6 Testing on 23-Oct-2020 (Day 6)
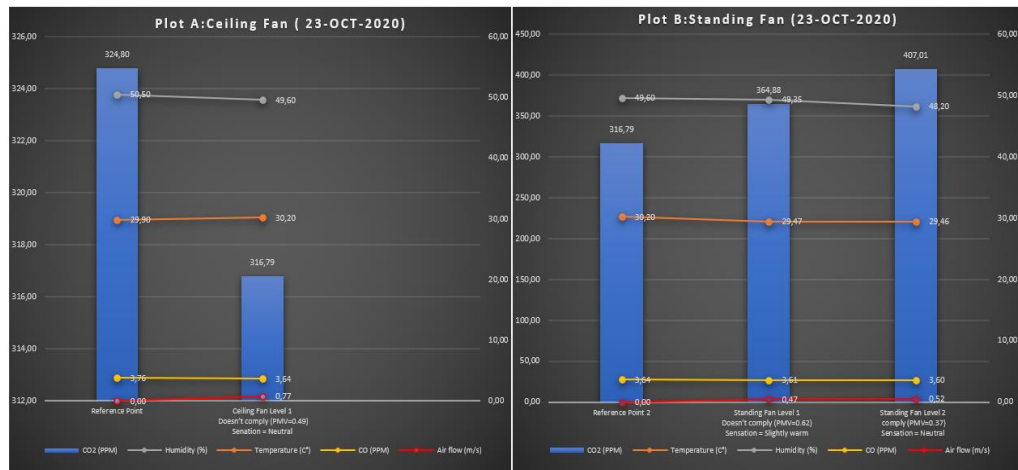
Figure 4.10: Ceiling Fan Data (A) and Standing Fan Data (B) (23-OCT-2020)

4.2.2.1.7 Testing on 24-Oct-2020 (Day 7)
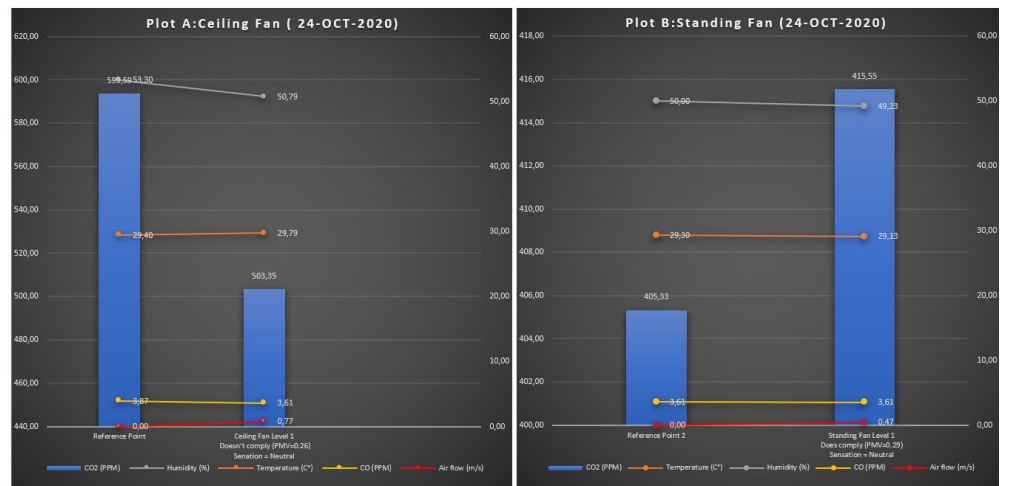
Figure 4.11: Ceiling Fan Data (A) and Standing Fan Data (B) (24-OCT-2020)

4.2.2.1.8 Summary for First Week Testing
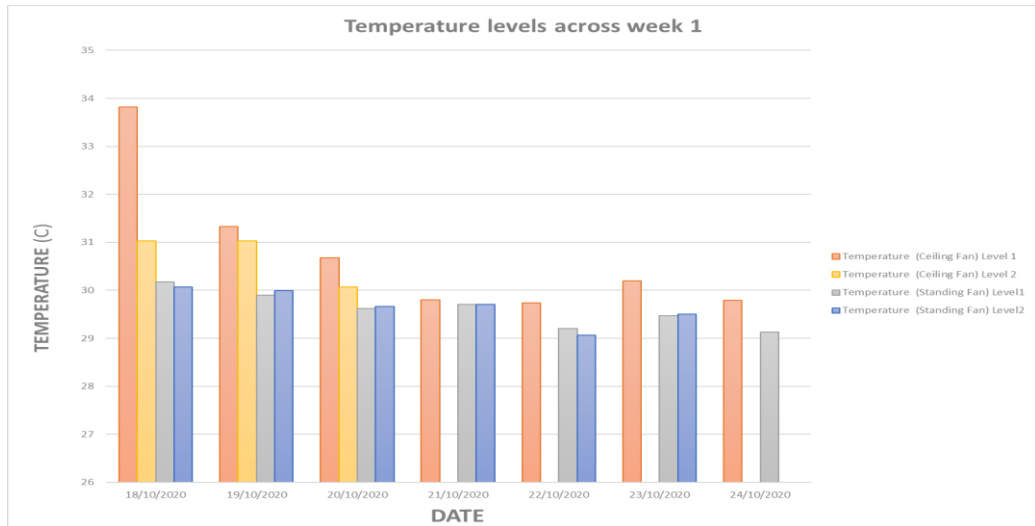
Figure 4.12: Temperature Levels at Different Fan Levels Across Week 1
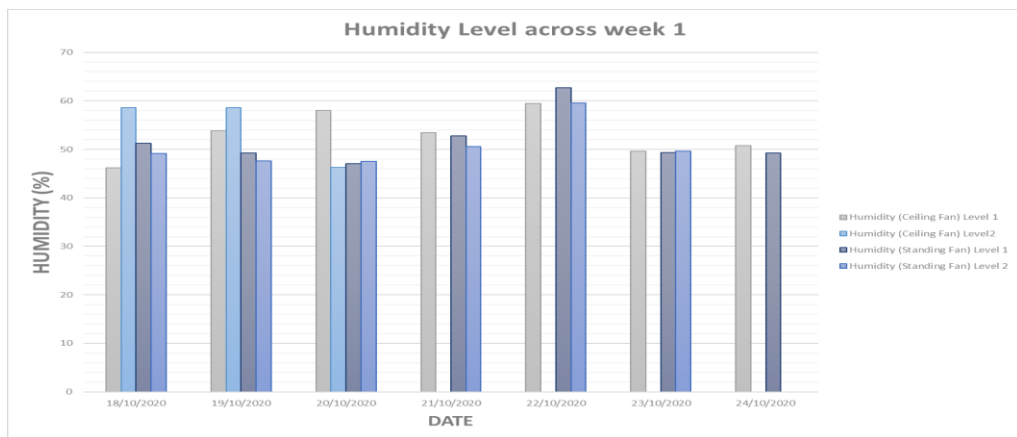
Figure 4.13: Humidity Levels at Different Fan Levels Across Week 1
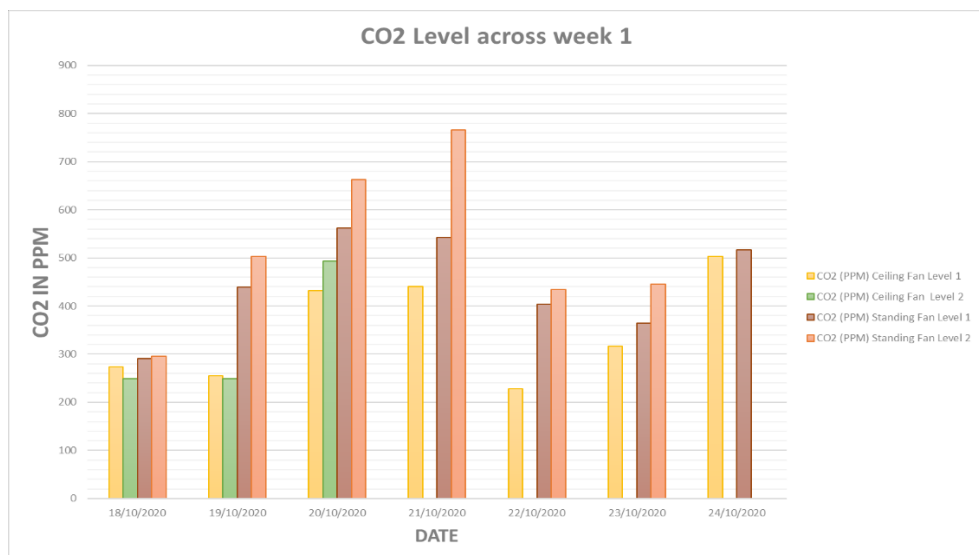
Figure 4.14: CO2 Levels at Different Fan Levels Across Week 1
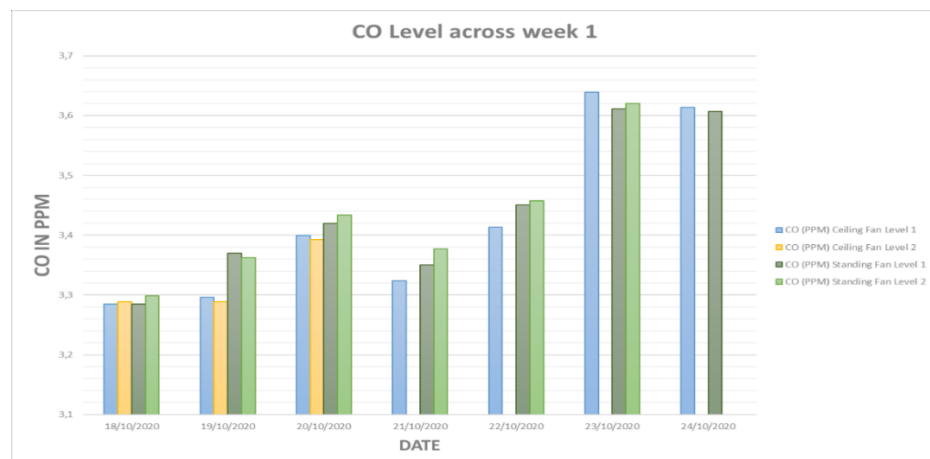
Figure 4.15: CO Levels at Different Fan Levels Across Week 1

The first week's results showed that both the humidity and temperature decrease as the fan speed level increases, whether using the ceiling fan or the standing fan. The results also that the temperature and humidity when using the standing fan were recorded to be less than the temperature and humidity level when using the ceiling fan, making the standing fan a better option in terms of thermal comfort.

As for indoor air quality, the ceiling fan was chosen to be a better option since the level of CO_2 was recorded at a higher level when using the standing fan than that of the ceiling fan. In contrast, the CO level doesn't differ much between the standing fan and ceiling fan condition, making CO_2 level the main concern for indoor air quality and occupants' health status.

Therefore, the standing fan can be categorized as a better option for thermal comfort but increases the carbon dioxide concentration, whereas the ceiling fan can achieve a better thermal comfort state without degrading the indoor air quality, however, another week of testing was conducted to support the first week's findings.

4.2.2.2   Case Study 3: Week 2 Indoor Air Quality and Thermal Comfort Analysis at Different Ceiling Fan and Standing Fan Speed Levels

4.2.2.2.1   Testing on 28-Oct-2020 (Day 8)
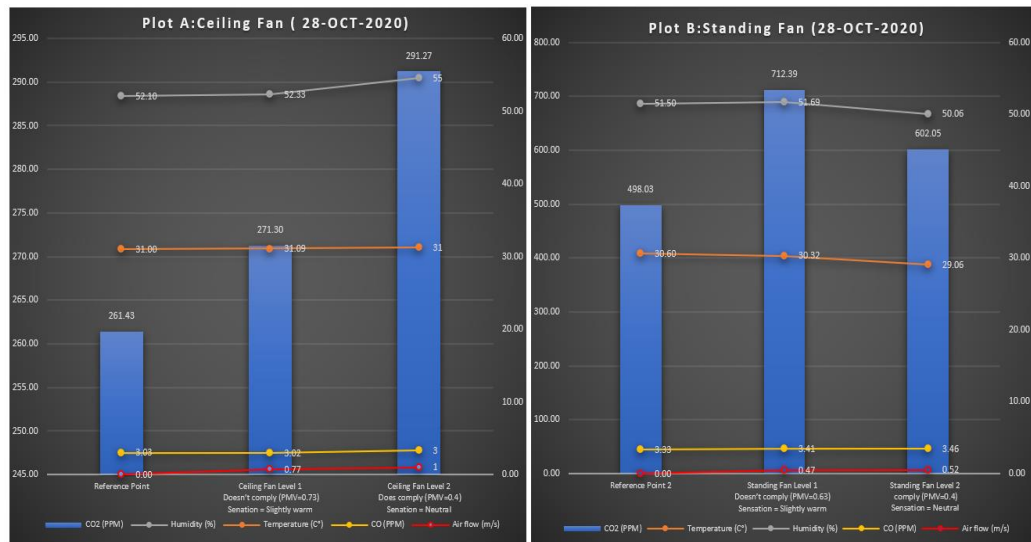
Figure 4.16: Ceiling Fan Data (A) and Standing Fan Data (B) (28-OCT-2020)

4.2.2.2.2   Testing on 29-Oct-2020 (Day 9)
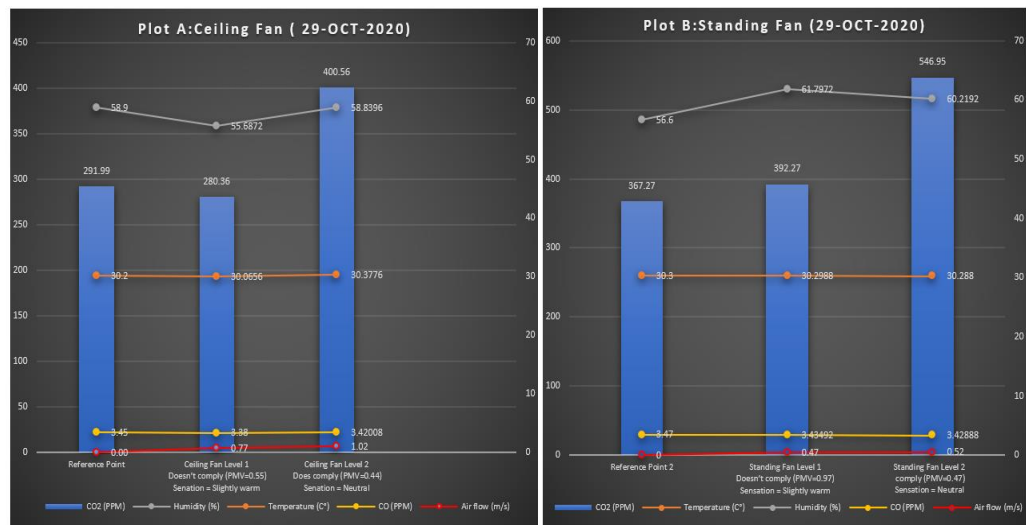
Figure 4.17: Ceiling Fan Data (A) and Standing Fan Data (B) (29-OCT-2020)

4.2.2.2.3 Testing on 31-Oct-2020 (Day 10)
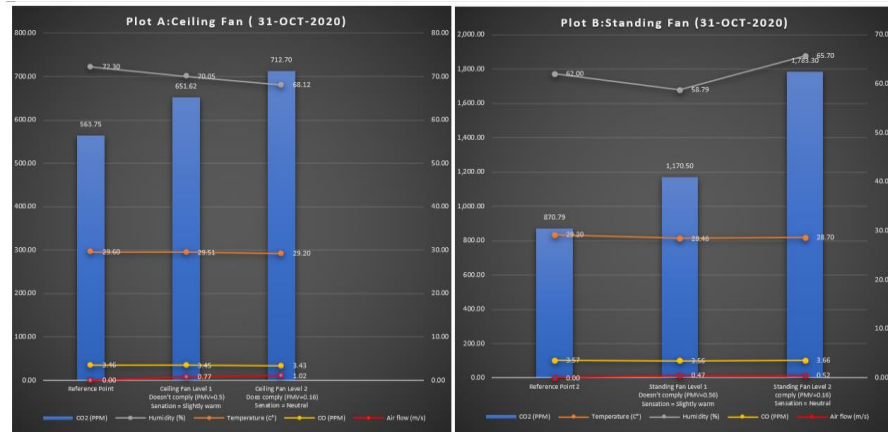
Figure 4.18: Ceiling Fan Data (A) and Standing Fan Data (B)(31-OCT-2020)

4.2.2.2.4 Testing on 1-Nov-2020 (Day 11)
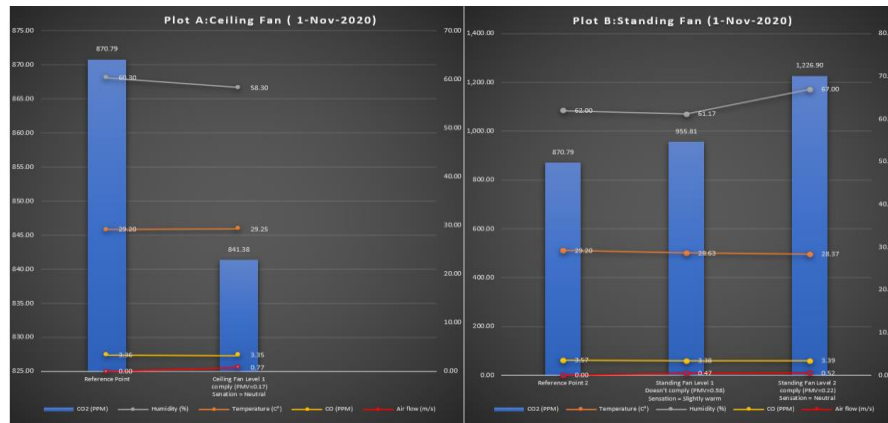
Figure 4.19: Ceiling Fan Data (A) and Standing Fan Data (B)(1-NOV-2020)

4.2.2.2.5 Testing on 2-Nov-2020 (Day 12)
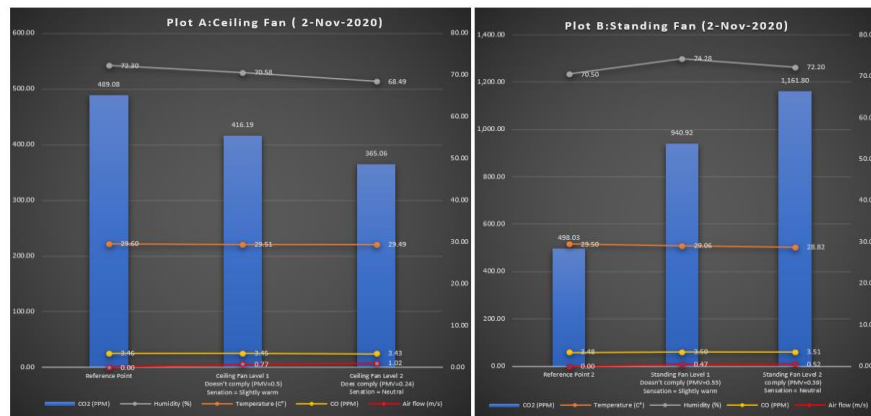
Figure 4.20: Ceiling Fan Data (A) and Standing Fan Data (B)(2-NOV-2020)

4.2.2.2.6 Testing on 3-Nov-2020 (Day 13)
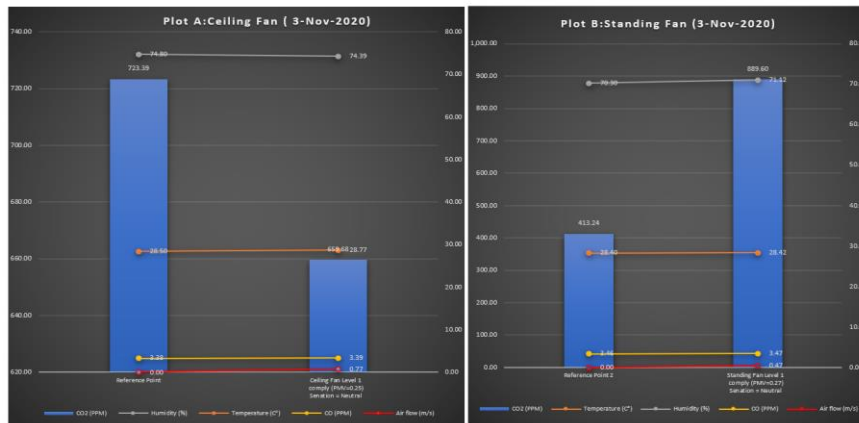
Figure 4.21: Ceiling Fan Data (A) and Standing Fan Data (B)(3-NOV-2020)

4.2.2.2.7 Testing on 4-Nov-2020 (Day 14)
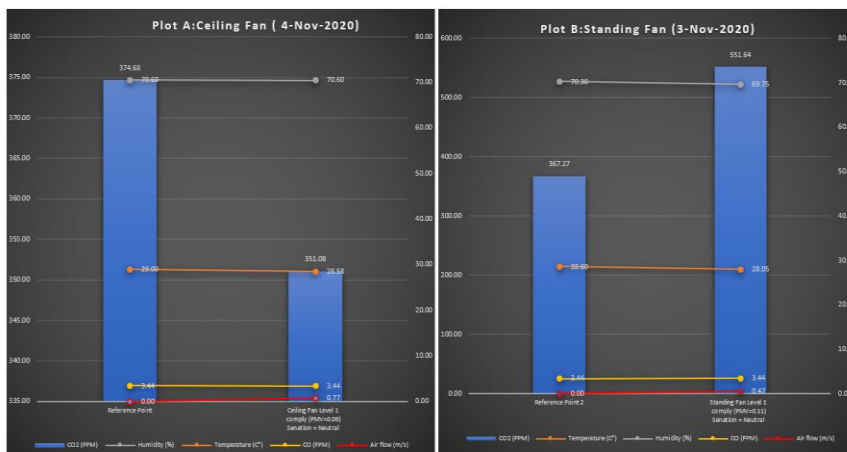
Figure 4.22: Ceiling Fan Data (A) and Standing Fan Data (B)(4-NOV-2020)

4.2.2.2.8 Summary for Second Week
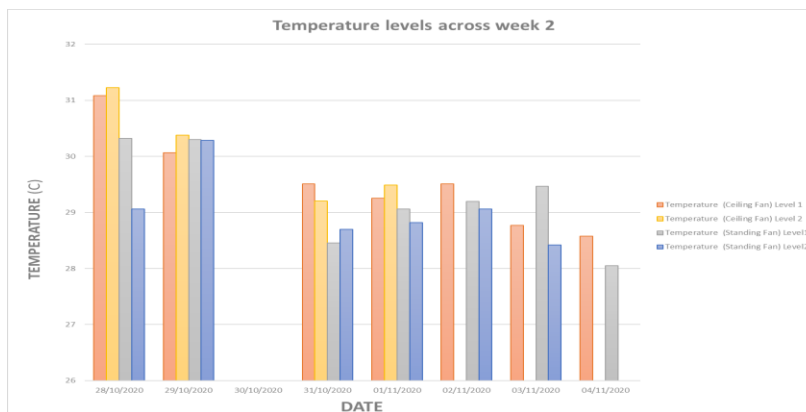
Figure 4.23: Temperature Levels at Different Fan Levels Across Week 2
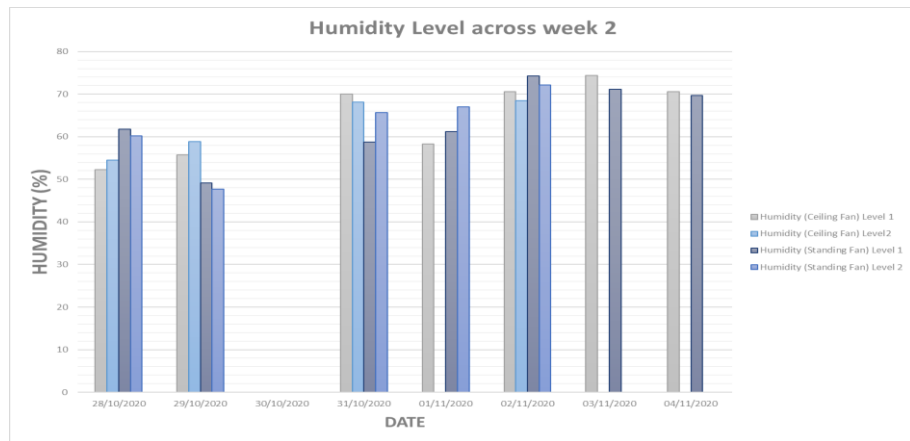
Figure 4.24: Humidity Levels at Different Fan Levels Across Week 2
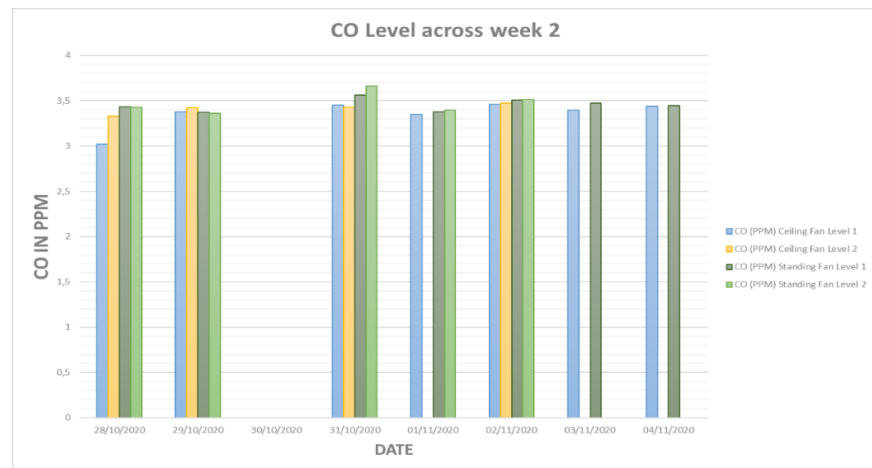
Figure 4.25: CO Levels at Different Fan Levels Across Week 2
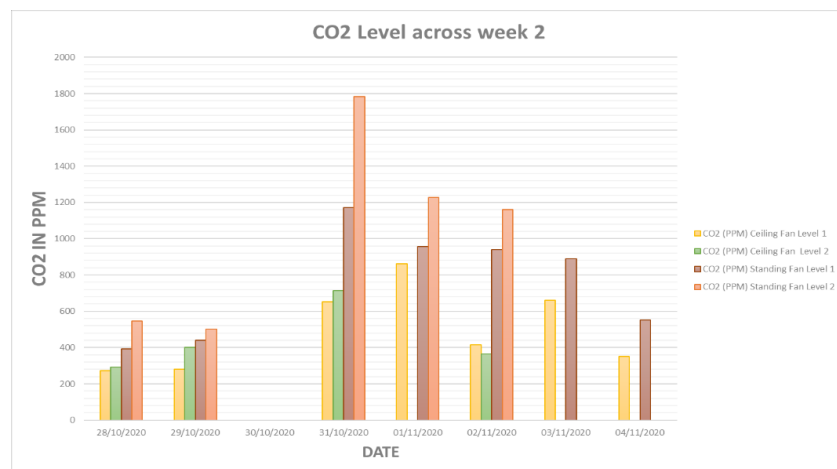
Figure 4.26: CO2 Levels at Different Fan Levels Across Week 2

The results obtained from week 2 are similar to week 1, showing that the temperature level reduces significantly when using a standing fan than when using a ceiling fan. The results have also shown that the CO_2 level increases substantially with a standing fan's usage, unlike the ceiling fan, where the CO_2 level changes are moderately acceptable.

Based on ICOP 2010, the CO_2 level is deemed to be acceptable when it is below 850ppm, which the indoor air quality complied to in week 1; however, in week 2, the CO_2 level has increased beyond that on the days from 31st October to 2nd November when using a standing fan.

The days between 31st October and 2nd November can be described as muggy days compared to the rest of the testing days since the humidity outdoors fluctuated between 70%-80% with a temperature of 32°C during testing (Refer to Appendix A). Still, despite the stuffy weather condition, ceiling fans managed to maintain the CO_2 levels within acceptable limits on the opposite of standing fans, where the CO_2 level surpassed 1000 PPM (shown in Figure 4.25).

After completing the 2-week testing, an investigation was done to understand why the CO_2 level increases substantially when using a ceiling fan. Despite finding no previous research explaining the logical reason for the CO_2 rate's escalation, previous research has discussed the disadvantages of standing fans, mentioning that it has caused dehydration and increased convective heat gain by blowing hot air over the body (Eyy and GuptaS, 2017)

The previous research also highlighted that the standing fan has more disadvantages than benefits during a heatwave, explaining why the CO2 level increased so dramatically when the temperature was 32°C. The research also emphasized that further research has to be conducted regarding electric standing fan disadvantages as limited data was found (Eyy and GuptaS, 2017).

Therefore, the ceiling fan was chosen as most suited to use in the temperature and humidity-based fan system for indoor environmental quality improvement as it provides both thermal comfort and indoor air quality.

4.2.3 The Benchmark Results for the Developed Energy Efficient Temperature and Humidity Based Fan System

From the results obtained from case 2 and case 3, the benchmark was developed, which is shown in Table 4-2. The table lists down the 11 main conditions that cover all the weather conditions that might be encountered and their corresponding fan speed that can achieve thermal satisfaction and occupant satisfaction following both the ASHRAE 55-2017 standard and the EN-16798 standard.

In conditions, where no fan speed can achieve thermal satisfaction, the ceiling fan is turned off as the need for air conditioner activation is crucial for the occupant's health.

The case condition 9 and 10 were listed down to ensure that indoor air quality is achieved by maintaining the CO_2 level below 800ppm and CO level below 8.7ppm following Table 2-4.

As for the final case, an alert turns on when the humidity is above 75% since no fan speed can ensure thermal comfort and it is beyond the ICOP limit of 70% as shown in Table 2-3. Hence sensors were connected to the fan motor to ensure that the speed level of the fan will change according to the benchmark setting and guarantee both indoor air quality satisfaction and thermal comfort at all times.

Table 4-2 : The benchmark results obtained from the two week analysis In Case 2 And Case 3

Case	Temperature (C°)	Humidity (H)	CO2 Value (PPM)	Air Flow m/s	Ceiling Fan level	PMV Max at H=75%	PPD Max at H=75%	ASHRAE Standard 55-2017	EN-16798	Comment
Case 1	=>32	>20%	<850	N/A	No-Fan	N/A	N/A	Does not Comply	Does not Comply	Need to activate Air Con
Case 2	31	>51%	<850	N/A	No-Fan	N/A	N/A	Does not Comply	Does not Comply	Need to activate Air Con
Case 3	31	<=50%	<850	1.27	Level 3	0.48	10%	Comply	Comply	
Case 4	30	<70%	<850	1.02	Level 2	0.48	10%	Comply	Comply	
Case 5	29	<75%	<850	0.768	Level 1	0.30	7%	Comply	Comply	
Case 6	28	<75%	<850	0.768	Level 1	-0.08	5%	Comply	Comply	
Case 7	27	<75%	<850	0.768	Level 1	-0.44	7 %	Comply	Comply	
Case 8	=< 26	<75%	<850	<0.768	Natural Ventilation	N/A	N/A	Comply	Comply	
Case 9	CO2 level beyond 800ppm will activate LED and stop fan for Alert purposes									
Case 10	CO level beyond 8.7 ppm will activate LED and stop fan for Alert purposes									
Case 11	Humidity level beyond 80 % will activate LED and stop fan for Alert purposes									

4.3 The Energy Efficiency Analysis

Fans are designed to provide its peak performance when the fan is running at full speed (100%), and the peak performance will consume high energy consumption, running cost and a reduction in the fan's expected life.

Pulse Width Modulation (PWM) is the method that was used to control the speed of the fan by reducing the amount of energy transferred to the fan through a rapid circulation between the on and off condition.

Hence by varying the PWM signals duty cycle, the fan speed can be controlled. In this experiment, the fan used is a ceiling fan with five-speed levels, so by considering the PWM signals complete duty cycle is 100%, where the fan will rotate at maximum speed at 100% (level 5) and a minimum rate at 0% (not activated), meaning that each speed level differs from the other by a duty cycle

$$\text{of } \frac{Pwm\ complete\ Duty\ Cycle}{number\ of\ speed\ levels} = \frac{100\%}{5\ levels} = 20\%. \tag{4.1}$$

Based on Table 4-2, only three fan speed levels are used instead of five, meaning that only 60% of the duty cycle will be needed and that will cause a reduction in energy consumption and cost as shown in Figure 4.27 and Table 4-3. Figure 4.27, illustrates the power efficiency at different fan speed level, highlighting a power saving of approximately 80% is achieved when setting the fan speed at level 1 when compared to the fan's maximum power consumption level.

The power-saving is approximately 60% and 40% when setting the fan at level 2 and level 3 respectively, summarising that the environmental fan system will not be operating the ceiling fan at its maximum power potential thus resulting in power consumption of 40% to 80%, a reduction in energy consumption and cut in the electricity bill.
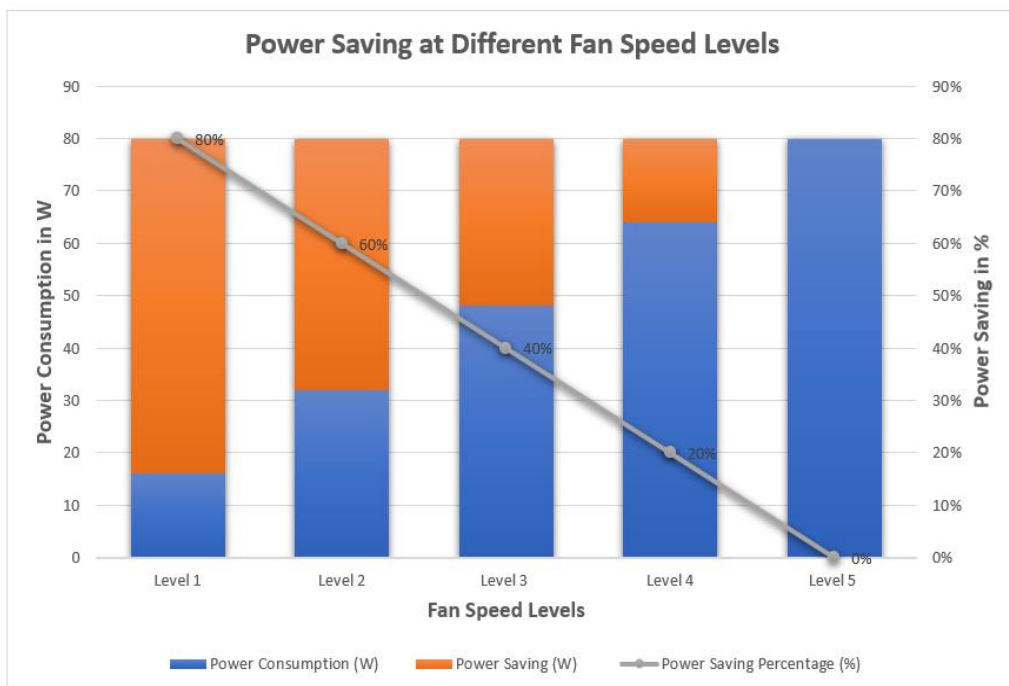
Figure 4.27: Plot illustrating the power saving at different fan levels

Table 4-3: Energy saving at different fan levels

Fan Speed	Power Consumption (W)	Power Saving (W)	Power Saving Percentage (%)	Duty Cycle (%)
Level 1	16	64	80%	20
Level 2	32	48	60%	40
Level 3	48	32	40%	60
Level 4	64	16	20%	80
Level 5	80	0	0%	100

In addition to the reduction of the fan speed level, the reliance on air conditioners is reduced to a large extend as only 2 cases out of 11 requests to open an air conditioner, whereas 6 cases out of 11 rely solely on fan usage as shown in Table 4-2. As for the last 3 cases, it is emergency cases where the weather condition will damage the human's health.

Thus, under normal circumstances without considering emergency cases, an overall of only 2 cases require activation of air conditioner out of 8. In contrast, the rest will rely on a ceiling fan, making the percentage of air conditioner usage limited to only 25% of the time.

When referring to previous research mentioned in section 1.1 general introduction that 70% of the time is spent at home (Argunhan and Avci, 2018)., which is approximately 17 hours a day so air conditioner operation will be limited to 4 and a half hours, which is a reduction of 30% of air conditioner usage since the average daily use in Malaysia is 6 hours Based on EnerDemand (The Global Efficiency and Demand Database).

To illustrate the difference of energy consumption, different types of air conditioner with different energy rating labels was used as an example as shown in Table 4-4. The power consumption for each air conditioner mentioned in Table 4-4 is for a 1 ton split AC and the data are based on Bureau of Energy Efficiency (BEE) sample of hourly power consumption (BEE, 2001).

Table 4-4: Energy saving before and after Environmental fan usage

Energy Rating Labels	Air conditioner's Ton	Hourly Power Consumption (Wh)	Energy Consumption before environmental fan usage (kWh)	Energy Consumption After environmental fan usage (kWh)	Energy saving
1 Star	0.5 (2HP)	677	6 hours ×677= 4.06	4.5 hours ×677= 3.06	24.63%
2 Star	0.5 (2HP)	639.5	6 hours × 639.5= 3.84	4.5 hours × 639.5= 2.88	25.00%
3 Star	0.5 (2HP)	587	6 hours × 587=3.55	4.5 hours × 587=2.64	25.63%
4 Star	0.5 (2HP)	550	6 hours × 550= 3.3	4.5 hours × 550= 2.48	24.85%
5 Star	0.5 (2HP)	532.5	6 hours × 532.5= 3.195	4.5 hours × 532.5= 2.39	25.20%
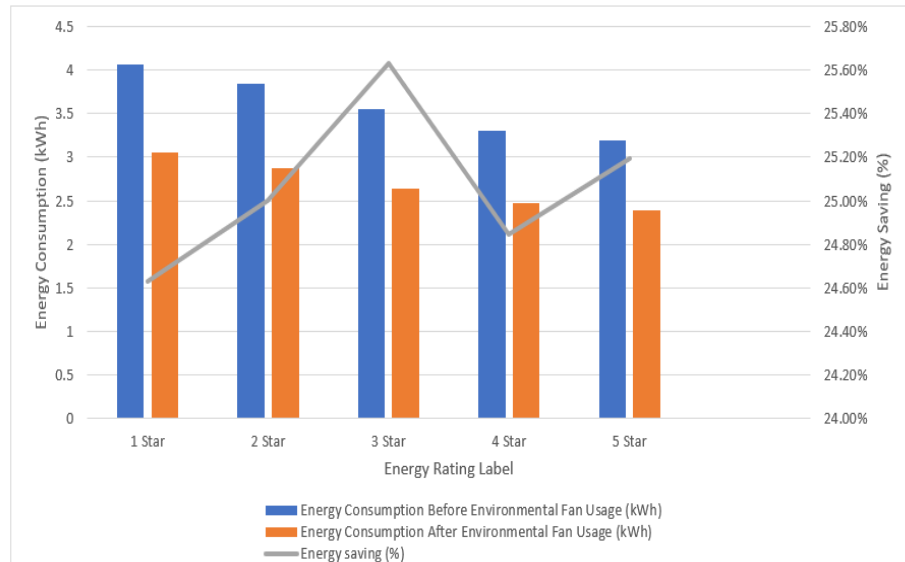
Figure 4.28: Energy saving before and after Environmental fan usage

Table 4-4 and Figure 4.28 illustrates the energy saving that ranges between 24% to 25% of the total energy consumption at different energy rating for the same type of air conditioner, which will result in a noticeable reduction of electricity bill costs as well.

4.4 Energy Efficient Temperature and Humidity Based Fan System Virtual Simulation

To ease the understanding of the temperature and humidity-based fan system, a virtual circuit was designed and simulated to illustrate the results. The system designed follows the hardware architecture in Figure 3.35, which includes four different sensors, the airflow detection sensor, humidity and temperature sensor, CO sensor and CO_2 sensor to monitor the indoor air quality and thermal comfort and control the fan speed accordingly as shown in Figure 4.29.

The four sensors are connected to a microcontroller (Arduino) to process the input and give three outcome signals (pins D9, D10, D11), which are connected to a 3-8 decoder to control the motor based on the cases mentioned in Table 4-2.

The 3-8 decoder is connected to the second microcontroller (Pic16F877A), which processed the input to control the motor accordingly. The instructions of control are shown in Table 4-3, where A, B, C represents the input of the decoder used, and Y0-Y7 represents the outcome of the decoder as shown in Table 4-3.

The motor was controlled by the second microcontroller (PIC16F877A), by relying on the decoder's outcome and adjusting the duty cycle accordingly as shown in Figure 4.29.

Table 4-5: 3-8 Decoder's input and output setting for motor speed adjustment

Input			Output								
A	B	C	Y0	Y1	Y2	Y3	Y4	Y5	Y6	Y7	
0	0	0	1	0	0	0	0	0	0	0	Case 1, Case 2 (0%)
0	0	1	0	1	0	0	0	0	0	0	Case 9 (0%)
0	1	0	0	0	1	0	0	0	0	0	Case 10 (0%)
0	1	1	0	0	0	1	0	0	0	0	Case 11 (0%)
1	0	0	0	0	0	0	1	0	0	0	Case 8 (fan level 1 duty cycle 20%)
1	0	1	0	0	0	0	0	1	0	0	Case 5, Case 6, Case 7 (fan level 1 duty cycle 20%)
1	1	0	0	0	0	0	0	0	1	0	Case 3 (fan level 3 duty cycle 60%)
1	1	1	0	0	0	0	0	0	0	1	Case 4 (fan level 2 duty cycle 40%)
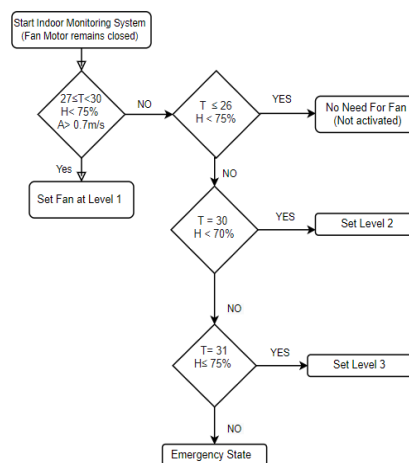
Figure 4.29: Energy Efficient Temperature and Humidity Based Fan System's Flowchart
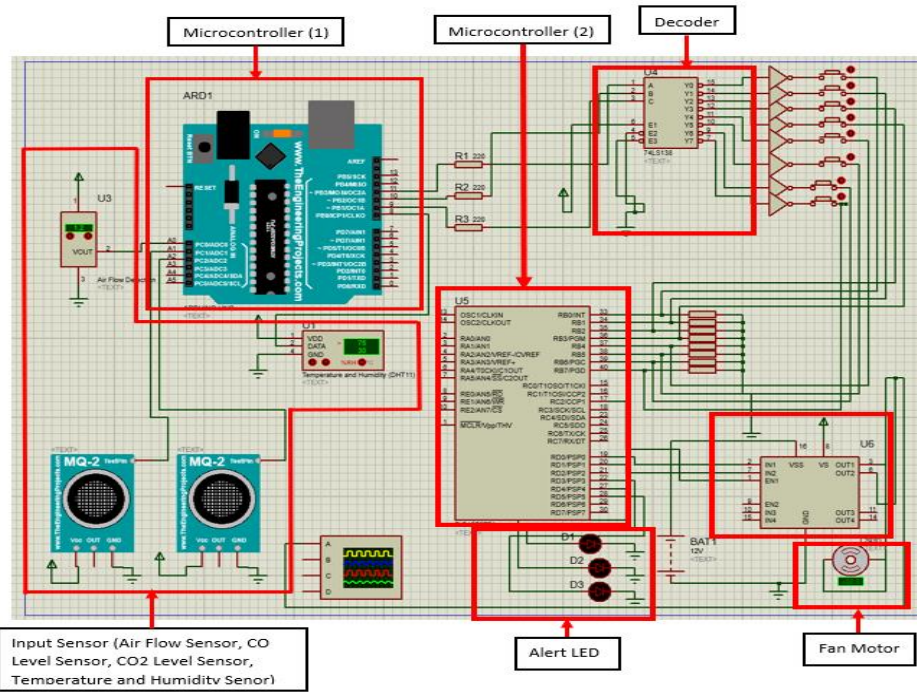
Figure 4.30: Energy Efficient Temperature and Humidity Based Fan System illustrating main structure
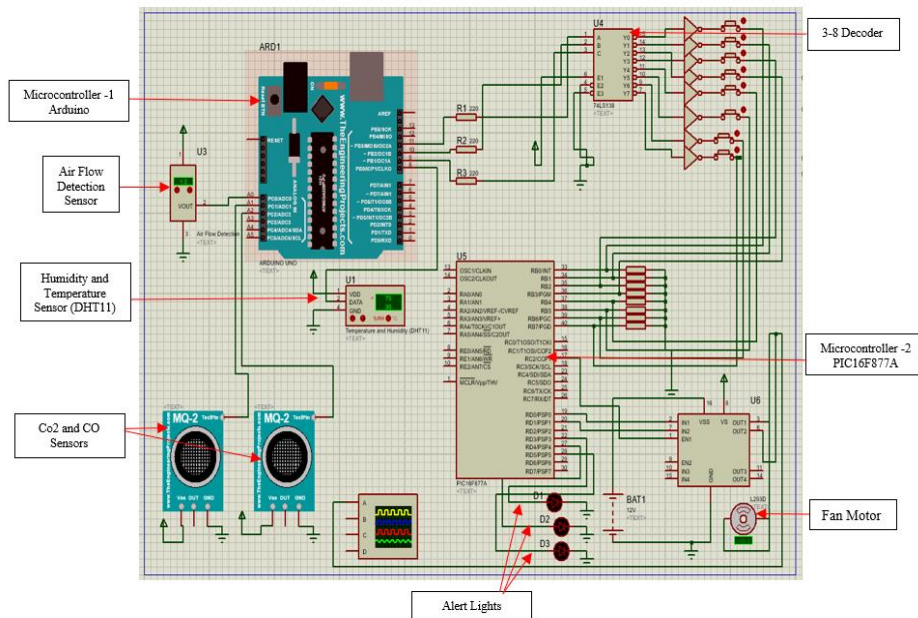
Figure 4.31: Energy Efficient Temperature and Humidity Based Fan System illustrating the main components

An oscilloscope channel A was connected to the fan's motor to indicate the motor's speed at different senor settings. The maximum speed of the motor used in the Proteus software is rated at 180 (Angle adjustment rating).

So, when adjusting the duty cycle at 20%, the resulting motor speed angle ranged between 37 to 39. In comparison, a duty cycle of 40% adjusted the motor speed angle at a range between 75 to 79, and finally, a duty cycle of 60% changed the motor speed angle at a range between 112 to 118.

As for the negative sign shown in the angle is because the fan was programmed to rotate Counter-clockwise, since the fans in summer are set to rotate Counter-clockwise direction for a cooling breeze below the fan.

4.4.1   Duty Cycle 20% Simulation

The first simulation testing was done by setting Case 8, where the input to the decoder is 100 (Arduino outcome signal is D9 =1 D10 = 0 D11 = 0) as shown in Figure 4.32 and the outcome of the decoder sets the duty cycle of the motor at 20% as shown in Table 4.5.
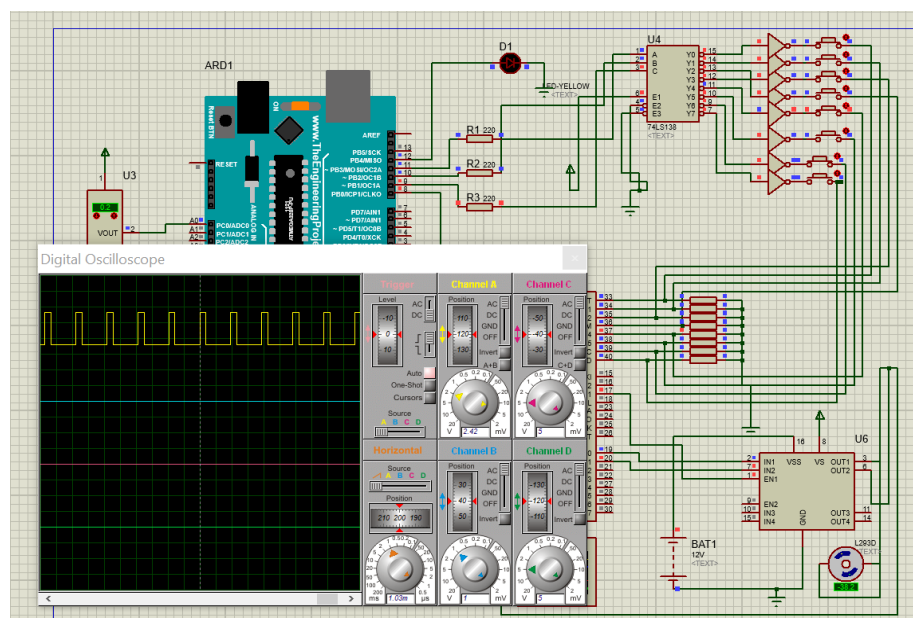
Figure 4.32: Oscilloscope illustration of 20% duty cycle with a motor speed angle of 38.2

4.4.2   Duty Cycle 40% Simulation

The second simulation testing was done by setting Case 4, where the input to the decoder is 111 (Arduino signal is D9 =1 D10 = 1 D11 = 1) as shown in Figure 4.33 and the outcome of the decoder sets the duty cycle of the motor at 40% as shown in Table 4.5.
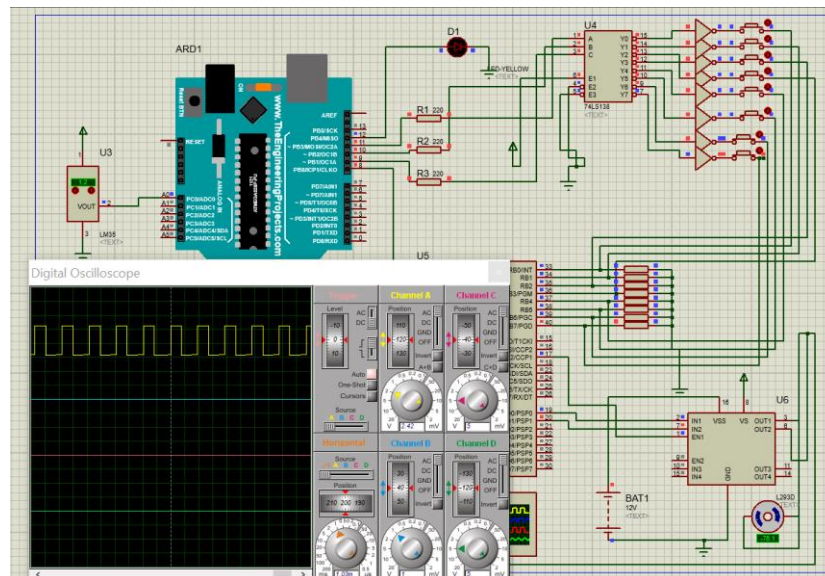
Figure 4.33: Oscilloscope illustration of 40% duty cycle with a motor speed angle of 76.1

4.4.3   Duty Cycle 60% Simulation

The Third simulation testing was done by setting Case 3, where the input to the decoder is 110 (Arduino signal is D9 =1 D10 = 1 D11 = 0) as shown in Figure 4.34 and the outcome of the decoder sets the duty cycle of the motor at 60% as shown in Table 4.5.
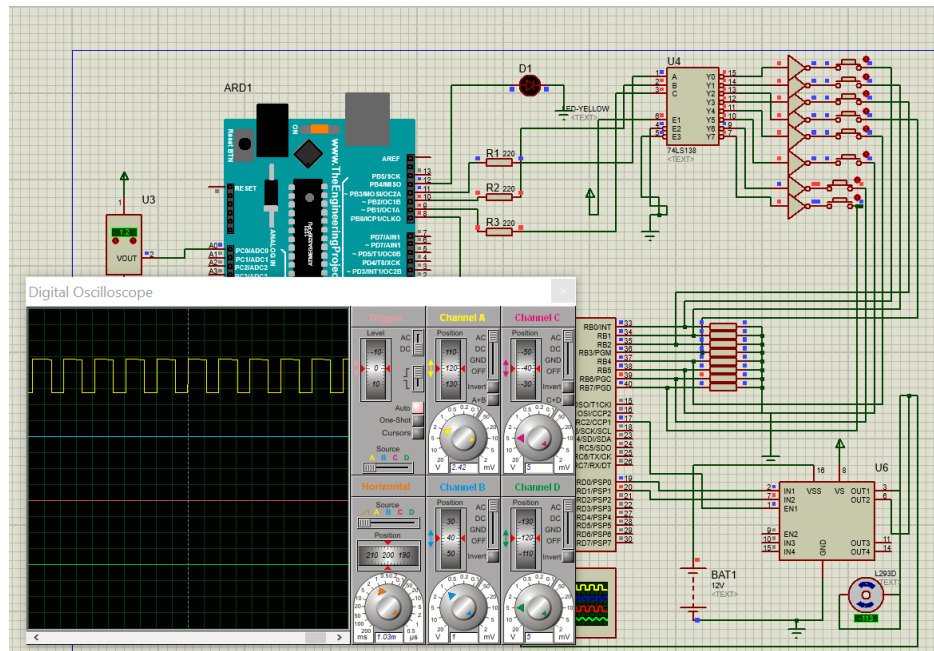
Figure 4.34: Oscilloscope illustration of 60% duty cycle with a motor speed angle of 113

CHAPTER 5

CONCLUSIONS AND RECOMMENDATIONS FOR FUTURE WORK

5.1   Conclusion

From the research that was carried out, the effectiveness of humidity and temperature-based fan systems in terms of providing indoor air quality without causing thermal discomfort was analysed through three different case studies. The research then computed the resulted reduction in terms of air conditioner reliance and energy consumption.

The first case study involved an inspection of IAQ and thermal comfort during open/ close doors, while the second and third case studies focused on monitoring the IAQ and thermal comfort at different fan speed levels with the usage of two different fan types across two preceding weeks.

From the three case studies, it showed that the most beneficial type of fan is the ceiling fan. Ceiling fans demonstrated noticeable advantages in terms of humidity level and temperature reduction while maintaining the CO_2 level under control when compared to the standing fan.

The results collected throughout the two-week analysis assisted in creating the benchmark-setting, in which the humidity and temperature-based fan system operated accordingly.

By applying the benchmark-setting created to the environmental fan system designed, a 25% reduction in air conditioner energy consumption is achieved and was proven by implementing the system onto a 0.5-ton (2HP) air conditioner with an energy label rating ranging from 1 star to 5 stars as an example.

In addition to a 25% energy consumption, the maximum speed level needed to achieve the IAQ and thermal comfort is level 3, meaning only a maximum PWM duty cycle of 60% is needed thus the fan will not operate at full capacity, which results in as added advantage in terms of energy consumption and fan's life span.

Finally, this research concludes that a high reliance on an environmental fan system in humid and hot countries like Malaysia is possible as the expected reliance was estimated to be 75% during normal weather conditions. In comparison, reliance on air conditioners was expected to be 25%, only needing it on days where heat waves occur or unbearable outdoor humidity levels.

5.2   Recommendation for Future Work

This research's outcome showed a 25% reduction in air conditioner energy consumption from the implementation of the environmental fan system. However, that percentage can be increased furthermore by connecting the system to the AC and thus activating and deactivation the AC according to weather conditions, therefore the long periods of AC activation in workplace, schools, universities and apartments will no longer be necessary.

REFERENCES

Anguera, J., Satapathy, S. and Bhateja, V., 2018. *Microelectronics, Electromagnetics and Telecommunications: Proceedings of ... - Google Books*, Springer.

Arens, E., Zhang, H., Pasut, W. and Org, E., 2013. *UC Berkeley HVAC Systems Title Air movement as an energy efficient means toward occupant comfort Permalink https://escholarship.org/uc/item/2d656203 Publication Date*,

Argunhan, Z. and Avci, A.S., 2018. Statistical Evaluation of Indoor Air Quality Parameters in Classrooms of a University. *Advances in Meteorology*. Available at: https://www.hindawi.com/journals/amete/2018/4391579/.

Arredondo, A., Roy, P. and Wofford, E., 2004. Implementing PWM Fan Speed Control to Decrease Energy Consumption, Reduce Acoustics, and Increase Fan Performance.

Attalage, R. and Sugathapala, A., 2001. Performance analysis of table and pedestal fans. Available at: http://dl.lib.mrt.ac.lk/handle/123/14543 [Accessed: 3 November 2020].

Babich, F. et al., 2017. Transient three-dimensional CFD modelling of ceiling fans. *Building and Environment*, 123, pp.37–49.

BEE, B. of E.E., 2001. THE ENERGY CONSERVATION ACT, 2001 No 52 OF 2001, Chapter III. *www.beeindia.in*. Available at: http://www.beeindia.in/about_bee/documents/ec_act/act_detail/CHAPTER II.pdf [Accessed: 8 December 2020].

Boddy, S. and Krigger, J., 2001. *Cooling Your Home with Fans and Ventilation*,

Boschi, N., 1999. *Education and Training in Indoor Air Sciences*, Springer Netherlands.

Carlos, M. and Da Silva, G., *SPREADSHEETS FOR THE CALCULATION OF THERMAL COMFORT INDICES PMV AND PPD*,

Chan, W.R., Parthasarathy, S., Fisk, W.J. and Mckone, T.E., 2016. Estimated effect of ventilation and filtration on chronic health risks in U.S. offices, schools, and retail stores. *Indoor Air*, 26(2), pp.331–343. Available at: https://pubmed.ncbi.nlm.nih.gov/25639183/ [Accessed: 3 July 2020].

Chaudhuri, T. et al., 2016. On assuming Mean Radiant Temperature equal to air temperature during PMV-based thermal comfort study in air-conditioned buildings. *IECON Proceedings (Industrial Electronics Conference)*. 21 December 2016 IEEE Computer Society, pp. 7065–7070.

Cheng, Y. et al., 2014. Uniformity of stratum-ventilated thermal environment and thermal sensation. *Indoor Air*, 24(5), pp.521–532.

Cincinelli, A. and Martellini, T., 2017. Indoor air quality and health. *International Journal of Environmental Research and Public Health*, 14(11). Available at: https://www.semanticscholar.org/paper/Indoor-Air-Quality-and-Health-Cincinelli-Martellini/ce0bf30c1d9dc9948fc158c3ebf5d1d7964a9ab8 [Accessed: 3 March 2020].

Daikin Global, 2018, *Increasing Air Conditioner Efficiency* [Online]. Available at:
https://www.daikin.com/csr/environment/climatechange/air_conditioner.html [Accessed: 18 July 2020].

Ehiagwina, F. and Onawola, H., 2016. Development of Temperature Control Monitoring System for Server Racks. *8TH INTERNATIONAL CONFERENCE OF THE SCHOOL OF ENGINEERING AND ENVIRONMENTAL*. 20 July 2016

Eyy, C. and GuptaS, M. V, 2017. Cochrane Library Cochrane Database of Systematic Reviews Electric fans for reducing adverse health impacts in heatwaves (Review). Available at: www.cochranelibrary.com [Accessed: 23 November 2020].

Fang, L., 1998. Impact of temperature and humidity on the perception of indoor air quality. *Indoor Air*, 8(2), pp.80–90. Available at: https://onlinelibrary.wiley.com/doi/abs/10.1111/j.1600-0668.1998.t01-2-

00003.x [Accessed: 6 March 2020].

He, Y. et al., 2017. Comfort, energy efficiency and adoption of personal cooling systems in warm environments: A field experimental study. *International Journal of Environmental Research and Public Health*, 14(11).

Ihtsham, S., Gilani, H., Khan, M.H. and Pao, W., 2015. ScienceDirect Thermal comfort analysis of PMV model Prediction in Air conditioned and Naturally Ventilated Buildings. , pp.1876–6102. Available at: www.sciencedirect.com [Accessed: 6 November 2020].

Jamaludin, N., Mohammed, N.I., Khamidi, M.F. and Wahab, S.N.A., 2015. Thermal Comfort of Residential Building in Malaysia at Different Micro-climates. *Procedia - Social and Behavioral Sciences*, 170, pp.613–623.

James, P.W. et al., 1996. *Are Energy Savings Due to Ceiling Fans Just Hot Air?*, Forida.

Karali, N. et al., 2020. Improving the energy efficiency of room air conditioners in China: Costs and benefits. *Applied Energy*, 258, p.114023.

Kelly, F.J. and Fussell, J.C., 2015. Air pollution and public health: emerging hazards and improved understanding of risk. *Environmental Geochemistry and Health*, 37(4), pp.631–649. Available at: https://link.springer.com/article/10.1007/s10653-015-9720-1?utm_source=mendeley&utm_medium=getftr&utm_campaign=getftr_pilot [Accessed: 4 March 2020].

Khare, M. and Katiyar, V., 2001. Indoor Air Quality-An Emerging Environmental Challenge. *CES Newsletter Enviroscan*. Available at: https://www.researchgate.net/publication/236605730_Indoor_Air_Quality-An_Emerging_Environmental_Challenge/references [Accessed: 3 March 2020].

Kim, J., de Dear, R., Parkinson, T. and Candido, C., 2017. Understanding patterns of adaptive comfort behaviour in the Sydney mixed-mode residential context. *Energy and Buildings*, 141, pp.274–283. Available at: https://www.sciencedirect.com/science/article/abs/pii/S0378778816308672?via

%3Dihub [Accessed: 6 March 2020].

Kubota, T., Jeong, S., Toe, D. and Ossen, D., 2011. Energy Consumption and Air-Conditioning Usage in Residential Buildings of Malaysia. *Journal of International Development and Cooperation*, 17(3), pp.61–69.

Leung, D.Y.C., 2015. Outdoor-indoor air pollution in urban environment: Challenges and opportunity. *Frontiers in Environmental Science*, 2(JAN).

Li, J. et al., 2014. Wireless sensor network for indoor air quality monitoring. *Sensors and Transducers*, 171(6), pp.86–90. Available at: https://www.sciencedirect.com/science/article/abs/pii/S1350453311002761.

Manickam, D., 2017. Designing and Controlling the Speed of Single Phase Induction Motor using Raspberry pi System. *Journal of Embedded Systems and Processing*, 2(1), pp.1–8. Available at: https://www.researchgate.net/publication/340792684_Designing_and_Controlling_the_Speed_of_Single_Phase_Induction_Motor_using_Raspberry_pi_System [Accessed: 5 December 2020].

Mendes, A. et al., 2013. Indoor air quality and thermal comfort - Results of a pilot study in elderly care centers in portugal. *Journal of Toxicology and Environmental Health - Part A: Current Issues*, 76(4–5), pp.333–344.

Mun, Kwak, Kim and Huh, 2019. A Comprehensive Thermal Comfort Analysis of the Cooling Effect of the Stand Fan Using Questionnaires and a Thermal Manikin. *Sustainability*, 11(18), p.5091. Available at: https://www.mdpi.com/2071-1050/11/18/5091 [Accessed: 20 July 2020].

ÖZDAMAR, M. and UMAROĞULLAR, F., 2018. THERMAL COMFORT AND INDOOR AIR QUALITY. *International Journal of Scientific Research and Innovative Technology*, 5(3), pp.90–109. Available at: https://link.springer.com/chapter/10.1007%2F978-1-4471-2336-1_1 [Accessed: 6 March 2020].

Phadke, A. et al., 2020. Chinese policy leadership would cool global air conditioning impacts: Looking east. *Energy Research and Social Science*, 66,

p.101570.

Polese, M. et al., 2014. *Crisma Crisma Version 2 of Dynamic vulnerability functions, Systemic vulnerability, and Social vulnerability*,

Purnomo, H.D. et al., 2016. Design and implementation of temperature and humidity monitoring system for poultry farm. *Fourth International Conference on Wireless and Optical Communications*. 2016

Raheem Hatem, H., 2019. Control of Pulse Width Modulation ON Direction and Speed of DC Motor using Arduino. *Journal of Engineering and Applied Sciences*, 14(4), pp.1493–1497.

Ramsden, E., 2006. *Hall-Effect Sensors*, Elsevier Inc.

Ranjbar, N., Zaki, S.A., Yusoff, N.M. and Hagishima, A., 2017. Time series data analysis of household electricity usage during el-nino in Malaysia. *Chemical Engineering Transactions*, 56, pp.379–384. Available at: https://www.cetjournal.it/index.php/cet/article/view/CET1756064 [Accessed: 18 July 2020].

Raza, N. et al., 2017. Recent advances in titania-based composites for photocatalytic degradation of indoor volatile organic compounds. *Asian Journal of Atmospheric Environment*, 11(4), pp.217–234.

Saha, S., Rahman, M.A. and Thakur, A., 2014. Design and implementation of SPI bus protocol with Built-in-self-test capability over FPGA. *1st International Conference on Electrical Engineering and Information and Communication Technology, ICEEICT 2014*. 8 October 2014 Institute of Electrical and Electronics Engineers Inc.

Schiavon, S. and Melikov, A.K., 2008. Energy saving and improved comfort by increased air movement. *Energy and Buildings*, 40(10), pp.1954–1960.

Schulze, F. et al., 2017. Air quality effects on human health and approaches for its assessment through microfluidic chips. *Genes*, 8(10), p.244. Available at: http://www.mdpi.com/2073-4425/8/10/244 [Accessed: 9 March 2020].

Shah, R.K., 2009. Automotive air-conditioning systems-historical developments, the state of technology, and future trends. *Heat Transfer Engineering*, 30(9), pp.720–735.

Sipani, J.P., Patel, R.H., Upadhyaya, T. and Patel, V.T., 2017. TEMPERATURE & HUMIDITY MONITORING & CONTROL SYSTEM BASED ON ARDUINO AND SIM900A GSM SHIELD. *International Journal Of Electrical, Electronics And Data Communication*, 5(11), pp.2320–2084. Available at: http://www.iraj.in/journal/journal_file/journal_pdf/1-423-151703294362-68.pdf [Accessed: 1 March 2020].

Spengler, J.D. and Sexton, K., 1983. Indoor air pollution: A public health perspective. *Science*, 221(4605), pp.9–17. Available at: https://pubmed.ncbi.nlm.nih.gov/6857273/ [Accessed: 3 July 2020].

Stazi, F., Naspi, F., Ulpiani, G. and Di Perna, C., 2017. Indoor air quality and thermal comfort optimization in classrooms developing an automatic system for windows opening and closing. *Energy and Buildings*, 139, pp.732–746. Available at: https://www.sciencedirect.com/science/article/abs/pii/S0378778817300592?via%3Dihub [Accessed: 6 March 2020].

Van Der Tempel, M., Wouters, I., Descamps, F. and Aerts, D., 2011. Ventilation techniques in the 19 th century: Learning from the past. *WIT Transactions on the Built Environment*. 2011 pp. 271–281.

Ujjan, G.M., Malik, A., Ahmed, S. and Abdullah, M.Z., 2019. Implementation of 4-bit data transmission for accessing SD card with FPGA embedded soft processor. *ACM International Conference Proceeding Series*. 2019 Association for Computing Machinery, pp. 67–72.

US EPA, 2015. Why Indoor Air Quality is Important to Schools. Available at: https://www.epa.gov/iaq-schools/why-indoor-air-quality-important-schools [Accessed: 3 July 2020].

Wafi, S.R., Ismail, M.R. and Ahmed, E.M., 2011. A Case Study of the Climate

Factor on Thermal Comfort for Hostel Occupants in Universiti Sains Malaysia (USM), Penang, Malaysia. *Journal of Sustainable Development*, 4(5).

Yu, B.F. et al., 2009. Review of research on air-conditioning systems and indoor air quality control for human health. *International Journal of Refrigeration*. Available at: https://www.sciencedirect.com/science/article/abs/pii/S0140700708000984?via%3Dihub.

Yu, T.C. and Lin, C.C., 2015. An Intelligent Wireless Sensing and Control System to Improve Indoor Air Quality: Monitoring, Prediction, and Preaction. *International Journal of Distributed Sensor Networks*, 11(8). Available at: https://journals.sagepub.com/doi/full/10.1155/2015/140978.

Zhai, Y. et al., 2015. Human comfort and perceived air quality in warm and humid environments with ceiling fans. *Building and Environment*, 90, pp.178–185. Available at: https://www.sciencedirect.com/science/article/abs/pii/S0360132315001614 [Accessed: 7 March 2020].

Zur, P., Baier, A. and Kolodziej, A., 2019. Influence of Selected Parameters of the Motor Controller on the Current Characteristics of the DC Brush Motor Used in the Silesian Greenpower's Vehicle. *IOP Conference Series: Materials Science and Engineering*. 17 April 2019 Institute of Physics Publishing.

APPENDICES

Appendix A

- **Day 1 Testing Results (18-10-2020)**

	Fan Speed		Temperature (C°)	Humidity (%)	CO2 (ppm)	CO (ppm)	Wind speed m/s	PMV	Sensation
	CEILING FAN								
	Fan Speed		Temperature (C°)	Humidity (%)	CO2 (ppm)	CO (ppm)	Wind speed m/s	PMV	Sensation
18-Oct (Outside) 28°C 77%	Level 1	Average	33,82	46,15	273,8	3,285	0.768	1.38	Slightly warm (Does not comply)
		Highest	35,2	50	285,7	3,3			
	Level 2	Average	31,0336	58,6156	248,6	3,289	1.02	0.7	Slightly warm (Does not comply)
		Highest	31,2	61,2	311,4	3,34			
	Level 3	Average	30,6944	52,9672	282,6	3,305	1.27	0.48	Neutral (Comply)
		Highest	31	54,6	311,4	3,33			
	STANDING FAN								
	Fan Speed		Temperature (C°)	Humidity (%)	CO2 (ppm)	CO (ppm)	Wind speed m/s	PMV	Sensation
	Level 1	Average	30,172400	51,2096	290,74	3,2847	0.47	0.63	Slightly warm (Does not comply)
		Highest	30,4	53	331,64	3,31			
	Level 2	Average	30,0648	49,1656	295,65	3,2987	0.52	0.36	Neutral (Comply)
		Highest	30,2	49,5	311,4	3,31			

- **Day 2 Testing Results (19-10-2020)**

	Fan Speed		Temperature (C°)	Humidity (%)	CO2 (ppm)	CO (ppm)	Wind speed m/s	PMV	Sensation
	CEILING FAN								
	Fan Speed		Temperature (C°)	Humidity (%)	CO2 (ppm)	CO (ppm)	Wind speed m/s	PMV	Sensation
19-Oct (Outside) 32°C 64%	Level 1	Average	31.3296	53.824	255.036	3.2962	0.768	0.82	Slightly warm (Does not comply)
		Highest	31.6	54.6	311.4	3.35			
	Level 2	Average	31.0336	58.6156	248.6	3.289	1.02	0.92	Slightly warm (Does not comply)
		Highest	31.2	61.2	311.4	3.34			
	Level 3	Average	30.6944	52.9672	510.75	3.35	1.27	-0.02	Neutral (Comply)
		Highest	31	54.6	526.1	3.535			
	STANDING FAN								
	Fan Speed		Temperature (C°)	Humidity (%)	CO2 (ppm)	CO (ppm)	Wind speed m/s	PMV	Sensation
	Level 1	Average	29.8936	49.202	439.81	3.3697	0.47	0.54	Slightly warm (Does not comply)
		Highest	30.1	50.8	462.86	3.4			
	Level 2	Average	29.9904	47.66	502.81	3.3624	0.52	0.5	Neutral (Comply)
		Highest	30.2	49.1	544.42	3.39			

- **Day 3 Testing Results (20-10-2020)**

	Fan Speed		Temperature (C°)	Humidity (%)	CO2 (ppm)	CO (ppm)	Wind speed m/s	PMV	Sensation
	CEILING FAN								
	Fan Speed		Temperature (C°)	Humidity (%)	CO2 (ppm)	CO (ppm)	Wind speed m/s	PMV	Sensation
20-Oct (Outside) 28°C 81%	Level 1	Average	30.6824	58.046	444,7	645,61	0.768	0.74	Slightly warm (Does not comply)
		Highest	31	59	479	3.99			
	Level 2	Average	30.0708	46.3188	492.85	3.39272	1.02	0.19	Neutral (Comply)
		Highest	30.1	47.5	504.86	3.41			
	STANDING FAN								
	Fan Speed		Temperature (C°)	Humidity (%)	CO2 (ppm)	CO (ppm)	Wind speed m/s	PMV	Sensation
	Level 1	Average	29.6152	47.06	562.28	3.41976	0.47	0.58	Slightly warm (Does not comply)
		Highest	29.7	46.4	1081.6	3.44			
	Level 2	Average	29.6668	47.482	663.3	3.43396	0.52	0.35	Neutral (Comply)
		Highest	29.8	48.5	1504.2	3.56			

- **Day 4 Testing Results (21-10-2020)**

			CEILING FAN						
	Fan Speed		Temperature (C°)	Humidity (%)	CO2 (ppm)	CO (ppm)	Wind speed m/s	PMV	Sensation
21-Oct (Outside) 27°C 82% (Raining)	Level 1	Average	29.7992	53.468	441.03	3.32396	0.768	0.29	Neutral (comply)
		Highest	30.1	54.8	832.23	3.47			
			STANDING FAN						
	Fan Speed		Temperature (C°)	Humidity (%)	CO2 (ppm)	CO (ppm)	Wind speed m/s	PMV	Sensation
	Level 1	Average	29.7056	52.7656	542.86	3.35004	0.47	0.68	Slightly warm (Does not comply)
		Highest	29.8	54.3	624.45	3.39			
	Level 2	Average	29.7084	50.5908	765.82	3.37696	0.52	0.38	Neutral (Comply)
		Highest	29.8	51.5	832.23	3.4			

- **Day 5 Testing Results (22-10-2020)**

			CEILING FAN						
	Fan Speed		Temperature (C°)	Humidity (%)	CO2 (ppm)	CO (ppm)	Wind speed m/s	PMV	Sensation
22-Oct (Outside) 25°C 87% Cloudy	Level 1	Average	29.7396	59.5036	227.88	3.4132	0.768	0.36	Neutral (comply)
		Highest	30.9	61	244.15	3.44			
			STANDING FAN						
	Fan Speed		Temperature (C°)	Humidity (%)	CO2 (ppm)	CO (ppm)	Wind speed m/s	PMV	Sensation
	Level 1	Average	29.1988	62.7472	403.44	3.4506	0.47	0.59	Slightly warm (Does not comply)
		Highest	29.2	63.1	462.86	3.48			
	Level 2	Average	29.0624	59.582	434.68	3.45728	0.52	0.31	Neutral (Comply)
		Highest	29.2	60.5	979.4	3.56			

- **Day 6 Testing Results (23-10-2020)**

			CEILING FAN						
	Fan Speed		Temperature (C°)	Humidity (%)	CO2 (ppm)	CO (ppm)	Wind speed m/s	PMV	Sensation
23-Oct (Outside) 29°C 79% (Cloudy and possible rain)	Level 1	Average	30.2016	49.6024	316.79	3.63916	0.768	0.49	Neutral (comply)
		Highest	30.4	50.8	338.57	3.77			
			STANDING FAN						
	Fan Speed		Temperature (C°)	Humidity (%)	CO2 (ppm)	CO (ppm)	Wind speed m/s	PMV	Sensation
	Level 1	Average	29.4676	49.3512	364.88	3.61168	0.47	0.62	Slightly warm (Does not comply)
		Highest	29.7	50	397.52	3.66			
	Level 2	Average	29.4616	48.1976	407.01	3.60356	0.52	0.37	Neutral (Comply)
		Highest	29.5	49.6	445.91	3.62			

- **Day 7 Testing Results (23-10-2020)**

			CEILING FAN						
	Fan Speed		Temperature (C°)	Humidity (%)	CO2 (ppm)	CO (ppm)	Wind speed m/s	PMV	Sensation
24-Oct (Outside) 27°C 82% (Raining)	Level 1	Average	29.786	50.7872	503.35	3.61384	0.768	0.26	Neutral (comply)
		Highest	29.9	53.3	593.59	3.87			
			STANDING FAN						
	Fan Speed		Temperature (C°)	Humidity (%)	CO2 (ppm)	CO (ppm)	Wind speed m/s	PMV	Sensation
	Level 1	Average	29.1292	49.2324	516.2	3.60728	0.47	0.29	Neutral (comply)
		Highest	29.3	50.2	537.4	3.72			

- ## **Day 8 Testing Results (28-10-2020)**

			CEILING FAN						
	Fan Speed		**Temperature (C°)**	**Humidity (%)**	**CO2 (ppm)**	**CO (ppm)**	**Wind speed m/s**	**PMV**	**Sensation**
28-Oct (Outside) 29°C 71%	Level 1	Average	31.0868	52.328	271.3	3.01788	0.768	0.73	Slightly warm (Does not comply)
		Highest	31.2	52.9	374.68	3.03			
	Level 2	Average	31.2284	54.5224	291.27	3.32844	1.02	0.40	Neutral (Comply)
		Highest	31.4	60.2	389.81	3.46			
			STANDING FAN						
	Fan Speed		**Temperature (C°)**	**Humidity (%)**	**CO2 (ppm)**	**CO (ppm)**	**Wind speed m/s**	**PMV**	**Sensation**
	Level 1	Average	30.3248	51.6892	712.39	3.41116	0.47	0.63	Slightly warm (Does not comply)
		Highest	30.6	52.9	1066.5	3.53			
	Level 2	Average	29.0624	50.0576	602.05	3.45728	0.52	0.4	Neutral (Comply)
		Highest	29.2	50.9	782.6	3.56			

- ## **Day 9 Testing Results (29-10-2020)**

			CEILING FAN						
	Fan Speed		**Temperature (C°)**	**Humidity (%)**	**CO2 (ppm)**	**CO (ppm)**	**Wind speed m/s**	**PMV**	**Sensation**
29-Oct 10:00am (Outside) 32°C 81%	Level 1	Average	30.0656	55.6872	280.36	3.38	0.768	0.55	Slightly warm (Does not comply)
		Highest	30.2	59	298.37	3.48			
	Level 2	Average	30.3776	58.8396	400.56	3.42008	1.02	0.44	Neutral (Comply)
		Highest	30.6	61.9	794.82	3.56			
			STANDING FAN						
	Fan Speed		**Temperature (C°)**	**Humidity (%)**	**CO2 (ppm)**	**CO (ppm)**	**Wind speed m/s**	**PMV**	**Sensation**
	Level 1	Average	30.2988	61.7972	392.27	3.43492	0.47	0.97	Slightly warm (Does not comply)
		Highest	30.4	65	554.03	3.51			
	Level 2	Average	30.288	60.2192	546.95	3.42888	0.52	0.47	Neutral (Comply)
		Highest	30.4	65	656.36	3.49			

- ## **Day 10 Testing Results (30-10-2020)**

			CEILING FAN						
	Fan Speed		**Temperature (C°)**	**Humidity (%)**	**CO2 (ppm)**	**CO (ppm)**	**Wind speed m/s**	**PMV**	**Sensation**
31-Oct (Outside) 32°C 81%	Level 1	Average	29.5128	70.0504	651.62	3.4524	0.768	0.50	Slightly warm (Does not comply)
		Highest	29.6	73.5	711.92	3.47			
	Level 2	Average	29.2008	68.1192	712.7	3.42604	1.02	0.16	Neutral (Comply)
		Highest	29.5	71	758.55	3.47			
			STANDING FAN						
	Fan Speed		**Temperature (C°)**	**Humidity (%)**	**CO2 (ppm)**	**CO (ppm)**	**Wind speed m/s**	**PMV**	**Sensation**
	Level 1	Average	28.4564	58.79	1170.5	3.56368	0.47	0.56	Slightly warm (Does not comply)
		Highest	29.4	63.2	1306.7	3.61			
	Level 2	Average	28.7	65.7	1783.3	3.66	0.52	0.16	Neutral (Comply)
		Highest	28.7	65.7	1825.8	3.64			

- **Day 11 Testing Results (1-11-2020)**

			CEILING FAN						
	Fan Speed		**Temperature (C°)**	**Humidity (%)**	**CO2 (ppm)**	**CO (ppm)**	**Wind speed m/s**	**PMV**	**Sensation**
	Level 1	Average	29.2504	58.3008	841.38	3.34876	0.768	0.17	Neutral
		Highest	29.4	60.3	924.03	3.38			(comply)
			STANDING FAN						
1-Nov (Outside) 32°C 70%	**Fan Speed**		**Temperature (C°)**	**Humidity (%)**	**CO2 (ppm)**	**CO (ppm)**	**Wind speed m/s**	**PMV**	**Sensation**
	Level 1	Average	28.6252	61.1704	955.81	3.37692	0.47	0.58	Slightly warm
		Highest	29	62	1036.9	3.4			(Does not comply)
	Level 2	Average	28.3684	67.0024	1226.9	3.39468	0.52	0.22	Neutral
		Highest	28.5	68.4	1272.8	3.42			(Comply)

- **Day 12 Testing Results (2-11-2020)**

			CEILING FAN						
	Fan Speed		**Temperature (C°)**	**Humidity (%)**	**CO2 (ppm)**	**CO (ppm)**	**Wind speed m/s**	**PMV**	**Sensation**
	Level 1	Average	29.508	70.5804	416.19	3.46312	0.768	0.50	Slightly warm
		Highest	29.6	72.5	554.03	3.49			(Does not comply)
	Level 2	Average	29.4924	68.4896	365.06	3.47008	1.02	0.24	Neutral
2-Nov (Outside) 32°C 82%		Highest	29.700000	70	389.81	3.49			(Comply)
			STANDING FAN						
	Fan Speed		**Temperature (C°)**	**Humidity (%)**	**CO2 (ppm)**	**CO (ppm)**	**Wind speed m/s**	**PMV**	**Sensation**
	Level 1	Average	29.0644	74.2824	940.92	3.5042	0.47	0.55	Slightly warm
		Highest	29.5	75.5	1111.9	3.54			(Does not comply)
	Level 2	Average	28.8184	72.2036	1161.8	3.51456	0.52	0.39	Neutral
		Highest	29	74.4	1256.1	3.55			(Comply)

- **Day 13 Testing Results (3-11-2020)**

			CEILING FAN						
	Fan Speed		**Temperature (C°)**	**Humidity (%)**	**CO2 (ppm)**	**CO (ppm)**	**Wind speed m/s**	**PMV**	**Sensation**
	Level 1	Average	28.7729	74.3915	659.68	3.392903	0.768	0.25	Neutral
		Highest	28.8	76.7	1272.8	3.44			(comply)
			STANDING FAN						
3-Nov (Outside) 28°C 80%	**Fan Speed**		**Temperature (C°)**	**Humidity (%)**	**CO2 (ppm)**	**CO (ppm)**	**Wind speed m/s**	**PMV**	**Sensation**
	Level 1	Average	28.418	71.1216	889.6	3.47264	0.47	0.27	Neutral
		Highest	28.5	70.9	1036.9	3.49			(comply)

- **Day 14 Testing Results (4-11-2020)**

	CEILING FAN								
	Fan Speed		**Temperature (C°)**	**Humidity (%)**	**CO2 (ppm)**	**CO (ppm)**	**Wind speed m/s**	**PMV**	**Sensation**
4-Nov (Outside) 28°C 76%	Level 1	Average	28.5776	70.5976	351.08	3.43908	0.768	0.06	Neutral (comply)
		Highest	29	70.7	374.68	3.48			
	STANDING FAN								
	Fan Speed		**Temperature (C°)**	**Humidity (%)**	**CO2 (ppm)**	**CO (ppm)**	**Wind speed m/s**	**PMV**	**Sensation**
	Level 1	Average	28.0516	69.752	551.64	3.44436	0.47	0.11	Neutral (comply)
		Highest	28.4	70.2	574.68	3.47			